이학박사학위논문

Development of a General Relativistic Hydrodynamic Code in Spherical Symmetry

구대칭 일반상대론적 유체역학 코드의 개발

2013년 2월

서울대학교 대학원

물리천문학부 물리학전공

박동호

Development of a General Relativistic Hydrodynamic Code in Spherical Symmetry

구대칭 일반상대론적 유체역학 코드의 개발

지도교수 이형목

이 논문을 이학박사 학위논문으로 제출함

2013년 2월

서울대학교 대학원

물리천문학부 물리학전공

박동호

박동호의 이학박사 학위논문을 인준함

2012년 12월

위 원 장 김웅태 (인)

부위원장 이형목 (인)

위 원 구본철 (인)

위 원 이창환 (인)

위 원 강궁원 (인)

To my mother

ABSTRACT

I develop a fully general relativistic hydrodynamic code that is designed to study a self-gravitating system of spherically symmetric perfect fluid numerically. It is based on 3+1 Arnowitt-Deser-Misner formalism and isotropic spatial coordinates. For spacetime geometry set of constraint equations are solved with maximal slicing gauge condition. For hydrodynamic fluid matter high resolution shock capturing schemes with approximated Riemann solvers are used in the Eulerian viewpoint. The convergence and the accuracy of my code are verified by performing several test problems. These include a relativistic blast wave, relativistic spherical accretion of matter onto a black hole, Tolman-Oppenheimer-Volkoff stars and Oppenheimer-Snyder (OS) dust collapses. In particular, a dynamical code test is done for the OS collapse by explicitly performing numerical coordinate transformations between coordinate system used in my code and the one used for the analytic solution. Finally, polytropic equilibrium star solutions are surveyed and the formation of singularity during a matter collapse to a black hole is investigated for the Eddington-inspired Born-Infeld gravity theory.

Keywords: General relativistic hydrodynamics, Spherically symmetric numerical code, Eddington-inspired gravity

Student Number: 2003-30091

Contents

List of Tables

List of Figures

1. INTRODUCTION

Highly energetic astronomical observations such as supernovae and gamma-ray bursts, are believed to involve high-density matter and its dynamics. The dynamics for unstable cores of very massive stars (above tens of the solar mass) during their last stages and neutron star-neutron star or neutron star-black hole binaries in the last phases of coalescence reveals strong self-gravitation and highly-relativistic motions. Those phenomena are beyond the Newtonian gravity limit, so general relativity should be considered to understand them. However, the Einstein equations comprise ten coupled non-linear partial differential equations. Thus, in general, it is almost impossible to solve them analytically. Moreover, if matter appears, one should solve the equations of motion for matter in conjunction with a spacetime metric. A feasible way to do this is to solve the Einstein equations numerically.

May and White [1] took the first step towards a numerical study of general relativistic hydrodynamics. There have been many works and developments since this pioneering work; see Refs. [2, 3, 4, 5] for reviews. I have developed a fully general relativistic hydrodynamic (GRHydro) code that can be used to simulate a system of spherically symmetric perfect fluid. Currently, finite difference schemes, smoothed particle hydrodynamics and spectral methods compete with each other. Here, I choose finite difference schemes which are widely used in hydrodynamic codes. There are two view points in fluid dynamics, namely, the Lagrangian and the Eulerian approaches. Because the Eulerian approach can be extended to multi-dimensions easily, I adopt this approach. In non-linear hydrodynamics, discontinuities are often occur, so one should handle them properly. The artificial viscosity approach and the high resolution shock capturing (HRSC) scheme are most widely used for that purpose. Here, I choose the HRSC scheme with approximated Riemann solvers.

In order to solve the Einstein equations and GRHydro equations fully but in a simple way I restricted spacetime and matter distribution to spherical symmetry. However, I followed the conventional formulations of 3+1 decompositions of the Einstein and the hydrodynamic equations with isotropic spatial coordinates in order to compare the simulation result with the one of other multi-dimensional codes easily. Since a spherically symmetric spacetime has no dynamical degree of freedom, i.e., it is a fully constrained system, here, the Einstein equations can be solved with constraint equations only.

To check whether my GRHydro code works properly and accurately, I considered several test problems. These include a relativistic blast wave, relativis-

tic spherical accretion of matter onto a black hole, Tolman-Oppenheimer-Volkoff (TOV) stars and Oppenheimer-Snyder (OS) dust collapses. The hydrodynamic part of my code was tested by addressing the relativistic blast wave problem, which is a sort of a shock tube test with spherical symmetry. Here, the metric is fixed as the flat Minkowski spacetime during its evolution. The relativistic spherical accretion problem is another hydrodynamic test, but on a curved spacetime. It addresses how well my code solves the steady-state spherical accretion of matter onto a fixed black hole spacetime metric. The TOV star is a static equilibrium solution of a self-gravitating fluid matter. The TOV star test checks both the spacetime metric and the hydrodynamic parts of my code together. I also analyze the oscillation modes of the TOV star under small perturbations. The mode frequencies are compared with the results of linearized perturbation calculations of radial pulsations. Finally, I perform a dynamical full code test by using the Oppenheimer-Snyder dust (pressureless) collapse solution. To compare simulation results of my code with the known analytic time-dependent solution [6], I explicitly performed numerical coordinate transformations between coordinate system used in my code and the one used for the analytic solution.

The Eddington-inspired Born-Infeld (EiBI) gravity theory is an alternative theory of gravity that was suggested very recently [7]. This theory differs from the Einstein general relativity in matter part only. Since the EiBI gravity is known to have not only the usual attractive nature, but also a repulsive effect on compact stars [8], studying TOV star solutions in this theory and seeing how they differ from those in general relativity are of interest.

My GRHydro code was developed by using Rapid Numerical Prototyping Language (RNPL), which was produced by Choptuik's Numerical Relativity Group at the University of British Columbia [9]. The `RNPL` program is needed to compile the GRHydro code. My code is posted on the web page http://www.ksc.re.kr/kcnr/research.htm.

The outline of the thesis is as follows. In Chapter 2, I review formulations of fully general relativistic hydrodynamics in the presence of spherical symmetry and present the equations to be solved numerically. In Chapter 3, the numerical methods used to solve these equations are explained. In Chapter 4, my GRHydro code is verified for several test problems such as the relativistic blast wave problem, relativistic spherical accretion of matter onto a black hole, Tolman-Oppenheimer-Volkoff star evolution, and Oppenheimer-Snyder dust collapse. In Chapter 5, some TOV star solutions in the Eddington-inspired Born-Infeld gravity theory are reported. Finally, I conclude with possible applications and further developments of my code.

Throughout this thesis, I use the geometrized units where the gravitational constant G, and the speed of light c, are set to be $G = c = 1$, except for the EiBI gravity theory in which I use $8\pi G = 1$ unit. The metric signature used is "$-+++$". Greek indices run from 0 to 3 whereas Latin indices (*e.g.*, $i, j, k, \cdots$)

run from 1 to 3 unless stated otherwise.

2. FORMULATIONS

The equations to solve are the Einstein equations and the conservation equations of the baryon rest-mass and the energy-momentum tensor. However, those equations are written in covariant tensor form, independent of the coordinate system one may choose. Because there is no direct tensor calculation in numerics, one should choose a coordinate system and rewrite the equations in order to make them a well-defined Cauchy problem. In this chapter, 3+1 decompositions of the Einstein and the hydrodynamic equations are presented.

2.1. 3+1 Decomposition of Einstein Equations

There are many good references for the formulations of 3+1 decomposition of Einstein equations. Here, I refer [10, 11, 12, 13, 14].

2.1.1. Spacetime foliation

If a spacetime manifold $(M, g_{\mu\nu})$ is *globally hyperbolic*, then one can choose a *global time function*, t, such that each surface of constant t is a *Cauchy surface*. Thus the spacetime manifold M can be foliated by Cauchy surfaces, $\{\Sigma_{t\in\mathbb{R}}\}$ and the topology of M is $\mathbb{R}\times\Sigma$.

Let n^μ be the timelike unit vector which is normal to the spacelike hypersurfaces, Σ. Then one can define the orthogonal projection operator onto Σ.

2.1.1.1. Metric decomposition

For each slice Σ one can choose three vector fields $(e_1)^a, (e_2)^a, (e_3)^a$, such that they are linearly independent at each point of Σ. Then the symmetric spacetime metric g_{ab} satisfies the following,

$$g_{ab}n^a n^b \equiv n^a n_a = -1\,, \tag{2.1}$$

$$g_{ab}(e_i)^a n^b = 0 \qquad (i = 1,2,3)\,, \tag{2.2}$$

$$g_{ab}(e_i)^a (e_j)^b = \gamma_{ij} \qquad (i,j = 1,2,3)\,. \tag{2.3}$$

The first and second equation tell us n^a is a unit vector and is orthogonal to Σ respectively. The last one, Eq. (2.3)) is the definition of 3-metric γ_{ij} and it is a positive definite metric inside Σ.

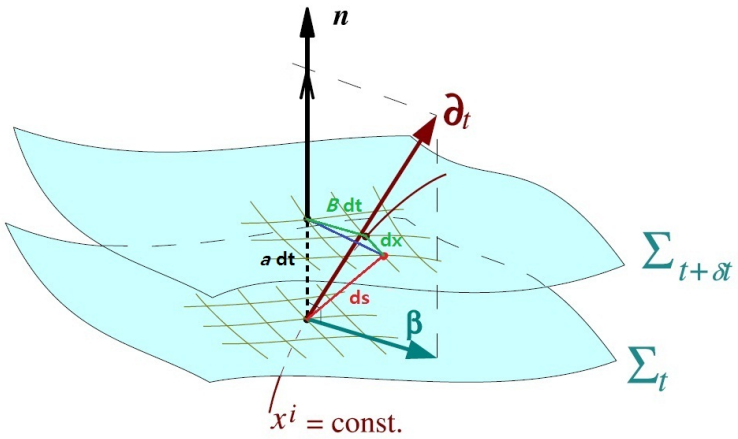

Figure 2.1: Two slices of the foliation of spacetime. ∂_t is the tangent vector field to the curves threading the foliation and $\mathbf{n}$ is the hypersurface orthogonal vector field. The relation between these vectors is defined by the lapse function α and the shift vector β^i. [Figure from Gourgoulhon (gr-qc/0703035)]

For a given foliation of spacetime, it is free to choose the timelike basis vector $(\partial_t)^a$. This is the coordinate or gauge freedom of general relativity and it is represented by the lapse function α and the shift vector β^i (see Fig. 2.1)

$$(\partial_t)^a \;=\; \alpha n^a + \beta^i (e_i)^a \,. \tag{2.4}$$

Therefore the metric components $g_{\mu\nu}$ become

$$g_{tt} \;=\; g_{ab}(\partial_t)^a(\partial_t)^b \;=\; -\alpha^2 + \gamma_{ij}\beta^i\beta^j \,, \tag{2.5}$$

$$g_{ti} \;=\; g_{ab}(\partial_t)^a(e_i)^b \;=\; \gamma_{ij}\beta^j \;\equiv\; \beta_i \,, \tag{2.6}$$

$$g_{ij} \;=\; \gamma_{ij} \,. \tag{2.7}$$

Then, the infinitesimal squared distance ds^2 can be represented by

$$ds^2 \;=\; (-\alpha^2 + \beta_i\beta^i)dt^2 + 2\beta_i dt dx^i + \gamma_{ij}dx^i dx^j \,. \tag{2.8}$$

Or one can calculate ds^2 considering vector sum of αdt and $\beta^i dt + dx^i$ from Fig. 2.1 as

$$ds^2 = \alpha^2 dt^2 + \gamma_{ij}(dx^i + \beta^i dt)(dx^j + \beta^j dt) \,. \tag{2.9}$$

2.1.1.2. Projection tensor

Consider a vector field v^a. The parallel part of v^a to n^a is $(n^b v_b)n^a$. Therefore the orthogonal part of v^a to n^a, in other words v^a's orthogonal projection onto

Σ is

$$v^a + (n^b v_b) n^a \,. \tag{2.10}$$

One may wonder that the '+' sign is wrong because one should subtract the parallel part of v^a to n^a from v^a. But if we substitute n^a for v^a, then we obtain the correct answer,

$$n^a + (n^b n_b) n^a \;=\; 0\,. \tag{2.11}$$

So, using the correct sign projection formula, Eq. (2.10) one can define the ***projection tensor*** $\gamma^a{}_b$ by

$$\gamma^a{}_b v^b \;\equiv\; v^a + (n^b v_b) n^a \;=\; (\delta^a{}_b + n^a n_b) v^b \,. \tag{2.12}$$

Let us consider $\gamma_{ab} \;=\; g_{ac}\gamma^c{}_b$.[1]

$$\gamma_{ab} \;=\; g_{ab} + n_a n_b \tag{2.13}$$

Before specifying the components of γ_{ab}, $\gamma_{\mu\nu}$, we need to know the components of n^a and n_a.

$$n^\mu \;=\; \frac{1}{\alpha}\left((\partial_t)^\mu - \beta^i (e_i)^\mu\right) \tag{2.14}$$

$$n^t \;=\; \frac{1}{\alpha}\left((\partial_t)^t - \beta^i (e_i)^t\right) \;=\; \frac{1}{\alpha} \tag{2.15}$$

$$n^i \;=\; \frac{1}{\alpha}\left((\partial_t)^i - \beta^j (e_j)^i\right) \;=\; -\frac{\beta^i}{\alpha} \tag{2.16}$$

$$n_\mu \;=\; g_{\mu\nu} n^\nu \;=\; \frac{1}{\alpha}\left(g_{\mu\nu}(\partial_t)^\nu - \beta^i g_{\mu\nu}(e_i)^\nu\right) \tag{2.17}$$

$$n_t \;=\; \frac{1}{\alpha}\left(g_{tt}(\partial_t)^t - \beta^i g_{tj}(e_i)^j\right) \;=\; \frac{1}{\alpha}\left(-\alpha^2 + \beta^i\beta_i - \beta^i\beta_i\right) = -\alpha \tag{2.18}$$

$$n_i \;=\; \frac{1}{\alpha}\left(g_{it}(\partial_t)^t - \beta^i g_{ij}(e_i)^j\right) \;=\; \frac{1}{\alpha}\left(\beta_i - \beta_i\right) = 0 \tag{2.19}$$

$$\therefore \quad n^\mu = \left(\frac{1}{\alpha}, -\frac{\beta^i}{\alpha}\right), \quad n_\mu = (-\alpha, 0, 0, 0) \tag{2.20}$$

Now we can specify $\gamma_{\mu\nu}$.

$$\gamma_{\mu\nu} \;=\; g_{\mu\nu} + n_\mu n_\nu \tag{2.21}$$

$$\gamma_{tt} \;=\; g_{tt} + n_t n_t \;=\; -\alpha^2 + \beta^i\beta_i + \alpha^2 \;=\; \beta^i\beta_i \tag{2.22}$$

$$\gamma_{ti} \;=\; g_{ti} + n_t n_i \;=\; \beta_i \tag{2.23}$$

[1] Note that 4 dimensional tensor indices are raised or lowered with the spacetime metric g^{ab} or g_{ab}.

And $\gamma_{ij} = g_{ij} + n_i n_j = g_{ij}$, the 3-metric! This is the reason why we use the same character γ to define the projection tensor, Eq.(2.12). The 3-metric γ_{ij} is related to $(0,2)$ tensor $\gamma_{ab} = g_{ab} + n_a n_b$ in this way.

Note that $\gamma^{ab} = g^{ab} + n^a n^b$ is not inverse of γ_{ab}.

$$\begin{aligned}\gamma^{ab}\gamma_{bc} &= (g^{ab} + n^a n^b)(g_{bc} + n_b n_c) \\ &= \delta^a{}_c + n^a n_c = \gamma^a{}_c \end{aligned} \tag{2.24}$$

But we want $\gamma^{ij} = g^{ij} + n^i n^j$ to be inverse of γ_{ij}. To impose this, we should specify $g^{\mu\nu}$ as follows.

$$\delta^\rho{}_\mu = g_{\mu\nu}g^{\nu\rho} = g_{\mu t}g^{t\rho} + g_{\mu j}g^{j\rho} \tag{2.25}$$

g^{ij} satisfies $g^{ij} = \gamma^{ij} - n^i n^j$ and we impose γ^{ij} is inverse of γ_{ij}. To obtain $g^{\mu\nu}$ we only need to know g^{tt} and g^{ti} from Eq. (2.25). Substitute $\mu = i$ and $\rho = k$.

$$g_{it}g^{tk} + \gamma_{ij}g^{jk} = \delta^k{}_i \tag{2.26}$$

$$g_{it}g^{tk} + \gamma_{ij}(\gamma^{jk} - n^j n^k) = \delta^k{}_i \tag{2.27}$$

$$\beta_i g^{tk} - \gamma_{ij}\frac{\beta^j\beta^k}{\alpha^2} = 0 \tag{2.28}$$

$$\therefore\ g^{ti} = \frac{\beta^i}{\alpha^2} \tag{2.29}$$

And substitute $\mu = t$ and $\rho = t$.

$$g_{tt}g^{tt} + g_{ti}g^{it} = 1 \tag{2.30}$$

$$g^{tt} = \frac{1 - g_{ti}g^{it}}{g_{tt}} = \frac{1}{\alpha^2}\frac{(\alpha^2 - \beta_i\beta^i)}{(-\alpha^2 + \beta_i\beta^i)} = -\frac{1}{\alpha^2} \tag{2.31}$$

$$\therefore\ g^{\mu\nu} = \begin{pmatrix} -\frac{1}{\alpha^2} & \frac{\beta^j}{\alpha^2} \\ \frac{\beta^i}{\alpha^2} & \gamma^{ij} - \frac{\beta^i\beta^j}{\alpha^2} \end{pmatrix} \tag{2.32}$$

Let us use the ***projection operator*** $\perp$ from York [11] . For a dual vector V_a, a vector V^a and a tensor T_{ab}, these projections are defined by

$$\begin{aligned}\perp V_a \equiv \gamma^b{}_a V_b &= (\delta^b{}_a + n_a n^b)V_b\,, \\ \perp V^a \equiv \gamma^a{}_b V^b &= (\delta^a{}_b + n^a n_b)V^b\,, \end{aligned} \tag{2.33}$$

$$\perp T_{ab} \equiv \gamma^c{}_a\gamma^d{}_b T_{cd}\,. \tag{2.34}$$

Therefore to obtain a projected tensor of any type we contract all indices of it with $\gamma^a{}_b$'s,

$$\perp T^{ab\cdots}_{cd\cdots} \equiv \gamma^a{}_p\gamma^b{}_q\cdots\gamma^r{}_c\gamma^s{}_d\cdots T^{pq\cdots}_{rs\cdots}\,. \tag{2.35}$$

Any projected tensor is orthogonal to n^a or n_a, because

$$\gamma^a{}_b n^b = n^a - n^a = 0\,, \tag{2.36}$$

$$\gamma^a{}_b n_a = n_b - n_b = 0\,. \tag{2.37}$$

So we could call projected tensors are *spatial*.

2.1.2. Normal vector

The gradient of the time function t, $\nabla_a t = (dt)_a$[2] is normal to Σ.

$$\perp \nabla_\mu t = \nabla_\mu t + n_\mu n^\nu \nabla_\nu t = 0 \tag{2.38}$$

Because the direction which is normal to Σ is unique, n_a should be proportional to $\nabla_a t$.

One could start to define a normal vector from the fact that for every vector field v^a tangent to Σ a closed 1-form $(dt)_a$ satisfies $(dt)_a(v^a) = 0$. Therefore $g^{ab}(dt)_b = g^{ab}\nabla_b t$ is a normal vector field to Σ, and choosing appropriate sign for direction of future and coefficient, we can define the unit normal vector n^a.

Anyway, n_a is related to $\nabla_a t$,

$$n_a = -\alpha \nabla_a t \tag{2.39}$$

Using this we obtain a useful property of n_a,

$$\begin{aligned} n_{[a}\nabla_b n_{c]} &= \alpha(\nabla_{[a}t)\nabla_b(\alpha\nabla_{c]}t) \\ &= \alpha(\nabla_{[a}t)(\nabla_b\alpha)\nabla_{c]}t + \alpha^2(\nabla_{[a}t)\nabla_b\nabla_{c]}t = 0\,. \end{aligned} \tag{2.40}$$

The last equality holds because a, c and b, c are symmetric inside the totally antisymmetric bracket.

2.1.3. Spatial covariant derivative

The ***spatial covariant derivative*** is defined by the projection of covariant derivative. Using the spatial covariant derivative operator, D_a, the spatial covariant derivative of a scalar ϕ and a dual spatial vector X_a, i.e., $n^a X_a = 0$, are

$$D_a\phi \equiv \perp \nabla_a\phi = (\delta^b{}_a + n_a n^b)\nabla_b\phi = \nabla_a\phi + n_a n^b \nabla_b\phi \tag{2.41}$$

$$\begin{aligned} D_a X_b \equiv \perp \nabla_a X_b &= (\delta^c{}_a + n_a n^c)(\delta^d{}_b + n_b n^d)\nabla_c X_d \\ &= \nabla_a X_b + n_a n^c \nabla_c X_b - n_b(X^d\nabla_a n_d + n_a n^c X^d \nabla_c n_d) \\ &= \nabla_a X_b + n_a n^c \nabla_c X_b + K_{ac}X^c n_b \end{aligned} \tag{2.42}$$

[2] $(\partial_t)^a\nabla_a t = 1 = (\partial_t)^a(dt)_a$

where we use the fact, $n^d \nabla_c X_d = -X^d \nabla_c n_d$ and K_{ab} is the extrinsic curvature

$$K_{ab} = -\nabla_a n_b - n_a n^c \nabla_c n_b = - \perp \nabla_a n_b \ . \tag{2.43}$$

The spatial covariant derivative of any dual vector field, $V_a = X_a - n_a n^b V_b$, where $X_a = \perp V_a = (\delta^b{}_a + n_a n^b) V_b$, is then

$$\begin{aligned}
D_a V_b &= \perp \nabla_a V_b = (\delta^c{}_a + n_a n^c)(\delta^d{}_b + n_b n^d) \nabla_c V_d \\
&= \nabla_a V_b + n_a n^c \nabla_c V_b + n_b n^d \nabla_a V_d + n_a n_b n^c n^d \nabla_c V_d \\
&= \nabla_a V_b + n_a n^c \nabla_c V_b + n_b \nabla_a (n^d V_d) - n_b V^d \nabla_a n_d + n_a n_b n^c \nabla_c (n^d V_d) - n_a n_b n^c V^d \nabla_c n_d \\
&= \nabla_a V_b + n_b \nabla_a (n^d V_d) + n_b V^d (-\nabla_a n_d - n_a n^c \nabla_c n_d) + n_a n^c (\nabla_c V_b + n_b \nabla_c (n^d V_d)) \\
&= \nabla_a X_b - (\nabla_a n_b) n^d V_d + n_b V^d K_{ad} + n_a n^c (\nabla_c X_b - (\nabla_c n_b) n^d V_d) \\
&= \nabla_a X_b + n_a n^c \nabla_c X_b + K_{ac} X^c n_b + \boxed{K_{ab} n^c V_c}
\end{aligned} \tag{2.44}$$

where we use the facts

$$\begin{aligned}
\nabla_a V_b + n_b \nabla_a (n^c V_c) &= \nabla_a (X_b - n_b n^c V_c) + n_b \nabla_a (n^c V_c) \\
&= \nabla_a X_b - (\nabla_a n_b) n^c V_c
\end{aligned} \tag{2.45}$$

between 4th and 5th line and

$$K_{ac} V^c n_b = K_{ac} X^c n_b \qquad \because n^c K_{ac} = 0 \tag{2.46}$$

between 5th and last line.

For a given metric there exists a unique compatible derivative operator. The compatible metric of D_a is γ_{ab},

$$D_a \gamma_{bc} = \perp \nabla_a (n_b n_c) = \perp (n_b \nabla_a n_c + n_c \nabla_a n_b) = 0 \, . \tag{2.47}$$

We already assume the metric g_{ab} is compatible with ∇_a, $\nabla_a g_{bc} = 0$.

2.1.4. Extrinsic curvature

The ***extrinsic curvature tensor***, K_{ab} is defined by the Lie derivative of 3-metric along the unit normal vector field n^a,

$$K_{ab} = -\frac{1}{2} \mathcal{L}_n \gamma_{ab} \, . \tag{2.48}$$

We can interpret the extrinsic curvature tensor as a "*velocity*" of the spatial 3-metric with respect to n^a.

The extrinsic curvature also can be defined as the spatial derivative of n_a.

$\mathcal{L}_n\gamma_{ab}$ can be written as

$$\begin{aligned}\mathcal{L}_n\gamma_{ab} &= n^c\nabla_c\gamma_{ab} + \gamma_{ac}\nabla_b n^c + \gamma_{bc}\nabla_a n^c \\ &= n^c\nabla_c(n_a n_b) + (g_{ac} + n_a n_c)\nabla_b n^c + (g_{bc} + n_b n_c)\nabla_a n^c \\ &= 2(\nabla_{(a}n_{b)} + n_{(a}n^c\nabla_{|c|}n_{b)})\,. \end{aligned} \tag{2.49}$$

However the symmetric brackets aren't needed because $\perp \nabla_{[a}n_{b]} = 0$. Let's investigate this in detail.

The spatial derivative of n_a is

$$D_a n_b \equiv \perp \nabla_a n_b = \nabla_a n_b + n_a n^c \nabla_c n_b\,. \tag{2.50}$$

Therefore

$$\perp \nabla_{[a}n_{b]} = \nabla_{[a}n_{b]} + n_{[a}n^c\nabla_{|c|}n_{b]}\,. \tag{2.51}$$

Using $n^a\nabla_b n_a = 0$,

$$\begin{aligned}2n^c n_{[a}\nabla_{|c|}n_{b]} &= n^c(n_a\nabla_c n_b - n_b\nabla_c n_a) \\ &= n^c(n_a\nabla_c n_b + n_c\nabla_b n_a + n_b\nabla_a n_c - n_b\nabla_c n_a - n_a\nabla_b n_c - n_b\nabla_c n_a) \\ &\quad + \nabla_b n_a - \nabla_a n_b \\ &= 6n^c n_{[a}\nabla_c n_{b]} - 2\nabla_{[a}n_{b]}\,. \end{aligned} \tag{2.52}$$

Using the property Eq. (2.40) we conclude as follows,

$$\nabla_{[a}n_{b]} = -n_{[a}n^c\nabla_{|c|}n_{b]} \quad \Rightarrow \quad \perp \nabla_{[a}n_{b]} = 0\,. \tag{2.53}$$

Therefore

$$D_a n_b \equiv \perp \nabla_a n_b = \perp \nabla_{(a}n_{b)} = \frac{1}{2}\mathcal{L}_n\gamma_{ab}\,, \tag{2.54}$$

and

$$\begin{aligned}K_{ab} &= -\frac{1}{2}\mathcal{L}_n\gamma_{ab} \\ &= -\perp \nabla_{(a}n_{b)} = -\perp \nabla_a n_b = -\nabla_a n_b - n_a n^c\nabla_c n_b\,. \end{aligned} \tag{2.55}$$

The trace of K_{ab} is

$$K \equiv g^{ab}K_{ab} = \nabla_a n^a\,. \tag{2.56}$$

2.1.5. Einstein tensor decomposition

The Einstein equation in tensor form is,

$$G_{\mu\nu} = 8\pi T_{\mu\nu}\,. \tag{2.57}$$

$G_{\mu\nu}$ is the Einstein tensor which is composed of Ricci tensor and Ricci scalar and contains first and second derivatives of the spacetime metric $g_{\mu\nu}$. The quantity $T_{\mu\nu}$ is called the energy-momentum tensor which describes matter.

2.1.5.1. Gauss-Codazzi relations and Ricci equations

The projected 4-dimensional Riemann tensor is related to the 3-dimensional Riemann tensor and the extrinsic curvature as following relations.

The ***Gauss relation***

$$\perp R_{abcd} = {}^{(3)}R_{abcd} + K_{ac}K_{bd} - K_{ad}K_{bc}\,, \tag{2.58}$$

the ***Codazzi-Mainardi relation***

$$\perp R_{abcd}\, n^d = D_b K_{ac} - D_a K_{bc}\,, \tag{2.59}$$

and the ***Ricci equation***

$$\perp R_{abcd}\, n^b n^d = \mathcal{L}_n K_{ac} + K_{ab}K^b_c + \frac{1}{\alpha} D_a D_b \alpha\,. \tag{2.60}$$

2.1.5.2. Ricci tensor decomposition

Contract the projected 4-dimensional Riemann tensor, we can decompose the projected Ricci tensor as

$$g^{cd} \perp R_{acbd} = \perp R_{ab} + \perp R_{acbd}\, n^c n^d \tag{2.61}$$

$$\Rightarrow \quad \perp R_{ab} = -\mathcal{L}_n K_{ab} - 2K_{ac}K^c_b - \frac{1}{\alpha} D_a D_b \alpha + {}^{(3)}R_{ab} + K_{ab}K\,, \tag{2.62}$$

and the Ricci scalar as

$$\perp R_{abcd}\, n^b n^d = R_{abcd}\, n^b n^d \tag{2.63}$$

$$\begin{aligned} g^{ab} \perp R_{ab} &= R + R_{ab}\, n^a n^b \\ &= g^{ab} g^{cd} \perp R_{acbd} - g^{ab} R_{acbd}\, n^c n^d \end{aligned} \tag{2.64}$$

$$\Rightarrow \quad R = g^{ab} g^{cd} \perp R_{acbd} - 2R_{ab}\, n^a n^b \tag{2.65}$$

Therefore, one can decompose Ricci tensor components as follows,

$$R_{\mu\nu}\, n^\mu n^\nu = \frac{1}{2}\left({}^{(3)}R + K^2 - K_{\rho\sigma}K^{\rho\sigma} - R\right) \tag{2.66}$$

$$\perp R_{\mu\nu}\, n^\nu = D_\mu K - D^\nu K_{\mu\nu} \tag{2.67}$$

$$\perp R_{\mu\nu} = -\mathcal{L}_n K_{\mu\nu} - 2K_{\mu\rho}K^{\rho}_{\nu} - \frac{1}{\alpha}D_\mu D_\nu \alpha + {}^{(3)}R_{\mu\nu} + K_{\mu\nu}K \tag{2.68}$$

2.1.5.3. Einstein tensor decomposition

The Einstein tensor is decomposed as

$$\bullet\ G_{ab}\, n^a n^b = \frac{1}{2} g^{ab} g^{cd} \perp R_{acbd} = \frac{1}{2}\left({}^{(3)}R + K^2 - K_{cd}K^{cd}\right), \tag{2.69}$$

$$\bullet\ \perp G_{ab}\, n^b = \perp R_{ab}\, n^b = \gamma^{cd} \perp R_{cadb}\, n^b = D_a K - D^b K_{ab}\,, \tag{2.70}$$

$$\begin{aligned}\bullet\ \perp G_{ab} &= \perp R_{ab} - \frac{1}{2}\gamma_{ab}R \\ &= -\mathcal{L}_n K_{ab} - 2K_{ac}K^{c}_{b} - \frac{1}{\alpha}D_a D_b \alpha + {}^{(3)}R_{ab} + K_{ab}K \\ &\left[-\frac{1}{2}\gamma_{ab}\left({}^{(3)}R + K^2 - K_{cd}K^{cd}\right) + \gamma_{ab}\left(\gamma^{cd}\mathcal{L}_n K_{cd} + K_{cd}K^{cd} + \frac{1}{\alpha}D_c D^c \alpha\right)\right].\end{aligned}$$

2.1.6. Energy-momentum tensor and hydrodynamic variables

We are going to describe matter as a perfect fluid. Its energy-momentum tensor is

$$T^{\mu\nu} = \rho_0 h u^\mu u^\nu + P g^{\mu\nu}\,. \tag{2.71}$$

where ρ_0 is the baryon rest-mass density, P is the pressure, u^μ is the fluid 4-velocity and h is the specific enthalpy,

$$h = 1 + \epsilon + \frac{P}{\rho_0}\,, \tag{2.72}$$

with the specific internal energy ϵ.

Here ρ_0, P and ϵ are related to the quantities measured by an observer who is following the fluid.[3] However, because we treat spacetime as a foliation of 3-dimensional spacelike hypersurfaces and calculate geometric and hydrodynamic variables at each slice, we need to consider the viewpoint of the observer whose 4-velocity is normal to the 3-dimensional hypersurface, i.e., n^μ. This observer is called the Eulerian observer.

The fluid 4-velocity u^μ can be decomposed into tangential and normal to the 3-dimensional spacelike hypersurfaces. Doing this there is an important scalar

[3] That observer is also called the comoving or Lagrangian observer. In the Lagrangian scheme those hydrodynamic variables are used in formulas directly.

quantity, namely the generalized Lorentz factor[4],

$$W = -n_\mu u^\mu \,. \tag{2.73}$$

Then u^μ can be decomposed by

$$u^\mu \equiv W(n^\mu + v^\mu) \tag{2.74}$$

where v^μ is the projected spatial velocity (satisfying $n_\mu v^\mu = 0$).

Now, we are ready to consider the projected quantities of the energy momentum tensor, i.e.,

$$E \equiv T_{\mu\nu} n^\mu n^\nu \,, \tag{2.75}$$

$$S_\mu \equiv - \perp T_{\mu\nu} n^\nu \,, \tag{2.76}$$

and

$$S_{\mu\nu} \equiv \perp T_{\mu\nu} \,. \tag{2.77}$$

These quantities can be expressed in terms of ρ_0, P, ϵ [5] (hence h) and the Lorentz factor W.

$$E = \rho_0 h W^2 - P \tag{2.78}$$

$$S_i = \rho_0 h W^2 v_i \tag{2.79}$$

$$S_{ij} = \rho_0 h W^2 v_i v_j + \gamma_{ij} P \tag{2.80}$$

Let's consider the trace of the stress tensor, $S_{\mu\nu}$,

$$S \equiv g^{\mu\nu} S_{\mu\nu} = g^{\mu\nu} \perp T_{\mu\nu} = \perp \gamma^{\mu\nu} T_{\mu\nu} = \gamma^{\mu\nu} \perp T_{\mu\nu} = \gamma^{\mu\nu} S_{\mu\nu} \tag{2.81}$$

where $\gamma^{\mu\nu} \equiv g^{\mu\nu} + n^\mu n^\nu$ is the projection tensor and we used the following property,

$$\gamma^{\mu\nu} = \perp g^{\mu\nu} \,. \tag{2.82}$$

Because $-1 = n^\mu n_\mu = n^0 n_0$ and $n^\mu = g^{\mu\nu} n_\nu = g^{\mu 0} n_0$,

$$\gamma^{\mu 0} = g^{\mu 0} + n^\mu n^0 = 0 \,. \tag{2.83}$$

Therefore

$$S = g^{\mu\nu} S_{\mu\nu} = \gamma^{\mu\nu} S_{\mu\nu} = \gamma^{ij} S_{ij} \,. \tag{2.84}$$

[4] In special relativity, a 4-velocity u^μ in a reference frame is

$$u^\mu = (\gamma, \gamma \boldsymbol{v}) \,,$$

where γ is the Lorentz factor,

$$\gamma = \frac{1}{\sqrt{1 - |\boldsymbol{v}|^2}} \,.$$

[5] Let's call these variables are primitive variables, because we are going to consider hydrodynamic variables which are transformed from these variables.

2.1.7. Einstein equation decomposition

2.1.7.1. Constraint equations

- The Hamiltonian constraint:

$$G_{ab}\, n^a n^b \;=\; 8\pi T_{ab}\, n^a n^b \tag{2.85}$$

With the projected Einstein tensor

$$G_{ab}\, n^a n^b \;=\; \frac{1}{2} g^{ab} g^{cd} \perp R_{acbd} \;=\; \frac{1}{2}\left({}^{(3)}R + K^2 - K_{cd}K^{cd}\right) \tag{2.86}$$

and the matter energy density

$$T_{ab}\, n^a n^b \;\equiv\; E \tag{2.87}$$

$$\rightarrow\; {}^{(3)}R + K^2 - K_{cd}K^{cd} \;=\; 16\pi E\,. \tag{2.88}$$

- The momentum constraints:

$$\perp G_{ab}\, n^b \;=\; 8\pi \perp T_{ab}\, n^b \tag{2.89}$$

With the projected Einstein tensor

$$\perp G_{ab}\, n^b \;=\perp R_{ab}\, n^b \;=\; \gamma^{cd} \perp R_{cadb}\, n^b \;=\; D_a K - D^b K_{ab} \tag{2.90}$$

and the matter momentum density

$$-\perp T_{ab}\, n^b \;\equiv\; p_a \tag{2.91}$$

$$\rightarrow D_a K - D^b K_{ab} \;=\; -8\pi p_a\,. \tag{2.92}$$

2.1.7.2. Evolution equations

$$\perp G_{ab} \;=\; 8\pi \perp T_{ab} \tag{2.93}$$

With the projected Einstein tensor

$$\begin{aligned}
\perp G_{ab} \;&=\perp R_{ab} - \frac{1}{2}\gamma_{ab} R \\
&= -\mathcal{L}_n K_{ab} - 2K_{ac}K^c_b - \frac{1}{\alpha} D_a D_b \alpha + {}^{(3)}R_{ab} + K_{ab}K \\
&\left[-\frac{1}{2}\gamma_{ab}\left({}^{(3)}R + K^2 - K_{cd}K^{cd}\right) + \gamma_{ab}\left(\gamma^{cd}\mathcal{L}_n K_{cd} + K_{cd}K^{cd} + \frac{1}{\alpha} D_c D^c \alpha\right)\right]
\end{aligned}$$

and the matter stress tensor

$$\perp T_{ab} \;\equiv\; S_{ab} \tag{2.94}$$

$$T \equiv g^{ab}T_{ab} = g^{ab} \perp T_{ab} - T_{ab}\, n^a n^b = (S - E) \tag{2.95}$$

where 4D Einstein theory,

$$R_{ab} = G_{ab} - \frac{1}{2} g_{ab} G \tag{2.96}$$

$$-R = G = 8\pi T \tag{2.97}$$

Then the evolution equations of the extrinsic curvature is

$$\begin{aligned}\partial_t K_{ij} &= \mathcal{L}_\beta K_{ij} - D_i D_j \alpha \\ &\quad + \alpha \left\{ {}^{(3)}R_{ij} - 2K_{ik}K^k{}_j + K_{ij}K - 8\pi \left[S_{ij} - \frac{1}{2}\gamma_{ij}(S - E) \right] \right\} .\end{aligned}$$

And the evolution equations of the 3-metric is (the definition of extrinsic curvature)

$$\partial_t \gamma_{ij} = \mathcal{L}_\beta \gamma_{ij} - 2\alpha K_{ij} \,. \tag{2.98}$$

2.1.8. 3+1 decomposition of spherically symmetric metric

Using 3+1 decomposition scheme and assuming spherical symmetry, $g_{\mu\nu}$ can be described in the form of the infinitesimal squared distance by

$$ds^2 = -\left(\alpha^2 - \psi^4\beta^2\right) dt^2 + 2\psi^4 \beta dt dr + \psi^4 \left[dr^2 + r^2(d\theta^2 + \sin^2\theta d\phi^2) \right] \tag{2.99}$$

where $\alpha(t, r)$, $\beta(t, r)$ and $\psi(t, r)$ are the lapse, shift and conformal factor respectively. Here we adopt conformal decomposition of 3-metric. It seems we have 3 independent degrees of freedom while there should be no degree of freedom in spherical symmetry. Later two of them will be fixed by the constraint equations of decomposed Einstein equations. Only one of them is left as a gauge freedom.

The general form of the spherically symmetric metric line element is

$$ds^2 = -A dt^2 + 2B dt d\mu + C d\mu^2 + R^2(d\theta^2 + \sin^2\theta d\phi^2) \tag{2.100}$$

where the metric components A, B, C and R are functions of μ and t. Without breaking spherical symmetry, one have freedom to choose the coordinates, i.e., the metric conserve its spherical symmetry under following gauge transformations,

$$t \to T(t, \mu) \,, \quad \mu \to \Upsilon(t, \mu) \,. \tag{2.101}$$

Let's consider the μ coordinate transformation only,

$$\mu \to r(t, \mu) \,, \tag{2.102}$$

and choose the coordinate function r such that the coefficient of dr^2 becomes

R'^2, where $R^2 = r^2 R'^2$. Then the metric form will be changed to

$$ds^2 = -A'dt^2 + 2B'dtdr + R'^2dr^2 + R'^2r^2(d\theta^2 + \sin^2\theta d\phi^2)\,. \tag{2.103}$$

Therefore one can write down a spherically symmetric, isotropic $3+1$ form metric[6] is

$$ds^2 = -\left(\alpha^2 - \psi^4\beta^2\right)dt^2 + 2\psi^4\beta dtdr + \psi^4\left[dr^2 + r^2(d\theta^2 + \sin^2\theta d\phi^2)\right]\,, \tag{2.104}$$

or

$$ds^2 = -\alpha^2 dt^2 + \psi^4\left[(dr + \beta dt)^2 + r^2(d\theta^2 + \sin^2\theta d\phi^2)\right]\,, \tag{2.105}$$

where $\alpha(t,r)$, $\beta(t,r)$ and $\psi(t,r)$ are the lapse, shift and conformal factor respectively and in order to preserve spherical symmetry, all of these are function of r and t. We also the metric $g_{\mu\nu}$ in matrix form on these $\{t, r, \theta, \phi\}$ coordinates basis,

$$g_{\mu\nu} = \begin{pmatrix} -(\alpha^2 - \psi^4\beta^2) & \psi^4\beta & 0 & 0 \\ \psi^4\beta & \psi^4 & 0 & 0 \\ 0 & 0 & \psi^4 r^2 & 0 \\ 0 & 0 & 0 & \psi^4 r^2\sin^2\theta \end{pmatrix}\,. \tag{2.106}$$

Its inverse, $g^{\mu\nu}$, can be calculated from the definition, $g^{\mu\rho}g_{\rho\nu} = \delta^\mu_\nu$.

$$g^{\mu\nu} = \begin{pmatrix} -\frac{1}{\alpha^2} & \frac{\beta}{\alpha^2} & 0 & 0 \\ \frac{\beta}{\alpha^2} & \frac{1}{\psi^4} - \frac{\beta^2}{\alpha^2} & 0 & 0 \\ 0 & 0 & \frac{1}{\psi^4 r^2} & 0 \\ 0 & 0 & 0 & \frac{1}{\psi^4 r^2\sin^2\theta} \end{pmatrix} \tag{2.107}$$

Here the 3-metric $\gamma_{ij} = g_{ij}$ is conformally flat, i.e., $\gamma_{ij} = \psi^4 f_{ij}$ where f_{ij} is a 3 dimensional flat metric.

The determinant of $g_{\mu\nu}$ is

$$\begin{aligned} g \equiv det\ g_{\mu\nu} &= -(\alpha^2 - \psi^4\beta^2)\psi^{12}r^4\sin^2\theta - \psi^4\beta\psi^{12}\beta r^4\sin^2\theta \\ &= -\alpha^2\psi^{12}r^4\sin^2\theta\,, \end{aligned} \tag{2.108}$$

and the determinant of γ_{ij} is $\gamma \equiv det\ \gamma_{ij} = \psi^{12}r^4\sin^2\theta$. Therefore,

$$\sqrt{-g} = \alpha\sqrt{\gamma} = \alpha\,\psi^6 r^2\sin\theta\,. \tag{2.109}$$

[6] cf. The isotropic Schwarzschild metric is

$$ds^2 = -\frac{\left(1 - \frac{M}{2r}\right)^2}{\left(1 + \frac{M}{2r}\right)^2}dt^2 + \left(1 + \frac{M}{2r}\right)^4\left[dr^2 + r^2(d\theta^2 + \sin^2\theta d\phi^2)\right]\,.$$

Because we have already expressed the spacetime metric in 3+1 form, we can write down the unit normal vector n^μ which is normal to the spacelike slices in terms of the lapse and shift.

n_μ is proportional to the gradient of the time t, $\nabla_\mu t$ which is normal to the 3-dimensional hypersurface. We set the proportionality is the lapse, α, i.e.,

$$n_\mu = -\alpha \nabla_\mu t \,. \tag{2.110}$$

Because $(\partial_t)^\mu \nabla_\mu t = (\partial_t)^\mu (dt)_\mu = 1$ and the orthonormality of coordinate basis vectors and its dual, n_μ has only the time t component,

$$n_\mu (\partial_t)^\mu = -\alpha \,. \tag{2.111}$$

Therefore one can obtain the unit normal vector n^μ using the (inverse) metric, $g^{\mu\nu}$

$$n^\mu = g^{\mu\nu} n_\nu = -\alpha g^{\mu 0} \tag{2.112}$$

The normal vector n^μ is therefore

$$n^\mu = \left(\frac{1}{\alpha}, -\frac{\beta}{\alpha}, 0, 0 \right) \qquad n_\mu = (-\alpha, 0, 0, 0) \tag{2.113}$$

and $n^\mu n_\mu = -1$.

In addition, I'd like to comment on the index of the shift. Dealing with a flat metric one does not need to distinguish upper and lower indices. So I do not write index of the shift in the metric. However the 3-metric has the conformal factor, is not completely flat, we should be careful in calculating any tensorial quantities related to the shift. If one restores index of the shift, then

$$\beta^r = \beta \qquad \beta_r = \psi^4 \beta \,. \tag{2.114}$$

2.1.9. Extrinsic curvature and slicing condition

In order to avoid singularity during the numerical calculation, we are going to impose maximal slicing condition, $K = 0$, which is one of the singularity avoiding gauge conditions.

$$K \equiv \mathrm{tr}(K_{ij}) = K^r{}_r + K^\theta{}_\theta + K^\phi{}_\phi = K^r{}_r + 2K^\theta{}_\theta = 0 \,. \tag{2.115}$$

To fix the gauge, we choose the maximal slicing condition, for which the trace of the extrinsic curvature vanishes ($K = 0$) during evolution ($\partial_t K = 0$). The non-zero components of the extrinsic curvature in spherical symmetry are $K^r{}_r$, $K^\theta{}_\theta$ and $K^\phi{}_\phi$ with

$$K^\theta{}_\theta = K^\phi{}_\phi \,, \qquad K^r{}_r - K^\theta{}_\theta = \frac{r}{\alpha} \left(\frac{\beta}{r} \right)' \,, \tag{2.116}$$

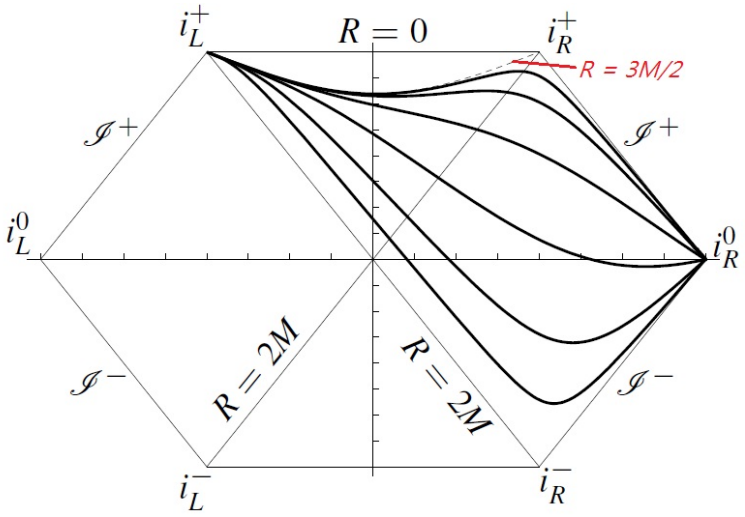

Figure 2.2: Penrose diagram of the maximal slicing [Figure from Ohme (SFB Video Seminar, 2008)]

where $'$ denotes $\frac{\partial}{\partial r}$. The maximal slicing condition, $K = K^r{}_r + K^\theta{}_\theta + K^\phi{}_\phi = 0$, therefore, gives

$$K^r{}_r = \frac{2}{3}\frac{r}{\alpha}\left(\frac{\beta}{r}\right)' . \tag{2.117}$$

This equation fixes one of degrees of freedom with the definition of the extrinsic curvature.

2.1.10. Einstein equation decomposition in spherical symmetry

Let us define the rest-mass density $D \equiv -\rho_0 u^\mu n_\mu$, the momentum density S_i, and $\tau \equiv E - D$, where E is the total energy density. With the generalized Lorentz factor $W = -n_\mu u^\mu$,

$$D = \rho_0 W , \tag{2.118}$$
$$S_i = \rho_0 h W^2 v_i , \tag{2.119}$$
$$E = \rho_0 h W^2 - P . \tag{2.120}$$

Then the spatial 3-velocity v^r is

$$v^r = \frac{v_r}{\psi^4} = \frac{1}{\psi^4}\frac{S_r}{\rho_0 h W^2} = \frac{1}{\psi^4}\frac{S_r}{\tau + D + P} . \tag{2.121}$$

The trace of the stress S_{ij} is

$$S = g^{\mu\nu}S_{\mu\nu} = \gamma^{ij}S_{ij} = \rho_0 h W^2 v^r v_r + 3P = \frac{1}{\psi^4}\frac{S_r^2}{\tau + D + P} + 3P\,. \quad (2.122)$$

The Hamiltonian constraint becomes

$$\psi'' + \frac{2}{r}\psi' + \frac{\psi^5}{12}\left[\frac{1}{\alpha}\left(\beta' - \frac{\beta}{r}\right)\right]^2 + 2\pi\psi^5\left(\tau + D\right) = 0\,, \quad (2.123)$$

and the momentum constraint is given by

$$\beta'' + \left(6\frac{\psi'}{\psi} - \frac{\alpha'}{\alpha} + \frac{2}{r}\right)\left(\beta' - \frac{\beta}{r}\right) - 12\pi\alpha S_r = 0\,. \quad (2.124)$$

Due to the gauge condition, $K_{ij}\partial_t\gamma^{ij} = 0$. Therefore

$$0 = \partial_t K = \partial\left(\gamma^{ij}K_{ij}\right) = \gamma^{ij}\partial_t K_{ij}\,. \quad (2.125)$$

The trace of the evolution equations of the extrinsic curvature gives rise to an equation for α:

$$\alpha'' + 2\alpha'\left(\frac{\psi'}{\psi} + \frac{1}{r}\right) - \frac{2}{3}\frac{\psi^4}{\alpha}\left(\beta' - \frac{\beta}{r}\right)^2 = 4\pi\alpha\left[\psi^4(\tau + D + 3P) + \frac{S_r^2}{\tau + D + P}\right]. \quad (2.126)$$

The definition of the extrinsic curvature with the maximal slicing condition gives a redundant hyperbolic evolution equation for ψ:

$$\dot{\psi} - \beta\left(\frac{\psi}{3r} + \psi'\right) - \frac{\psi\beta'}{6} = 0\,. \quad (2.127)$$

At $r = 0$, we impose the regularity conditions

$$\begin{aligned} \psi'(t,0) &= 0\,, \\ \alpha'(t,0) &= 0\,, \\ \beta(t,0) &= 0\,, \end{aligned} \quad (2.128)$$

and at the outer numerical grid, at some finite radius, we impose the Robin boundary conditions:

$$\begin{aligned} \psi' + (\psi - 1)/r &= 0\,, \\ \alpha' + (\alpha - 1)/r &= 0\,, \\ \beta' + \beta/r &= 0\,. \end{aligned} \quad (2.129)$$

2.2. Hydrodynamic Equations in Conservative Form

2.2.1. Decomposition of hydrodynamic equations

The ***perfect fluids*** are characterized by an isotropic pressure, an energy density and an equation of state. These specific form of the energy-momentum tensor T_{ab} is practically useful to treat the energy-momentum conservation equations which are implied by Einstein equation.

$$\boxed{\nabla_a T^a{}_b = 0} \tag{2.130}$$

2.2.1.1. Thermodynamic quantities

The energy-momentum tensor T_{ab} of a perfect fluid can be written as

$$T_{ab} = (\rho + P)u_a u_b + P g_{ab} \tag{2.131}$$

where u^a is 4-velocity of the fluid and ρ and P are the proper energy density and the proper pressure respectively measured by comoving observer with the fluid. [15]

$$u_a u^a = -1 \tag{2.132}$$

$$T^a{}_b u^b = -\rho u^a \tag{2.133}$$

which tells us a eigenvalue relation, u^a is the timelike eigenvector of $T^a{}_b$ and ρ is the corresponding eigenvalue.

In "*Taub's viewpoint*",

$$\rho = \rho_0(1 + \varepsilon) \tag{2.134}$$

where ρ_0 is the proper material density or the ***rest-mass energy density***, and ε is the ***proper specific internal energy***. The word, *specific* means a quantity divided by ρ_0. $\varepsilon = \varepsilon(\rho_0, P)$ depend on the internal structure of the fluid.

Let us introduce the ***specific enthalpy***,

$$h \equiv 1 + \varepsilon + \frac{P}{\rho_0}\,. \tag{2.135}$$

Recall the thermodynamic enthalpy is defined as $H \equiv E + PV$.

$$\rho_0 h = \rho + P \tag{2.136}$$

The definition of the ***proper temperature*** T of the fluid and its ***specific proper entropy*** $\mathcal{S}$,

$$T d\mathcal{S} \equiv d\varepsilon + P d\left(\frac{1}{\rho_0}\right) \tag{2.137}$$

Using h,

$$Td\mathcal{S} = dh - \frac{dP}{\rho_0} \tag{2.138}$$

2.2.1.2. Energy-momentum conservation equations

The energy-momentum conservation equation,

$$\nabla_a T^a{}_b = 0\,, \tag{2.139}$$

can be written for a perfect fluid model as

$$\nabla_a[(\rho + P)u^a u_b] + \nabla_a(P g^a{}_b) = 0 \tag{2.140}$$

$$\hookrightarrow u^a u_b \nabla_a(\rho + P) + (\rho + P)u_b \nabla_a u^a + (\rho + P)u^a \nabla_a u_b + \nabla_b P = 0 \tag{2.141}$$

2.2.1.3. Decomposition with u^a

1. u^a parallel part of the energy-momentum conservation equation:

$$n^b \nabla_a T^a{}_b = 0 \tag{2.142}$$

$$\hookrightarrow -u^a \nabla_a(\rho + P) - (\rho + P)\nabla_a u^a + u^b \nabla_b P = 0 \tag{2.143}$$

$$\hookrightarrow \nabla_a[(\rho + P)u^a] = u^a \nabla_a P \qquad : \text{energy equation} \tag{2.144}$$

2. The rest part of the energy-momentum conservation equation:
Substitute above result into Eq. (2.141), we get

$$(\rho + P)u^b \nabla_b u^a + (g^{ab} + u^a u^b)\nabla_b P = 0 \qquad : \text{Euler's equations} \tag{2.145}$$

- Energy equation:

$$\nabla_a(\rho_0 h u^a) = u^a \nabla_a P \tag{2.146}$$

$$\hookrightarrow \rho_0 u^a \nabla_a h + h\nabla_a(\rho_0 u^a) = u^a \nabla_a P \tag{2.147}$$

$$\hookrightarrow h\nabla_a(\rho_0 u^a) = -\rho_0 u^a \left(\nabla_a h - \frac{\nabla_a P}{\rho_0}\right) = -\rho_0 T u^a \nabla_a \mathcal{S} \tag{2.148}$$

where we use the relation

$$Td\mathcal{S} = dh - \frac{dP}{\rho_0} \tag{2.149}$$

$$\hookrightarrow h\nabla_a(\rho_0 u^a) + \rho_0 T u^a \nabla_a \mathcal{S} = 0 \tag{2.150}$$

Because h, ρ_0 and T are all positive,

$$\nabla_a(\rho_0 u^a) = 0 \quad \Leftrightarrow \quad u^a \nabla_a \mathcal{S} = 0\,. \tag{2.151}$$

That is, for a perfect fluid the material density is conserved(left) if and only if

the fluid is locally adiabatic(right).

- Euler's equations:

$$hu^b\nabla_b u^a \;=\; -(g^{ab}+u^a u^b)\frac{\nabla_b P}{\rho_0} \tag{2.152}$$

$$\hookrightarrow hu^b\nabla_b u^a \;=\; -(g^{ab}+u^a u^b)\left(\nabla_b h - T\nabla_b \mathcal{S}\right) \tag{2.153}$$

$$\hookrightarrow u^b\nabla_b u^a \;=\; -(g^{ab}+u^a u^b)\left(\frac{\nabla_b h}{h} - \frac{T}{h}\nabla_b \mathcal{S}\right) \tag{2.154}$$

For an ***isentropic fluid***, i.e., $d\mathcal{S} = 0$,

$$u^b\nabla_b u^a + (g^{ab}+u^a u^b)\frac{\nabla_b h}{h} \;=\; 0\,. \tag{2.155}$$

2.2.1.4. Decomposition with n^a

There could be another decomposition of the energy-momentum conservation equation. Using n^a instead of u^a, Shibata [16] decomposed the equation as follows.

- $\gamma^\nu{}_\rho\nabla_\mu T^\mu{}_\nu \;=\; 0$

$$\begin{aligned}\gamma^\nu{}_\rho\nabla_\mu T^\mu{}_\nu \;=\; &\partial_\mu\left(\sqrt{-g}T^\mu{}_\rho\right) - \frac{1}{2}\sqrt{-g}T^{\mu\nu}\partial_\rho g_{\mu\nu} \\ &+ n_\rho\left\{n^\nu\partial_\mu\left(\sqrt{-g}T^\mu{}_\nu\right) - \frac{1}{2}\sqrt{-g}T^{\mu\sigma}n^\nu\partial_\nu g_{\mu\sigma}\right\} \;=\; 0\end{aligned} \tag{2.156}$$

- $n^\nu\nabla_\mu T^\mu{}_\nu \;=\; 0$

$$\sqrt{-g}n^\nu\nabla_\mu T^\mu{}_\nu \;=\; \partial_\mu\left(\sqrt{-g}T^\mu{}_\nu n^\nu\right) - \sqrt{-g}T^{\mu\nu}\nabla_\mu n_\nu \;=\; 0 \tag{2.157}$$

However,

$$\partial_\mu\left(\sqrt{-g}T^\mu{}_\nu n^\nu\right) - \sqrt{-g}T^{\mu\nu}\nabla_\mu n_\nu \;=\; n^\nu\partial_\mu\left(\sqrt{-g}T^\mu{}_\nu\right) - \frac{1}{2}\sqrt{-g}T^{\mu\sigma}n^\nu\partial_\nu g_{\mu\sigma} \tag{2.158}$$

and

$$\sqrt{-g}\nabla_\mu T^\mu{}_\nu \;=\; \partial_\mu\left(\sqrt{-g}T^\mu{}_\nu\right) - \frac{1}{2}\sqrt{-g}T^{\mu\rho}\partial_\nu g_{\mu\rho}\,. \tag{2.159}$$

So $\gamma^\nu{}_\rho\nabla_\mu T^\mu{}_\nu \;=\; 0$ is reduced to

$$\partial_\mu\left(\sqrt{-g}T^\mu{}_\rho\right) - \frac{1}{2}\sqrt{-g}T^{\mu\nu}\partial_\rho g_{\mu\nu} \;=\; 0\,, \tag{2.160}$$

This is nothing but the original conservation equation, $\sqrt{-g}\nabla_\mu T^\mu{}_\rho \;=\; 0$.

2.2.2. Hydrodynamic equations in spherical symmetry

As for the evolution equations, we use the baryonic rest-mass density and the energy-momentum conservation equations for the hydrodynamic variables. In order to use the HRSC scheme, one should recast those equations into conservative form. If the conservative variables defined above are used, the rest-mass density conservation equation $\nabla_\mu(\rho_0 u^\mu) = 0$ becomes

$$\partial_t \left(r^2 \tilde{D}\right) + \partial_r \left[\alpha r^2 \tilde{D} \left(v^r - \frac{\beta}{\alpha}\right)\right] \;=\; 0\,, \tag{2.161}$$

and the energy-momentum conservation equation $\nabla_\mu T^{\mu\nu} = 0$ can be decomposed into

$n^\nu(\nabla_\mu T^\mu{}_\nu) = 0$

$$\Rightarrow \quad \partial_t \left(r^2 \tilde{\tau}\right) + \partial_r \left[\alpha r^2 \left\{\tilde{\tau}\left(v^r - \frac{\beta}{\alpha}\right) + \tilde{P} v^r\right\}\right]$$

$$= \alpha r^2 \left\{-\frac{\alpha'}{\alpha}\frac{\tilde{S}_r}{\psi^4} + \frac{2}{3}\frac{r}{\alpha}\left(\frac{\beta}{r}\right)' \frac{\tilde{S}_r{}^2}{\psi^4(\tilde{\tau} + \tilde{D} + \tilde{P})}\right\}, \tag{2.162}$$

$\gamma^\nu{}_r(\nabla_\mu T^\mu{}_\nu) = 0$

$$\Rightarrow \quad \partial_t \left(r^2 \tilde{S}_r\right) + \partial_r \left[\alpha r^2 \left\{\tilde{S}_r \left(v^r - \frac{\beta}{\alpha}\right) + \tilde{P}\right\}\right]$$

$$= \alpha r^2 \left\{2\frac{\psi'}{\psi}\left(\frac{\tilde{S}_r{}^2}{\psi^4(\tilde{\tau} + \tilde{D} + \tilde{P})} + 3\tilde{P}\right) + \frac{\beta'}{\alpha}\tilde{S}_r - \frac{\alpha'}{\alpha}(\tilde{\tau} + \tilde{D}) + \frac{2}{r}\tilde{P}\right\}, \tag{2.163}$$

where $\tilde{\tau} = \psi^6\tau$, $\tilde{D} = \psi^6 D$, $\tilde{S}_r = \psi^6 S_r$, and $\tilde{P} = \psi^6 P$.

The above equations can be written in the following conservative form:

$$\partial_t(r^2\mathbf{q}) + \partial_r(\alpha r^2 \mathbf{F}) \;=\; \alpha r^2 \mathbf{S}\,, \tag{2.164}$$

with the dynamical variables

$$\mathbf{q} \;=\; \begin{bmatrix} \tilde{D} \\ \tilde{S}_r \\ \tilde{\tau} \end{bmatrix}, \tag{2.165}$$

fluxes

$$\mathbf{F} \;=\; \begin{bmatrix} \tilde{D}\left(v^r - \frac{\beta}{\alpha}\right) \\ \tilde{S}_r\left(v^r - \frac{\beta}{\alpha}\right) + \tilde{P} \\ \tilde{\tau}\left(v^r - \frac{\beta}{\alpha}\right) + \tilde{P} v^r \end{bmatrix}, \tag{2.166}$$

and sources

$$\mathbf{S} = \begin{bmatrix} 0 \\ 2\frac{\psi'}{\psi}\left(\frac{\tilde{S_r}^2}{\psi^4(\tilde{\tau}+\tilde{D}+\tilde{P})} + 3\tilde{P}\right) + \frac{\beta'}{\alpha}\tilde{S}_r - \frac{\alpha'}{\alpha}(\tilde{\tau}+\tilde{D}) + \frac{2}{r}\tilde{P} \\ -\frac{\alpha'}{\alpha}\frac{\tilde{S}_r}{\psi^4} + \frac{2}{3}\frac{r}{\alpha}\left(\frac{\beta}{r}\right)'\frac{\tilde{S_r}^2}{\psi^4(\tilde{\tau}+\tilde{D}+\tilde{P})} \end{bmatrix}. \tag{2.167}$$

At $r = 0$, we impose regularity conditions as the geometry part:

$$\begin{aligned} \tilde{D}'(t,0) &= 0\,, \\ \tilde{S}_r(t,0) &= 0\,, \\ \tilde{\tau}'(t,0) &= 0\,. \end{aligned} \tag{2.168}$$

Also at the outer numerical grid, we impose the outflow boundary condition by using ghost cells, as explained in Chapter 3.

3. NUMERICAL METHODS

First we solve the geometry part equations (2.123), (2.124) and (2.126) with the boundary conditions (2.128) and (2.129) for an assumed matter profile. Then, we solve the matter part equations (2.161), (2.162) and (2.163) with the boundary conditions, assuming the spacetime to be fixed. Repeatedly doing this, we can calculate the whole spacetime structure and the matter profile.

3.1. Geometry Part

Using the Newton-Raphson method for ODEs, we solve the non-linear coupled second-order ODEs. We will describe the method briefly. Consider an ODE

$$\psi'' + \frac{2}{r}\psi' + \frac{2\pi}{\psi}\left(\tilde{\tau} + \tilde{D}\right) = 0 \tag{3.1}$$

with boundary conditions $\psi'(0) = 0$ and $\psi'(R) + (\psi(R) - 1)/R = 0$. Its finite difference equations are

$$f_i(\psi_j) = \frac{\psi_{i+1} - 2\psi_i + \psi_{i-1}}{\Delta r^2} + \frac{2}{r_i}\frac{\psi_{i+1} - \psi_{i-1}}{2\Delta r} + \frac{2\pi}{\psi_i}\left(\tilde{\tau}_i + \tilde{D}_i\right) = 0\,, \tag{3.2}$$

$$-\frac{3\psi_1 - 4\psi_2 + \psi_3}{2\Delta r} = 0\,, \tag{3.3}$$

$$\frac{3\psi_{Nr} - 4\psi_{Nr-1} + \psi_{Nr-2}}{2\Delta r} + \frac{\psi_{Nr} - 1}{r_{Nr}} = 0\,. \tag{3.4}$$

Then, the solution can be written as

$$\psi_i = \psi_i^{trial} + \delta\psi_i\,, \tag{3.5}$$

where ψ_i^{trial} is a trial solution of the equation and $\delta\psi_i$ is the solution of the matrix equation

$$J_{ij}\delta\psi_j = -f_i(\psi_k)\,. \tag{3.6}$$

J_{ij} is the Jacobian matrix

$$J_{ij} \equiv \frac{\partial f_i}{\partial \psi_j}\,. \tag{3.7}$$

The routine is iterated until all the metric variables converge at a certain level.

3.2. Hydrodynamic Part: HRSC

We adopt the finite-volume approach to the integral form of the conservative equations,

$$\int \partial_t(r^2\mathbf{q})dtdr + \int \partial_r(\alpha r^2\mathbf{F})dtdr \;=\; \int \alpha r^2\mathbf{S}dtdr\,, \tag{3.8}$$

as with the averaged quantities (upwind scheme)

$$\bar{\mathbf{q}}_i^{n+1} = \bar{\mathbf{q}}_i^n - \frac{\Delta t}{\Delta r}\frac{1}{r_i^2}\left(\alpha_{i+\frac{1}{2}}^{n+\frac{1}{2}} r_{i+\frac{1}{2}}^2 \hat{\mathbf{F}}_{i+\frac{1}{2}}^{n+\frac{1}{2}} - \alpha_{i-\frac{1}{2}}^{n+\frac{1}{2}} r_{i-\frac{1}{2}}^2 \hat{\mathbf{F}}_{i-\frac{1}{2}}^{n+\frac{1}{2}}\right) + \Delta t \alpha_i^{n+\frac{1}{2}} \bar{\mathbf{S}}_i^{n+\frac{1}{2}}\,. \tag{3.9}$$

The problem is how to calculate the time-averaged flux $\hat{\mathbf{F}}$ without knowing the evolved variables $\bar{\mathbf{q}}_i^{n+1}$.

At each cell (spacetime grid), we should solve a Riemann problem. However, approximated Riemann solvers are preferred over an exact Riemann solver because of less complexity and better numerical efficiency without loss of significant accuracy. In this paper, we implement HRSC schemes with approximated Riemann solvers using Roe's [17] and Harten et al.'s (HLLE) methods [18, 19].

3.2.1. Characteristic structure and approximated Roe flux

To calculate the approximated Roe numerical flux, we should know the characteristic structure of the conservative hydrodynamic equations. With the Jacobian $\mathbf{J} \equiv \alpha\partial\mathbf{F}/\partial\mathbf{q}$, the eigenvalue equation

$$\mathbf{J}\mathbf{r}_\alpha = \lambda_\alpha \mathbf{r}_\alpha \tag{3.10}$$

can be diagonalized with the characteristic variables $\mathbf{w}$. Then, the approximated flux is

$$\hat{\mathbf{F}} = \frac{1}{2}\left[\mathbf{F}(\tilde{\mathbf{p}}^R) + \mathbf{F}(\tilde{\mathbf{p}}^L) - \Sigma|\lambda_\alpha|(w_\alpha^R - w_\alpha^L)\mathbf{r}_\alpha\right]\,, \tag{3.11}$$

where

$$\lambda_0 = \alpha v^r - \beta\,, \tag{3.12}$$

$$\lambda_\pm = \frac{\alpha}{1-v^2c_s^2}\left\{v^r(1-c_s^2) \pm c_s\sqrt{(1-v^r)\left[\frac{1}{\psi^4}(1-v^2c_s^2) - v^r v^r(1-c_s^2)\right]}\right\} - \beta\,, \tag{3.13}$$

with $c_s^2 \equiv \left(\frac{\partial P}{\partial\rho}\right)_s = \frac{1}{h}\left(\chi + \frac{P}{\rho_0^2}\kappa\right)$, $\chi \equiv \left(\frac{\partial P}{\partial\rho_0}\right)_\epsilon$, $\kappa \equiv \left(\frac{\partial P}{\partial\epsilon}\right)_{\rho_0}$,

$$\mathbf{r}_0 = \begin{pmatrix} \frac{\mathcal{K}}{hW} \\ v_r \\ 1 - \frac{\mathcal{K}}{hW} \end{pmatrix}\,, \tag{3.14}$$

$$\mathbf{r}_{\pm} = \begin{pmatrix} 1 \\ hW\mathcal{C}^r_{\pm} \\ hW\tilde{\mathcal{A}}^r_{\pm} - 1 \end{pmatrix}, \tag{3.15}$$

with

$$\mathcal{K} = \frac{\frac{\kappa}{\rho_0}}{\frac{\kappa}{\rho_0} - c_s^2}, \tag{3.16}$$

$$\mathcal{C}^r_{\pm} = v_r - \mathcal{V}^r_{\pm}, \tag{3.17}$$

$$\mathcal{V}^r_{\pm} = \frac{v^r - \Lambda^r_{\pm}}{\frac{1}{\psi^4} - v^r\Lambda^r_{\pm}}, \tag{3.18}$$

$$\Lambda^r_{\pm} = \frac{\lambda_{\pm}}{\alpha} + \frac{\beta}{\alpha}, \tag{3.19}$$

$$\tilde{\mathcal{A}}^r_{\pm} = \frac{\frac{1}{\psi^4} - v^r v^r}{\frac{1}{\psi^4} - v^r\Lambda^r_{\pm}}. \tag{3.20}$$

3.2.2. HLLE flux

The Harten Lax van Leer Einfeld (HLLE) flux can be obtained more easily with information on only the eigenvalues:

$$\hat{\mathbf{F}}_{i+\frac{1}{2}} = \frac{b^+_{i+\frac{1}{2}}\mathbf{F}(\tilde{\mathbf{p}}^L) - b^-_{i+\frac{1}{2}}\mathbf{F}(\tilde{\mathbf{p}}^R)}{b^+_{i+\frac{1}{2}} - b^-_{i+\frac{1}{2}}} + \frac{b^+_{i+\frac{1}{2}}b^-_{i+\frac{1}{2}}}{b^+_{i+\frac{1}{2}} - b^-_{i+\frac{1}{2}}}(\tilde{\mathbf{p}}^R - \tilde{\mathbf{p}}^L) \tag{3.21}$$

where $b^+_{i+\frac{1}{2}} = \max(0, \max\{\lambda_{i+\frac{1}{2}}\})$ and $b^-_{i+\frac{1}{2}} = \min(0, \min\{\lambda_{i+\frac{1}{2}}\})$.

3.2.3. Calculating the primitive variables

When we solve the Riemann problem at each cell, the variables are reconstructed at the cell boundary by using a monotonized central-difference (MC) limiter. In order to increase numerical stability, it is common to reconstruct the primitive variables ρ_0, v^r and ϵ rather than the conservative variables. In Eqs. (3.11) and (3.21), $\tilde{\mathbf{p}}^L$ and $\tilde{\mathbf{p}}^R$ stand for the reconstructed primitive variables.

With the calculated numerical flux, we can update the conservative variables by using Eq. (3.9). After that, we need to calculate the primitive variables from the updated conservative variables in order to calculate the flux for the next time step. Unlike the calculation of the conservative variables from primitive variables, the reverse is a non-trivial task.

For the equation of state, we consider the ideal fluid

$$P = P(\rho_0, \epsilon) = (\Gamma - 1)\rho_0\epsilon, \tag{3.22}$$

where Γ is the adiabatic index. Which variable is calculated first from the conservative variables is not unique. If the P variable is considered first, the equation for the pressure is

$$f(P) \equiv W\left(D + \frac{PW}{\Gamma - 1}\right) + P(W^2 - 1) - D - \tau = 0\,, \tag{3.23}$$

where

$$W^2 = \frac{(\tau + D + P)^2}{(\tau + D + P)^2 - S_r S^r}\,. \tag{3.24}$$

Four roots of the pressure exist. One can obtain the physical root of the pressure by using a polynomial-root-finding method. However, the numerical Newton-Raphson method is more practical because the explicit form of the root is complicated. With the derivative of f with respect to P,

$$\frac{df}{dP} = \frac{W^2}{\Gamma - 1}\left[\frac{P\Gamma}{\tau + D + P}(1 - W^2) + 1\right] = 0\,, \tag{3.25}$$

we can obtain the solution for P. Then, the primitive variables are

$$v^r = \frac{1}{\psi^4}\frac{S_r}{\tau + D + P}\,, \tag{3.26}$$

$$\rho_0 = D\sqrt{1 - \psi^4 v^r v^r}\,, \tag{3.27}$$

$$h = \frac{\rho_0}{D^2}(\tau + D + P)\,, \tag{3.28}$$

$$\epsilon = h - 1 - \frac{P}{\rho_0}\,. \tag{3.29}$$

3.2.4. Time stepping scheme

As mentioned before, we evolve the conservative variables with Eq. (3.9). In the space grid, we adopt second-order discretization for the metric as well as the flux. It, therefore, shows second-order accuracy in space in smooth regions, and no more than first-order accuracy in space in discrete regions. However, in the time direction, Eq. (3.9) shows only first-order discretization in time. To obtain more than second-order accuracy in spacetime, we need higher-order time stepping scheme.

We choose a second-order time-stepping scheme such as

$$\begin{cases} \bar{\mathbf{q}}_i^{n+\frac{1}{2}} = \bar{\mathbf{q}}_i^n + \frac{\Delta t}{2} G_i^n \\ \bar{\mathbf{q}}_i^{n+1} = \bar{\mathbf{q}}_i^n + \Delta t G_i^{n+\frac{1}{2}}, \end{cases} \tag{3.30}$$

where

$$G_i^{n+\frac{1}{2}} = -\frac{1}{\Delta r}\frac{1}{r_i^2}\left(\alpha_{i+\frac{1}{2}}^{n+\frac{1}{2}} r_{i+\frac{1}{2}}^2 \hat{\mathbf{F}}_{i+\frac{1}{2}}^{n+\frac{1}{2}} - \alpha_{i-\frac{1}{2}}^{n+\frac{1}{2}} r_{i-\frac{1}{2}}^2 \hat{\mathbf{F}}_{i-\frac{1}{2}}^{n+\frac{1}{2}}\right) + \alpha_i^{n+\frac{1}{2}} \bar{\mathbf{S}}_i^{n+\frac{1}{2}}. \tag{3.31}$$

We also try a fourth-order Runge-Kutta time-stepping scheme

$$\begin{cases} \bar{\mathbf{q}}_i^{n+k_2} = \bar{\mathbf{q}}_i^n + \frac{\Delta t}{2} G_i^n \\ \bar{\mathbf{q}}_i^{n+k_3} = \bar{\mathbf{q}}_i^n + \frac{\Delta t}{2} G_i^{n+k_2} \\ \bar{\mathbf{q}}_i^{n+k_4} = \bar{\mathbf{q}}_i^n + \Delta t G_i^{n+k_3} \\ \bar{\mathbf{q}}_i^{n+1} = \bar{\mathbf{q}}_i^n + \frac{\Delta t}{6}\left\{G_i^n + G_i^{n+k_4} + 2(G^{n+k_2} + G^{n+k_3})\right\}. \end{cases} \tag{3.32}$$

3.2.5. Atmosphere

In HRSC schemes, we cannot treat pressureless regions or vacuum regions in which we cannot calculate the approximated flux. One solution is to use a very tenuous stationary fluid, "atmosphere," when the density becomes lower than a certain small value. In practice, we follow the `Whisky` code prescription [20].

4. CODE TESTS

4.1. Relativistic Blast Wave Problem

We solve the spherical relativistic blast wave problem to test the hydrodynamic part of the code. Two chambers are separated by a spherical shell and are filled with gases that have different densities and pressures and are at rest initially. After the shell is removed, shock, contact discontinuity and rarefaction waves develop and propagate due to the initial differences in the densities and pressures. The spacetime metric is fixed on a flat Minkowski spacetime. Because this problem has no exact solution, we compared the results with those in Ref. [21] in which two cases, *weak* and *strong* blast wave, are treated. The domain of the simulation is $r \in [0, 1]$, and the initial discontinuity is located at $r = 0.5$. The fluid obeys the ideal equation of state (EoS) with $\Gamma = 1.4$ and is initially at rest. The parameters are for the weak blast wave case, ($\rho_{0L} = 1.0,\ P_L = 1.0$), ($\rho_{0R} = 0.125,\ P_R = 0.1$) and for the strong blast wave case, ($\rho_{0L} = 10.0,\ P_L = 133.33$), ($\rho_{0R} = 1.0,\ P_R = 0.125$). The spatial resolution used is $\Delta r = 2 \times 10^{-4}$, and the courant factor is $\Delta t/\Delta r = 0.25$.

Figures 4.1 and 4.2 show the results obtained from our code. In order to compare with Ref. [21] we plot the evolved hydrodynamic variables at $t = 0.4$. Our results are in good agreement with those in Ref. 15. We also perform convergence tests. Although we use a second-order spatial finite-difference scheme, for the discontinuous part of a solution like the one to this test problem, the HRSC scheme shows first-order convergence. Figure 4.3 shows the difference of ρ_0 for different levels of resolutions. The resolutions of *level 0* is $\Delta r = 2.5 \times 10^{-4}$, *level 1* is $\Delta r/2$, *level 2* is $\Delta r/4$, and *level 3* is $\Delta r/8$; i.e., we increase the resolution by factors of two. For nth-order convergence, the differences (*level 0* - *level 1*) and $2^n\times$ (*level 1* - *level 2*) coincide. In Figure 4.3, we plot the three differences of four different resolution levels. The Figure shows first-order convergence.

4.2. Relativistic Spherical Accretion

The solution for spherical, stationary, adiabatic accretion is wellknown, so we can use the solution as a code test. The general relativistic version of the Bondi [22] equation is shown by Michel [23], and in the appendix of Ref. [24] one can find a good explanation of relativistic spherical accretion. Papadopoulos and Font [25] obtained the same solution with the horizon-adapted coordinate system and reported the resolution benefits obtained by using that coordinate

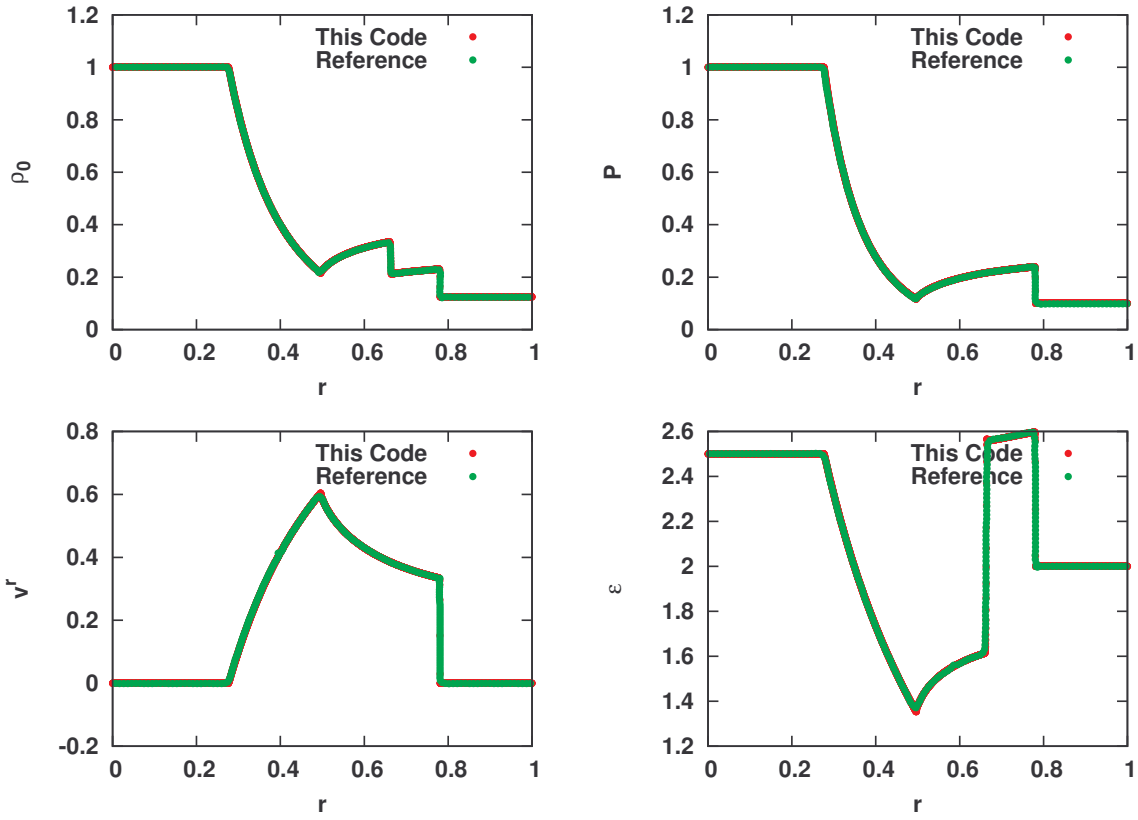

Figure 4.1: Evolution data at $t = 0.4$ for the weak blast wave case.

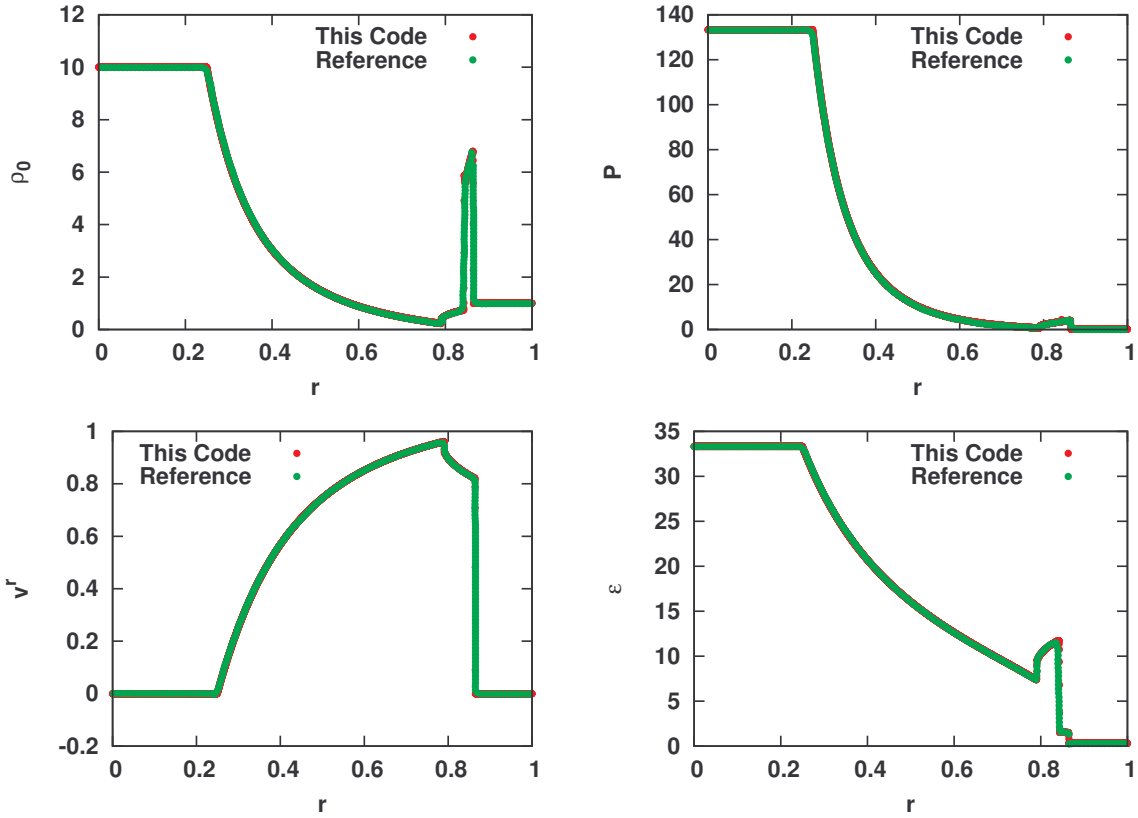

Figure 4.2: Evolution data at $t = 0.4$ for the strong blast wave case.

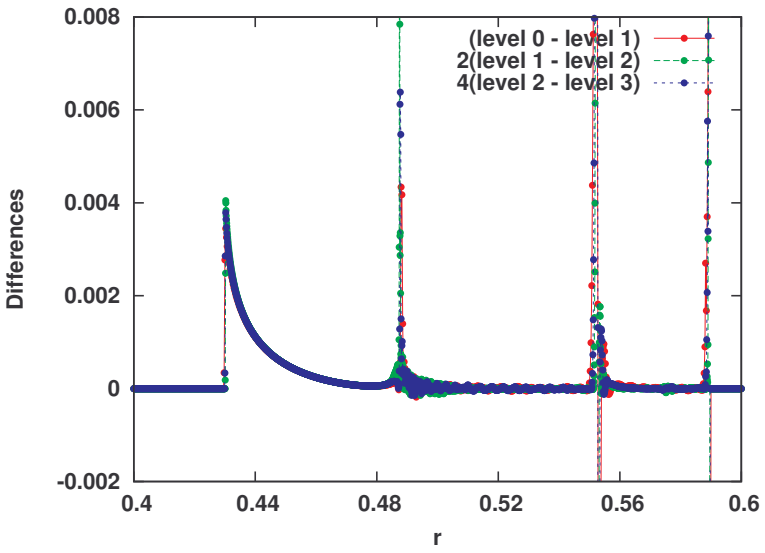

Figure 4.3: Convergence test of ρ_0 at $t = 0.125$. It shows the first order convergence.

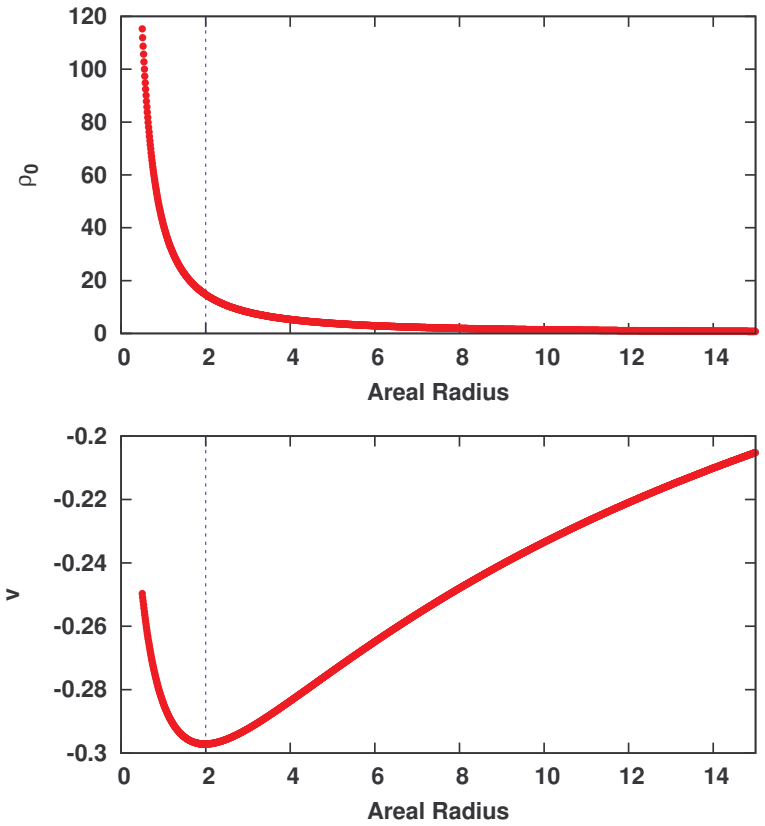

Figure 4.4: Exact solutions of spherical accretion of an ideal fluid with $\Gamma = \frac{4}{3}$ in horizon-adapted coordinates. The top panel shows the rest-mass density, and the bottom shows the physical velocity defined by $\sqrt{\gamma_{rr}}v^r$. The vertical dotted line indicates the event horizon of the black-hole.

system due to elimination of the divergence in the Lorentz factor at the horizon. Here, we adopt a conformal version of horizon-adapted coordinates.

The solution procedure is explained in Ref. [25] With the value of the critical radius $r_c = 400M$ and the rest-mass density at the critical point $(\rho_0)_c = 0.01$, we can obtain the integration constants C_1 and C_2 of the spherically-symmetric, stationary hydrodynamic equations:

$$r^2 \rho_0 u^r = C_1 \,, \tag{4.1}$$

$$r^2 (\rho + P) u^r u_t = C_2 \,. \tag{4.2}$$

Assuming the adiabatic, ideal EoS, one can rewrite Eqs. (4.1) and (4.2) to a non-linear algebraic equation for u^r. The equation is hard to solve algebraically, so we find the solution numerically by using the Newton-Raphson method. Fig-

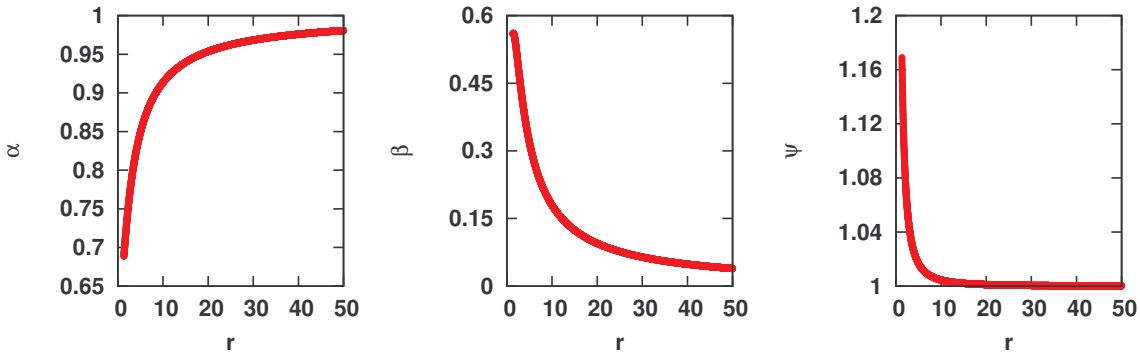

Figure 4.5: Metric components of the black hole in conformal horizon-adapted coordinates.

ure 4.4 shows the numerically-obtained solutions. In order to compare the results with those in Ref. [25] we use the same values of the parameters, and the results are seen to be in good agreement. Then, we transform the solution to the conformal metric coordinates as in Eq. (2.99). The black-hole metric in the horizon-adapted coordinate system is

$$ds^2 = -\left(1-\frac{2M}{\bar{r}}\right)dt^2+\frac{4M}{\bar{r}}dtd\bar{r}+\left(1+\frac{2M}{\bar{r}}\right)d\bar{r}^2+\bar{r}^2(d\theta^2+\sin^2\theta d\phi^2)\,. \quad (4.3)$$

The transformation of r to $\bar{r}$ is

$$\bar{r} = \psi^2 r\,, \quad (4.4)$$

$$\frac{d\psi}{dr} = -\frac{\psi}{2r}\left(1-\frac{\psi}{\sqrt{\psi^2+\frac{2M}{r}}}\right)\,. \quad (4.5)$$

Figure 4.5 shows the metric components of the black-hole in terms of the conformal horizon-adapted coordinates. We use those metric components in the code, and as initial data for the hydrodynamic variables ρ_0 and v^r, we use a homogeneous ρ_0 with the value of the exact solution at the numerical boundary and $v^r = 0$ everywhere. The initial data evolved well and approached the coordinate transformed exact solution (Figure 4.6).

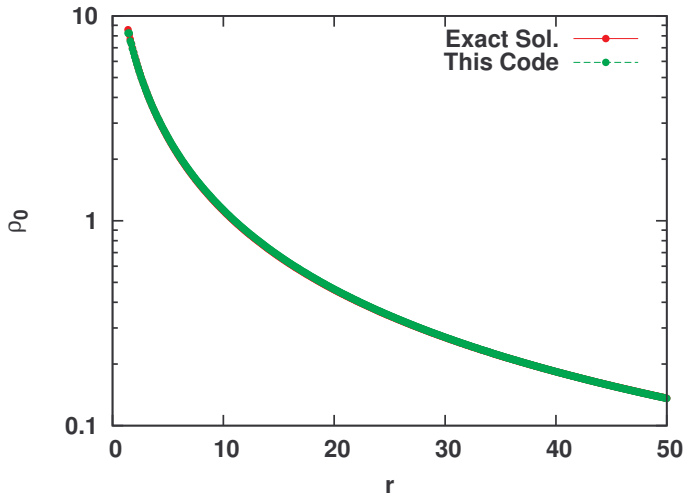

Figure 4.6: Rest-mass density profile in conformal horizon-adapted coordinates. The evolved data approach the red line which represents the exact solution.

4.3. TOV Star Evolution

4.3.1. TOV equations

Tolman-Oppenheimer-Volkoff(TOV) equations are

$$\frac{d}{dr}P(r) = -\frac{(\rho(r)+P(r))\left(M(r)+4\pi P(r)r^3\right)}{r^2\left(1-\frac{2M(r)}{r}\right)}$$
$$\frac{d}{dr}M(r) = 4\pi\rho(r)r^2 \tag{4.6}$$

4.3.2. TOV test

$$ds^2 \;=\; -\alpha^2 dt^2 + \psi^4\left[dr^2 + r^2(d\theta^2 + \sin^2\theta d\phi^2)\right] \tag{4.7}$$

where the lapse and conformal factor are functions of the radial coordinate r only, i.e., $\alpha = \alpha(r)$ and $\psi = \psi(r)$.

$$\sqrt{-g} \;=\; \alpha\,\psi^6\,r^2\sin\theta \tag{4.8}$$

where $g = det(g_{\mu\nu})$.

It is convenient to find the differential equation for the pressure P.

$$\nabla_\mu T^\mu{}_\nu \;=\; 0 \tag{4.9}$$

where $T_{\mu\nu} = (\rho + P)u_\mu u_\nu + P g_{\mu\nu}$ and the fluid 4-velocity u^μ is

$$u^\mu = \left(\frac{1}{\alpha}, 0, 0, 0\right) \qquad u_\mu = (-\alpha, 0, 0, 0) \tag{4.10}$$

$$\boxed{\hookrightarrow P' + \frac{\alpha'}{\alpha}(\rho + P) = 0} \tag{4.11}$$

where $' = \frac{d}{dr}$.

The Einstein equations $G_{\mu\nu} = 8\pi T_{\mu\nu}$ give rise to three independent ODEs.

- $G_{tt} = 8\pi T_{tt}$

$$\boxed{\hookrightarrow \psi'' + \frac{2}{r}\psi' + 2\pi\psi^5\rho = 0} \tag{4.12}$$

: the Hamiltonian constraint equation

- $G_{rr} = 8\pi T_{rr}$

$$\hookrightarrow \frac{\alpha'}{\alpha}\left(2\psi' + \frac{\psi}{r}\right)\psi + 2\psi'\left(\psi' + \frac{\psi}{r}\right) = 4\pi P\psi^6 \tag{4.13}$$

Rewrite

$$2\psi'^2 + 2\left(\frac{\alpha'}{\alpha} + \frac{1}{r}\right)\psi\psi' + \frac{\alpha'}{\alpha}\frac{\psi^2}{r} = 4\pi P\psi^6 \tag{4.14}$$

- $G_{\theta\theta} = 8\pi T_{\theta\theta}$

$$\hookrightarrow \frac{\psi^2}{r}\frac{\alpha'}{\alpha} - 2\psi'^2 + 2\frac{\psi'}{r}\psi + 2\psi\psi'' + \frac{\alpha''}{\alpha}\psi^2 = 8\pi P\psi^6 \tag{4.15}$$

$G_{rr} + G_{\theta\theta}$ gives

$$\boxed{\hookrightarrow \alpha'' + 2\alpha'\left(\frac{\psi'}{\psi} + \frac{1}{r}\right) = 4\pi\alpha\psi^4(\rho + 3P)} \tag{4.16}$$

$$\left(2\psi' + \frac{\psi}{r}\right)\psi\left(\frac{\alpha'}{\alpha}\right)^2 + \left(2\psi'^2 + 8\frac{\psi'}{r}\psi + 3\frac{\psi^2}{r^2}\right)\frac{\alpha'}{\alpha} + 6\frac{\psi'}{r}\left(\psi' + \frac{\psi}{r}\right)$$
$$= -4\pi\psi^6\left(P' - \frac{3P}{r} + \frac{\alpha'}{\alpha}\rho\right) = 4\pi\psi^6\left(\frac{\alpha'}{\alpha} + \frac{3}{r}\right)P \tag{4.17}$$

Nothing but

$$\left(\frac{\alpha'}{\alpha}+\frac{3}{r}\right)\left[\frac{\alpha'}{\alpha}\left(2\psi'+\frac{\psi}{r}\right)\psi+2\psi'\left(\psi'+\frac{\psi}{r}\right)\;=\;4\pi P\psi^6\right] \tag{4.18}$$

$G_{rr}-G_{\theta\theta}$ gives merely the same equation,

$$3\left[\frac{\alpha'}{\alpha}\left(2\psi'+\frac{\psi}{r}\right)\psi+2\psi'\left(\psi'+\frac{\psi}{r}\right)\;=\;4\pi P\psi^6\right] \tag{4.19}$$

4.3.3. Isotropic vs. Schwarzschild coordinates

$$ds^2_{Schw}\;=\;-\left(1-\frac{2M}{r}\right)dt^2+\frac{1}{\left(1-\frac{2M}{r}\right)}dr^2+r^2(d\theta^2+\sin^2\theta d\phi^2) \tag{4.20}$$

where $M=m(R)$ is

$$m(R)\;=\;4\pi\int_0^R\rho(r)r^2dr \tag{4.21}$$

and $P(r\geqq R)=0$.

$$ds^2_{Iso}\;=\;-\frac{\left(1-\frac{M}{2\bar{r}}\right)^2}{\left(1+\frac{M}{2\bar{r}}\right)^2}dt^2+\left(1+\frac{M}{2\bar{r}}\right)^4\left[d\bar{r}^2+\bar{r}^2(d\theta^2+\sin^2\theta d\phi^2)\right] \tag{4.22}$$

$$R\;=\;\bar{R}\left(1+\frac{M}{2\bar{R}}\right)^2 \tag{4.23}$$

$$\hookrightarrow\bar{R}\;=\;\frac{1}{2}\left[R-M\pm\sqrt{R(R-2M)}\right] \tag{4.24}$$

4.3.4. Boundary conditions for metric components

At the origin ($\bar{r}=0$), the lapse α and the conformal metric factor ψ satisfy the regularity condition for scalar, i.e.,

$$\alpha'\;=\;0\;\big|_{\bar{r}=0} \tag{4.25}$$

$$\psi'\;=\;0\;\big|_{\bar{r}=0} \tag{4.26}$$

At the outer boundary ($\bar{r}=\bar{r}_{max}$), the conformal metric factor ψ satisfies

$$\psi\;=\;1+\frac{M}{2\bar{r}}\;\Big|_{\bar{r}\geq\bar{R}} \tag{4.27}$$

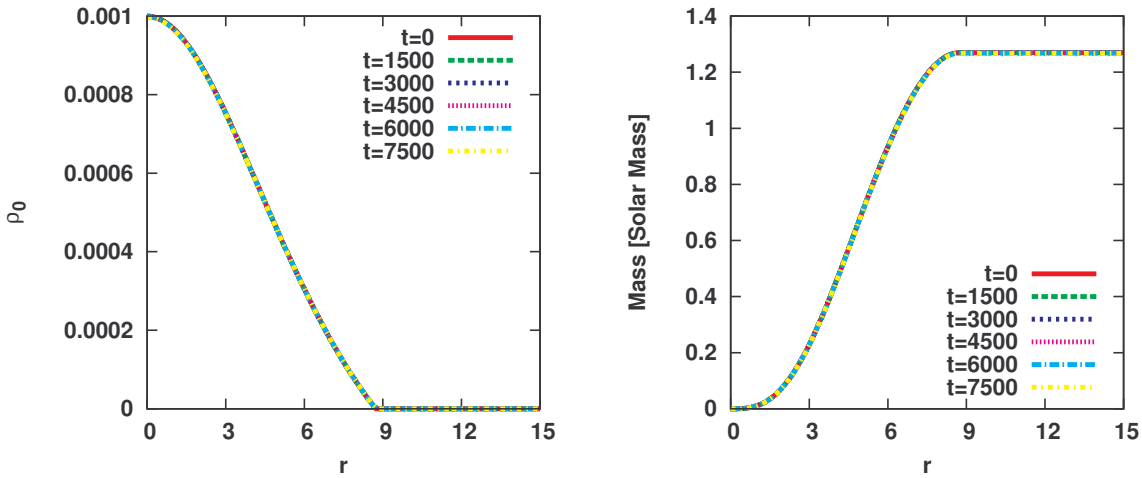

Figure 4.7: Evolved TOV star solution. We choose $(\rho_0)_c = 0.001$, $\kappa = 100$ and $\Gamma = 2$.

$\psi' = -\frac{M}{2\bar{r}^2}$ then the boundary condition becomes

$$\psi' = \frac{(1-\psi)}{\bar{r}} \Big|_{\bar{r}=\bar{r}_{max}} \tag{4.28}$$

The lapse α should satisfy

$$\alpha = \frac{1-\frac{M}{2\bar{r}}}{1+\frac{M}{2\bar{r}}} \Big|_{\bar{r}\geq\bar{R}} \tag{4.29}$$

$\alpha' = \frac{M}{\bar{r}^2}\left(1+\frac{M}{\bar{r}^2}\right)^{-2}$ then the boundary condition becomes

$$\alpha' = \frac{(1-\alpha)^2}{M} \Big|_{\bar{r}=\bar{r}_{max}} \tag{4.30}$$

However, this boundary condition contains the value of M which could be obtained after numerical simulation. Using Eq. (4.29) we can replace M to other quantities,

$$M = 2\bar{r}\frac{1-\alpha}{1+\alpha} \tag{4.31}$$

Then the boundary condition becomes

$$\alpha' = \frac{1-\alpha^2}{2\bar{r}} \Big|_{\bar{r}=\bar{r}_{max}} \tag{4.32}$$

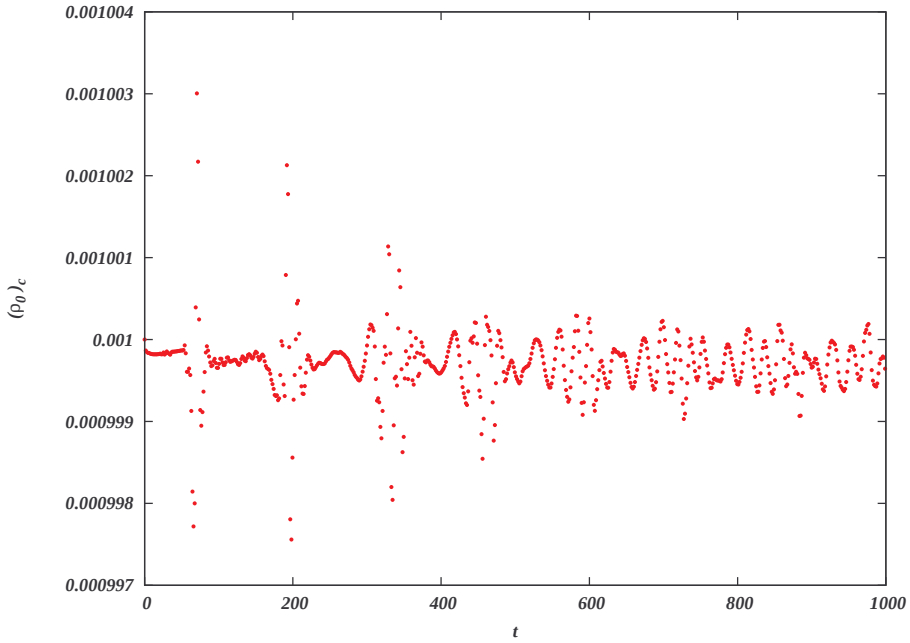

Figure 4.8: Central density pulsation during TOV evolution

4.3.5. TOV star code test

The TOV star solution is a self-gravitating GR solution for a stationary perfect fluid. We assume a polytropic fluid, $P = \kappa\rho_0^\Gamma$. Solving the TOV equation and transforming to the conformal coordinate system, we can obtain the static rest-mass density profile. Using that profile as initial data, we evolve it using our code. The test is whether the profile remains unchanged during evolution or not. Figure 4.7 shows the result of the evolution. As we expected, the profile is almost fixed during evolution. However, it oscillates slightly because we cannot avoid small numerical errors. (See Fig. 4.8) To investigate the oscillation modes, we perform a Fourier transformation analysis and obtain the power spectral density (PSD) of the central density. We then compare the oscillation mode frequencies with those from a linear perturbation analysis of the radial pulsation. The linear perturbation mode frequencies of radial pulsation can be obtained by solving the linear perturbation GR equation of the Lagrangian displacement function. In Chap. 26 in Ref. [26] the linear perturbation theory of the radial pulsation of general relativistic stellar models is well described. Also, one can find a solution procedure to obtain the mode frequencies in Refs. [27] and [28].

From the trial value of the oscillation frequency ω of a renormalized displacement function $\zeta = \zeta(r)e^{-i\omega t}$, we integrate the linear perturbation equation by using a Runge-Kutta method. Then, examining $\zeta'(r)$ at the star's surface, we

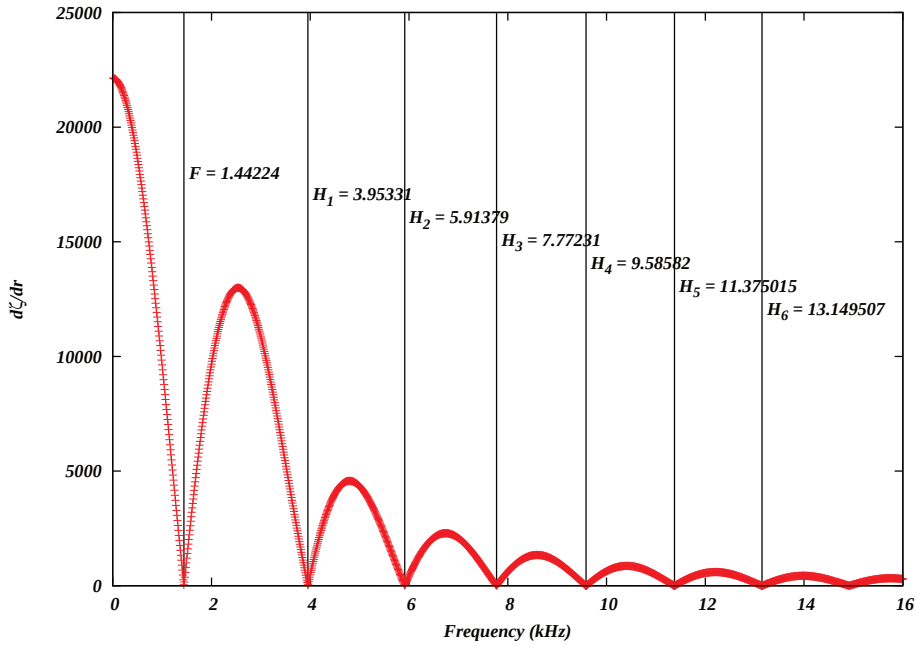

Figure 4.9: Radial pulsation frequencies from the linear perturbation analysis

Table 4.1: Radial pulsation frequencies from the numerical linear perturbation analysis, the data of Font et al., the PSD of the evolved TOV obtained using our GRHydro code, and the relative difference between the linear perturbation analysis and the evolved TOV of our code.

Mode	Linear Pert. (kHz)	Ref. (kHz)	Evolved (kHz)	Difference (%)
F	1.442	1.442	1.442	0.00
H1	3.953	3.955	3.952	0.03
H2	5.914	5.916	5.901	0.22
H3	7.772	7.776	7.724	0.62
H4	9.586			
H5	11.38			
H6	13.15			

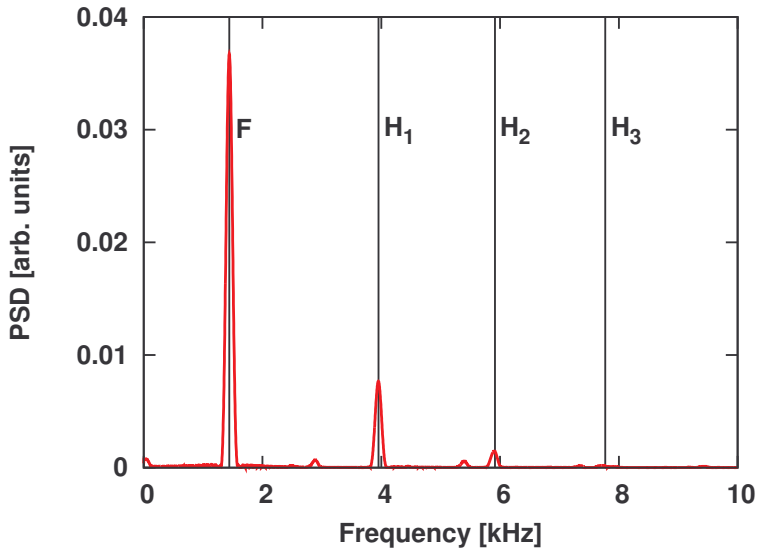

Figure 4.10: PSD of the central density change during evolution.

can determine the proper value of ω. (See Fig. 4.9) In Table 4.1, we present the radial pulsation mode frequencies using linear perturbation analysis. Also the frequency values are compared with other data from Ref. [29]. To test the evolution of TOV obtained from the GRHydro code, we compare the pulsation mode frequencies with those from linear perturbation theory. Figure 4.10 shows the PSD of the change of the central density during evolution.

4.4. Oppenheimer-Snyder Dust Collapse

Assuming spherical symmetry and pressureless matter (dust), one can solve the Einstein equations exactly [6].

4.4.1. The exact solution

The solution of the Einstein equations for this homogeneous dust star consists of two parts. Inside the star, the metric is the closed Friedmann

$$ds^2 = -d\tau^2 + a^2\left(d\chi^2 + \sin^2\chi d\Omega^2\right) . \tag{4.33}$$

where $a(\tau)$ can be written in terms of the conformal time η as

$$a = a_0(1 + \cos\eta) , \tag{4.34}$$

and

$$\tau = a_0(\eta + \sin\eta) . \tag{4.35}$$

The conformal metric of the closed Friedmann is

$$ds^2 \;=\; -a^2\left(d\eta^2 + d\chi^2 + \sin^2\chi d\Omega^2\right)\,. \tag{4.36}$$

Outside the star, the metric is Schwarzschild

$$ds^2 \;=\; -\left(1-\frac{2M}{R}\right)d\bar{t}^2 + \frac{dR^2}{\left(1-\frac{2M}{R}\right)} + R^2 d\Omega^2\,, \tag{4.37}$$

where M is the mass of the dust star.

a_0 is related to both M and initial areal radius $R_{\max}$. First, two metrics should be matched at the star surface, $\chi = \chi_s$,

$$R = a\sin\chi_s \tag{4.38}$$

and

$$ad\chi = \frac{dR}{\sqrt{1-\frac{2M}{R}}} \;=\; \frac{a\cos\chi_s d\chi}{\sqrt{1-\frac{2M}{R}}}\,. \tag{4.39}$$

Then

$$a\sin^3\chi_s = 2M \tag{4.40}$$

at the star surface. Second, at the beginning of collapse ($\eta = 0$, $a = 2a_0$) the star has maximum areal radius $R_{\max}$

$$R_{\max} = 2a_0\sin\chi_s\,. \tag{4.41}$$

Then we get

$$a_0 = \sqrt{\frac{R_{\max}^3}{8M}}\,. \tag{4.42}$$

The comoving rest-mass density is given by

$$\rho_0 \;=\; \frac{1}{8\pi}\frac{6a_0}{a^3} \tag{4.43}$$

η runs from 0 to π, a runs from $2a_0$ to 0 (complete collapse) and τ runs from 0 to πa_0

A kind of a Lagrangian radial coordinate χ has range [0,χ_s]

$$\chi_s = \arcsin\sqrt{\frac{2M}{R_{\max}}} \tag{4.44}$$

4.4.2. Coordinate transformations

From the closed Friedmann metric

$$ds^2 \;=\; -d\tau^2 + a^2\left(d\chi^2 + \sin^2\chi d\Omega^2\right) \tag{4.45}$$

and the Schwarzschild metric

$$ds^2 \;=\; -\left(1-\frac{2M}{R}\right)d\vec{t}^2 + \frac{dR^2}{\left(1-\frac{2M}{R}\right)} + R^2 d\Omega^2 \tag{4.46}$$

we are going to transform the metric to the 3+1 ADM metric

$$ds^2 \;=\; -\left(\alpha^2 - A^2\beta^2\right)dt^2 + 2A^2\beta dt dr + A^2 dr^2 + A^2 r^2 d\Omega^2 \tag{4.47}$$

The inner part equations are,

$$\left.\frac{\partial T}{\partial \chi}\right|_t \;=\; -\left(1-T^2\right)\left[3\cot\frac{\eta}{2} + 2T\cot\chi\right] \tag{4.48}$$

$$\left.\frac{\partial \eta}{\partial \chi}\right|_t = T \tag{4.49}$$

$$\left.\frac{\partial r}{\partial \chi}\right|_t = \frac{r}{\sin\chi}\sqrt{1-T^2} \tag{4.50}$$

$$\frac{\partial}{\partial\chi}\left(\left.\frac{\partial r}{\partial t}\right|_\chi\right)\Bigg|_t = \frac{\sqrt{1-T^2}}{\sin\chi}\left.\frac{\partial r}{\partial t}\right|_\chi - \frac{r}{\sin\chi}\frac{T}{\sqrt{1-T^2}}\left.\frac{\partial T}{\partial t}\right|_\chi \tag{4.51}$$

$$\begin{aligned}\frac{\partial}{\partial\chi}\left(\left.\frac{\partial T}{\partial t}\right|_\chi\right)\Bigg|_t \;=\; &\left[6T\cot\frac{\eta}{2} + 2\cot\chi(3T^2-1)\right]\left.\frac{\partial T}{\partial t}\right|_\chi \\ &+ \frac{3}{2}\frac{1-T^2}{\sin^2\frac{\eta}{2}}\left.\frac{\partial \eta}{\partial t}\right|_\chi\end{aligned} \tag{4.52}$$

$$\frac{\partial}{\partial\chi}\left(\left.\frac{\partial \eta}{\partial t}\right|_\chi\right)\Bigg|_t = \left.\frac{\partial T}{\partial t}\right|_\chi \tag{4.53}$$

The boundary conditions,

$$T \to -\chi\cot\frac{\eta}{2} \quad \text{as} \quad \chi\to 0 \tag{4.54}$$

η_c

$$\eta = \eta_c \quad \text{at} \quad \chi = 0 \tag{4.55}$$

$$r \to \chi\frac{a}{A} \quad \text{as} \quad \chi\to 0 \tag{4.56}$$

$$\left.\frac{\partial T}{\partial t}\right|_{\chi} \to \frac{\chi}{2\sin^2\frac{\eta}{2}}\left.\frac{\partial \eta}{\partial t}\right|_{\chi} = \frac{\alpha_c}{a_0}\frac{\chi}{\sin^2\eta} \quad \text{as} \quad \chi \to 0 \tag{4.57}$$

α_c and A_c

$$\left.\frac{\partial \eta}{\partial t}\right|_{\chi} = \frac{\alpha_c}{a_0(1+\cos\eta_c)} = \frac{\alpha_c}{a} \quad \text{at} \quad \chi = 0 \tag{4.58}$$

$$\left.\frac{\partial r}{\partial t}\right|_{\chi} \to -\chi\frac{\alpha_c}{A_c}\tan\frac{\eta}{2} \quad \text{as} \quad \chi \to 0 \tag{4.59}$$

The relations of variables are

lapse

$$\alpha = \frac{1}{\sqrt{1-T^2}}\left.\frac{\partial \tau}{\partial t}\right|_{\chi} = \frac{a}{\sqrt{1-T^2}}\left.\frac{\partial \eta}{\partial t}\right|_{\chi} \tag{4.60}$$

conformal factor

$$A = \sqrt{1-T^2}\frac{a}{\left.\frac{\partial r}{\partial \chi}\right|_t} \tag{4.61}$$

shift

$$\beta = -\left.\frac{\partial r}{\partial t}\right|_{\chi} - \frac{T\alpha}{A} \tag{4.62}$$

where

$$\tau = a_0(\eta + \sin\eta) \tag{4.63}$$

$$a = a_0(1+\cos\eta) \tag{4.64}$$

$$a_0 = \sqrt{\frac{R_{\max}^3}{8M}} \tag{4.65}$$

The equations of outer part are

$$\bar{t} = t - \int_0^{\frac{1}{R}} du \frac{B}{(1-2Mu)\sqrt{1-2Mu+B^2u^4}} \tag{4.66}$$

$$\ln r = \ln R + \int_0^{\frac{1}{R}} \frac{du}{u}\left(1 - \frac{1}{\sqrt{1-2Mu+B^2u^4}}\right) \tag{4.67}$$

$$\ln A = \ln R - \ln r = \int_0^{\frac{1}{R}} \frac{du}{u}\left(\frac{1}{\sqrt{1-2Mu+B^2u^4}} - 1\right) \tag{4.68}$$

$$\alpha = \sqrt{1-\frac{2M}{R}+\frac{B^2}{R^4}}\left\{1 - \frac{dB}{dt}\int_0^{\frac{1}{R}} \frac{du}{(1-2Mu+B^2u^4)^{\frac{3}{2}}}\right\} \tag{4.69}$$

$$\beta = -\frac{B}{AR^2}\left\{1 + \frac{dB}{dt}\int_0^{\frac{1}{R}} du \frac{R^3u^3-1}{(1-2Mu+B^2u^4)^{\frac{3}{2}}}\right\} \tag{4.70}$$

$$B = R^2 \cos\chi_s \frac{T - \tan\chi_s \tan\frac{\eta}{2}}{\sqrt{1-T^2}} \tag{4.71}$$

$$\begin{aligned}\frac{dB}{dt} =& -\frac{\partial\eta}{\partial t}\Big|_{\chi_s}\left[2B\tan\frac{\eta}{2} + R^2\frac{1}{2\cos^2\frac{\eta}{2}}\frac{\sin\chi_s}{\sqrt{1-T^2}}\right] \\ &+ \frac{\partial T}{\partial t}\Big|_{\chi_s} R^2\cos\chi_s\frac{1 - T\tan\chi_s\tan\frac{\eta}{2}}{(1-T^2)^{\frac{3}{2}}}\end{aligned} \tag{4.72}$$

$$R = 2M\frac{\cos^2\frac{\eta}{2}}{\sin^2\chi_s} \tag{4.73}$$

Parameterize solutions by α_c and A_c

$$d\tilde{t} = \alpha_c dt \ , \qquad \tilde{r} = A_c r \tag{4.74}$$

Then

$$\frac{\partial T}{\partial t} = \alpha_c \frac{\partial T}{\partial \tilde{t}} \tag{4.75}$$

$$\frac{\partial r}{\partial t} = \frac{\alpha_c}{A_c}\frac{\partial \tilde{r}}{\partial \tilde{t}} - \frac{\tilde{r}\alpha_c}{A_c^2}\frac{\partial A_c}{\partial \tilde{t}} \tag{4.76}$$

Define $\tilde{\alpha}$, $\tilde{A}$ and $\tilde{\beta}$ as

$$\tilde{\alpha} = \frac{a}{\sqrt{1-T^2}}\frac{\partial\eta}{\partial\tilde{t}}\Big|_{\chi} \tag{4.77}$$

$$\tilde{A} = \frac{a\sin\chi}{\tilde{r}} \tag{4.78}$$

$$\tilde{\beta} = -\frac{\partial\tilde{r}}{\partial\tilde{t}}\Big|_{\chi} - \frac{T\tilde{\alpha}}{\tilde{A}} \tag{4.79}$$

Then $\alpha = \alpha_c\tilde{\alpha}$, $A = A_c\tilde{A}$ and $\beta = \frac{\alpha_c}{A_c}\tilde{\beta} + \frac{\tilde{r}\alpha_c}{A_c}\frac{\partial}{\partial\tilde{t}}\ln A_c\,\big|_{\chi}$.
Compare the value of α of inner part with the outer part.

$$\alpha_c = \frac{1}{\frac{\tilde{\alpha}}{\sqrt{1-\frac{2M}{R}+\frac{B^2}{R^4}}} + \frac{dB}{d\tilde{t}}\int_0^{\frac{1}{R}}\frac{du}{(1-2Mu+B^2u^4)^{\frac{3}{2}}}} \tag{4.80}$$

Compare the value of A of inner part with the outer part.

$$A_c = \frac{A\tilde{r}}{R} \tag{4.81}$$

where

$$A = \exp^{\int_0^{\frac{1}{R}} \frac{du}{u}\left(\frac{1}{\sqrt{1-2Mu+B^2u^4}}-1\right)} \tag{4.82}$$

$\frac{\partial}{\partial\tilde{t}} \ln A_c \Big|_\chi$
At the surface $A_c = \frac{A\tilde{r}}{R}$, and

$$\frac{\partial}{\partial\tilde{t}} \ln A_c \Big|_\chi = \frac{\partial}{\partial\tilde{t}} \ln A \Big|_\chi + \frac{\partial}{\partial\tilde{t}} \ln \tilde{r} \Big|_\chi - \frac{\partial}{\partial\tilde{t}} \ln R \Big|_\chi \tag{4.83}$$

Therefore

$$\begin{aligned}\frac{\partial}{\partial\tilde{t}} \ln A_c \Big|_\chi =& \frac{\tan\frac{\eta}{2}}{\sqrt{1-\frac{2M}{R}+\frac{B^2}{R^4}}} \frac{\partial\eta}{\partial\tilde{t}} \Big|_\chi \\ & - B\frac{dB}{d\tilde{t}} \int_0^{\frac{1}{R}} du \frac{u^3}{(1-2Mu+B^2u^4)^{\frac{3}{2}}} + \frac{\partial}{\partial\tilde{t}} \ln \tilde{r} \Big|_\chi \end{aligned} \tag{4.84}$$

4.4.3. Code test

Using this exact solution, researchers have tested their codes [30, 31]. However, in order to perform such a code test, we need to treat the pressureless limit and coordinate transformations.

Using the HRSC scheme requires special treatment in order to handle a pressureless fluid. The characteristic structure is changed, so the code needs to be modified to the Oppenheimer-Snyder(OS) collapse test. One may circumvent this problem by using a polytropic fluid with a very small value of the polytropic constant κ. Romero et al. [30] and O'Connor and Ott [31] did the OS test in this way.

The OS solution has a simple form when we use the Friedmann metric inside and the Schwarzschild metric outside. However, one usually fixes the coordinate system when one develops a general relativistic hydrodynamic code, so coordinate transformations are necessary before comparing the results. Petrich et al. [32] already did the coordinate transformation between the Friedmann and Schwarzschild metric and the 3+1 conformal metric (isotropic coordinates) with the maximal slicing condition, so we follow their approach. The transformation procedure is quite complex, and one may refer to Ref. [32].

Fig. 4.11 shows the result for the OS test. Initially, we use the OS solution as initial data. Then, we evolve the system fully, not only the matter part but also the metric part. After that, we compare the evolved data with the coordinate-transformed exact OS solution. As can be seen in Fig. 4.11, our numerical evolution results are in good agreement with those analytic ones except in the vicinities of the origin and the star's surface. This is probably due to

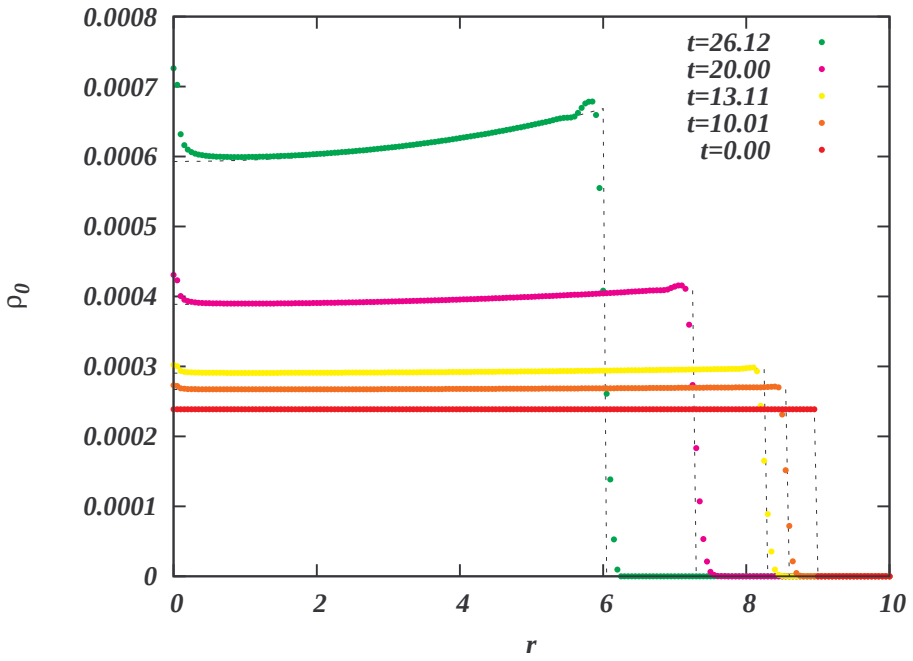

Figure 4.11: Oppenheimer-Snyder dynamical code test results.

the small, but non-zero, pressure effect we assumed around the origin and to the discrete boundary effect at the surface, which is also argued in Ref. [31]. Fig. 4.12 shows that the disagreement between our numerical results and the exact analytic solution is less than 0.45% in the designated region.

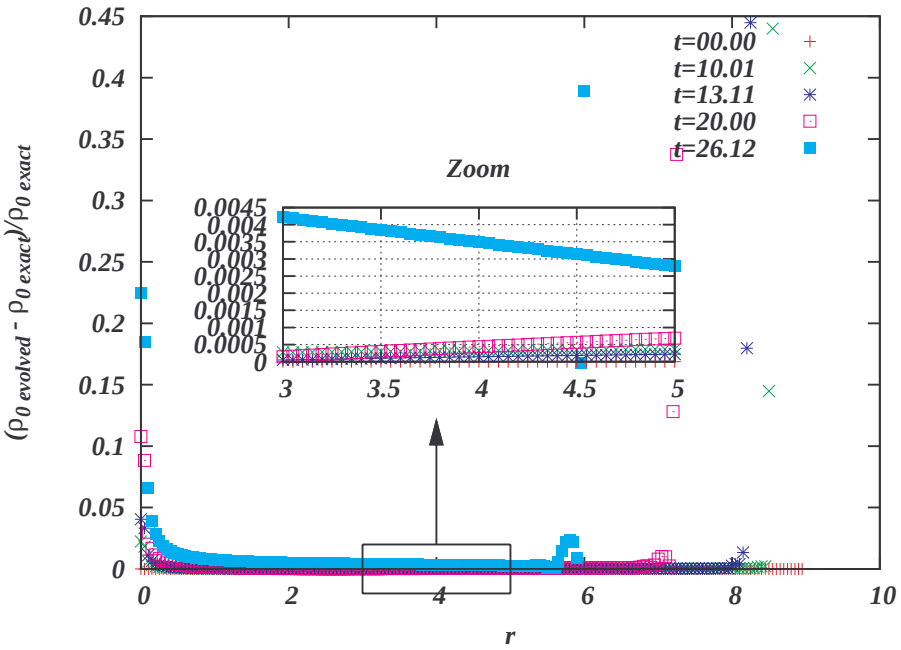

Figure 4.12: Accuracy in the OS dynamical code test.

5. EiBI GRAVITY THEORY

5.1. EiBI Gravity

Very recently, Eddington-inspired Born-Infeld (EiBI) gravity theory was suggested as an alternative theory of gravity [7]. The action of the EiBI gravity can be written as

$$S = \frac{2}{\kappa}\int d^4x\left(\sqrt{|g_{ab}+\kappa R_{ab}|}-\lambda\sqrt{-g}\right)+S_M[g_{ab},\Psi_M] \tag{5.1}$$

where $|M_{ab}|$ means the determinant of M_{ab}, $g\equiv|g_{ab}|$, R_{ab} are constructed from the connection Γ^a_{bc} which are independent of g_{ab}. κ is the only additional theory parameter to the gravitational constant (we set $8\pi G=1$). λ is a dimensionless parameter which is related with the cosmological constant by $\Lambda=(\lambda-1)/\kappa$. ($\lambda=1$ corresponds to the zero cosmological constant.) The Ricci tensor $R_{\mu\nu}(\Gamma)$ is evaluated solely by the connection, and the matter filed Ψ is coupled only to the gravitational field $g_{\mu\nu}$. The theory reduces to the theory of general relativity (GR) in vacuum, while it deviates from GR in the presence of matter. The equations of motion can be written as follows

$$q_{ab} = g_{ab}+\kappa R_{ab} \tag{5.2}$$

$$\sqrt{-q}q^{ab} = \lambda\sqrt{-g}g^{ab}-\kappa\sqrt{-g}T^{ab} \tag{5.3}$$

where q_{ab} is the auxiliary metric by which the connection Γ^a_{bc} is defined.

In Refs. [7, 33], it was investigated in EiBI gravity that the Universe driven by barotropic fluid with $w\equiv P/\rho>0$ is free from the initial singularity; there exists a state of minimum size for which one takes infinite time to reach from the present for $\kappa>0$. More interestingly, the initial state of the Universe driven by pressureless dust ($w=0$) approaches the de Sitter state of which effective cosmological constant is given by $\Lambda_{\rm eff}=8/\kappa$.[33]

In Refs. [8, 34], the authors investigated compact stars composed of pressureless dust and polytropic fluid. Studying the Poisson equation in EiBI gravity, they obtained singularity-free solutions. For pressureless dust, they could even find the static star solution in the Newtonian limit. In the Newtonian limit of EiBI gravity, the Poisson equation becomes

$$\nabla^2\Phi=4\pi G\rho+\frac{1}{4}\kappa\nabla^2\rho, \tag{5.4}$$

where Φ is the Newtonian potential. The second term in the right-hand side which is the EiBI correction, provides the repulsive nature of gravity.

More subjects in EiBI gravity have been studied such as the cosmological and astrophysical constraints on the EiBI theory [35, 36], the constraint on the value of κ by using the solar model [37], the tensor perturbation [38], bouncing cosmology [39], the five dimensional brane model [40], the effective stress tensor and energy conditions [41], cosmology with scalar fields [42], the instability of compact stars [43], the surface singularity of the compact star [44], etc.

5.2. Research Motivation

In GR, the singularity theorem states that a singularity must be formed in matter collapses provided that the strong-energy condition is satisfied. As all matter collapses towards a center, the matter density at the center will diverge finally, resulting in the appearance of a curvature singularity mostly enclosed by an event horizon, *e.g.*, a black hole solution. Such a formation of singularities simply means the breakdown of Einstein gravity in extremely high density, and it has been believed that some quantum nature of gravity may play a role to resolve such a problem.

EiBI gravity theory has some aspect of quantum gravity as mentioned above. It is already shown that the initial singularity is absent This is probably due to the repulsive nature appearing when the gravity in EiBI theory interacts with matter. As pointed out in Ref. [34], therefore, it will be very interesting to see whether curvature singularities are still formed during matter collapses in EiBI gravity, or the repulsive nature becomes strong enough in extremely dense matter to prevent their formation.

If the repulsive gravity in EiBI gravity is strong enough to prevent the formation of singularity during its final stage of matter collapse, the final state of matter collapse will be static at the center without a curvature singularity. Such star solutions would be expected to be enclosed by an event horizon. Thus, we numerically obtain spherically symmetric static (TOV) star solutions for various polytropic matters, and check if there exists any solution whose size is smaller than its Schwarzschild radius (*i.e.*, $R < 2M$). We found no such solution in EiBI gravity, implying that there exists no singularity-free black hole solution in EiBI gravity theory as a final state of polytropic type matter collapse.

5.3. Static Case

Assuming static and spherically symmetric spacetime, the spacetime metric g_{ab} and the auxiliary metric q_{ab} which are compatible with Γ^a_{bc} are

$$g_{ab} = \begin{pmatrix} -F(r) & 0 & 0 & 0 \\ 0 & B(r) & 0 & 0 \\ 0 & 0 & A(r)r^2 & 0 \\ 0 & 0 & 0 & A(r)r^2\sin^2\theta \end{pmatrix} \tag{5.5}$$

$$q_{ab} = \begin{pmatrix} -s(r) & 0 & 0 & 0 \\ 0 & h(r) & 0 & 0 \\ 0 & 0 & r^2 & 0 \\ 0 & 0 & 0 & r^2\sin^2\theta \end{pmatrix} \tag{5.6}$$

From (5.2), the differential equations of $s(r)$ and $h(r)$ are

$$F(r) = s(r) - \frac{\kappa\left[s'(r)\left\{rs(r)h'(r) + h(r)(-4s(r) + rs'(r))\right\} - 2rh(r)s(r)s''(r)\right]}{4rh^2(r)s(r)} \tag{5.7}$$

$$B(r) = F(r)\frac{h(r)}{s(r)} - \frac{\kappa}{r}\left(\frac{s'(r)}{s(r)} + \frac{h'(r)}{h(r)}\right) \tag{5.8}$$

$$A(r) = 1 + \frac{\kappa}{r^2}\left(\frac{1}{h(r)} - 1\right) + \frac{\kappa}{2rh(r)}\left(\frac{s'(r)}{s(r)} - \frac{h'(r)}{h(r)}\right) \tag{5.9}$$

And from (5.3), the components of the spacetime metric and the auxiliary metric are related as

$$F(r) = s(r)A(r)\frac{\lambda + \kappa\rho(r)}{\lambda - \kappa P(r)} \tag{5.10}$$

$$B(r) = h(r)A(r) \tag{5.11}$$

$$A(r) = \frac{1}{\sqrt{(\lambda - \kappa P(r))(\lambda + \kappa\rho(r))}} \tag{5.12}$$

Rearranging the equations (5.8) and (5.9) as

$$\frac{h'(r)}{h(r)} = \frac{r}{2\kappa}\left[F(r)\frac{h(r)}{s(r)} - B(r) - 2h(r)(A(r) - 1)\right] - \frac{1}{r}(h(r) - 1) \tag{5.13}$$

$$\frac{s'(r)}{s(r)} = \frac{r}{2\kappa}\left[F(r)\frac{h(r)}{s(r)} - B(r) + 2h(r)(A(r) - 1)\right] + \frac{1}{r}(h(r) - 1) \tag{5.14}$$

The conservation of the stress-energy tensor, $\nabla_a T^{ab} = 0$ gives rise to

$$2F(r)P'(r) + F'(r)\left[\rho(r) + P(r)\right] = 0 \tag{5.15}$$

5.4. $P = 0$ Static Case

For dust case, $P = 0$, we can get the equation of $\rho = \rho_0$ by putting $K = 0$ in (5.23)

$$\begin{aligned}\rho_0'(r) &= -\frac{(\lambda+\kappa\rho_0(r))\left(s(r)\left(2\left(h(r)\left(r^2A(r)+\kappa-r^2\right)-\kappa\right)-r^2B(r)\right)+r^2F(r)h(r)\right)}{\kappa^2 r s(r)} \\ &= -\frac{2\left(\lambda+\kappa\rho_0(r)\right)}{\kappa}\frac{s'(r)}{s(r)} \end{aligned} \tag{5.16}$$

or from (5.24)

$$\frac{F'(r)}{F(r)} = \frac{s'(r)}{s(r)} + \frac{a'(r)}{a(r)} = \frac{s'}{s} + \frac{\kappa}{2a^2}\rho_0' = 0 \tag{5.17}$$

where $a = \sqrt{\lambda+\kappa\rho_0}$.

5.5. Numerical Integrations for the Polytropic Stars

5.5.1. Integration of the equations for the EiBI static case

In order to close the set of equations to solve, we need one more equation, i.e., the equation of state (EoS).

Considering the polytropic EoS case,

$$P = K\rho_0^\Gamma \tag{5.18}$$

where $\rho = \rho_0(1+\epsilon)$ and for an isentropic case ($s = 0$)

$$\rho_0\epsilon = \frac{P}{\Gamma-1} \tag{5.19}$$

$$\rho = \rho_0 + \frac{P}{\Gamma-1} = \rho_0 + \frac{K\rho_0^\Gamma}{\Gamma-1} \tag{5.20}$$

Therefore, ρ and P are related as

$$P = K\left(\rho - \frac{P}{\Gamma-1}\right)^\Gamma \tag{5.21}$$

Actually we impose ρ_0 satisfies the conservation equation,

$$\nabla_\mu(\rho_0 u^\mu) = 0 \tag{5.22}$$

However, for the static case, this equation becomes trivial.

Using (5.18), the equation (5.15) can be written as

$$\begin{aligned}\frac{d\rho_0(r)}{dr} \;=\; & \rho_0(r)\left(\Gamma K\rho_0(r)^{\Gamma}+(\Gamma-1)\rho_0(r)\right)\left(\kappa K\rho_0(r)^{\Gamma}-\lambda\right)\\ & \left((\Gamma-1)\lambda+\kappa K\rho_0(r)^{\Gamma}+(\Gamma-1)\kappa\rho_0(r)\right)\\ & \left(s(r)\left(2\left(h(r)\left(r^2A(r)+\kappa-r^2\right)-\kappa\right)-r^2B(r)\right)+r^2F(r)h(r)\right)\\ & /\\ & \kappa r s(r)(-2(\Gamma-2)\Gamma\kappa^2K^3\rho_0(r)^{3\Gamma}-\Gamma\left(\Gamma^2-6\Gamma+5\right)\kappa^2K^2\rho_0(r)^{2\Gamma+1}\\ & -\Gamma\left(\Gamma^2-10\Gamma+8\right)\kappa\lambda K^2\rho_0(r)^{2\Gamma}+\Gamma\left(7\Gamma^2-12\Gamma+5\right)\kappa\lambda K\rho_0(r)^{\Gamma+1}\\ & +(\Gamma-1)^2(3\Gamma-1)\kappa^2K\rho_0(r)^{\Gamma+2}\\ & +4(\Gamma-1)^2\Gamma\lambda^2K\rho_0(r)^{\Gamma}+(\Gamma-1)^2\kappa\lambda\rho_0(r)^2)\end{aligned} \tag{5.23}$$

Let us write down the equation (5.23) in a neat form. From the equation (5.15),

$$\frac{2P'(r)}{[\rho(r)+P(r)]}+\frac{F'(r)}{F(r)} \;=\; 0 \tag{5.24}$$

$\frac{F'(r)}{F(r)}$ can be written using $a\equiv\sqrt{\lambda+\kappa\rho}$ and $b\equiv\sqrt{\lambda-\kappa P}$ as

$$\begin{aligned}F(r) \;&=\; \frac{sa}{b^3}\\ \frac{F'(r)}{F(r)} \;&=\; \frac{s'(r)}{s(r)}+\frac{a'(r)}{a(r)}-3\frac{b'(r)}{b(r)}\end{aligned} \tag{5.25}$$

$a'(r)$ and $b'(r)$ are

$$a'(r) \;=\; \frac{\kappa\rho'(r)}{2a(r)}\;, \qquad b'(r) \;=\; -\frac{\kappa P'(r)}{2b(r)} \tag{5.26}$$

Introducing the sound speed c_s

$$c_s^2 \;\equiv\; \left(\frac{\partial P}{\partial\rho}\right)_s \tag{5.27}$$

For the isentropic process and the polytropic EoS case,

$$c_s^2 \;=\; \frac{P'(r)}{\rho'(r)} \;=\; \frac{\Gamma P}{\rho+P} \tag{5.28}$$

where

$$P'(r) \;=\; \frac{\Gamma P}{\rho_0}\rho_0'\;, \qquad \rho'(r) \;=\; \frac{\rho+P}{\rho_0}\rho_0' \tag{5.29}$$

Then the equation (5.24) becomes

$$\left[\frac{2}{\rho(r)+P(r)}+\frac{\kappa}{2}\left(\frac{3}{b^2}+\frac{1}{a^2c_s^2}\right)\right]P'(r)+\frac{s'(r)}{s(r)} = 0 \tag{5.30}$$

We can remove the theory parameter κ by rescaling ρ, P and r

$$\tilde{\rho} = \kappa\rho \ , \qquad \tilde{P} = \kappa P \tag{5.31}$$

$$\tilde{r} = \frac{r}{\sqrt{\kappa}} \ , \qquad \frac{\partial}{\partial\tilde{r}} = \sqrt{\kappa}\frac{\partial}{\partial r} \tag{5.32}$$

Then (5.13), (5.14) and (5.15) become

$$\frac{h'(\tilde{r})}{h(\tilde{r})} = \frac{\tilde{r}}{2}\left[F(\tilde{r})\frac{h(\tilde{r})}{s(\tilde{r})}-B(\tilde{r})-2h(\tilde{r})(A(\tilde{r})-1)\right]-\frac{1}{\tilde{r}}(h(\tilde{r})-1) \tag{5.33}$$

$$\frac{s'(\tilde{r})}{s(\tilde{r})} = \frac{\tilde{r}}{2}\left[F(\tilde{r})\frac{h(\tilde{r})}{s(\tilde{r})}-B(\tilde{r})+2h(\tilde{r})(A(\tilde{r})-1)\right]+\frac{1}{\tilde{r}}(h(\tilde{r})-1) \tag{5.34}$$

$$2F(\tilde{r})\tilde{P}'(\tilde{r})+F'(\tilde{r})\left[\tilde{\rho}(\tilde{r})+\tilde{P}(\tilde{r})\right] = 0 \tag{5.35}$$

λ is related to the cosmological constant Λ

$$\Lambda = \frac{(\lambda-1)}{\kappa} \tag{5.36}$$

In order to integrate (5.13), (5.14) and (5.23) we need to know the value of h, s and ρ_0 at a certain starting point. To obtain the values we impose regularity conditions at the center, $r=0$. Then one can expand h, s and ρ_0 as

$$\begin{aligned} s(r) &= s_0+s_1r+s_2r^2+s_3r^3+\cdots \\ h(r) &= h_0+h_1r+h_2r^2+h_3r^2+\cdots \\ \rho_0(r) &= \rho_C+\rho_1r+\rho_2r^2+\rho_3r^3+\cdots \end{aligned} \tag{5.37}$$

We also need to expand P at the center because ρ_0 and P are not related by integer power.

$$P(r) = P_0+P_1r+P_2r^2+P_3r^2+\cdots \tag{5.38}$$

5.5.2. Boundary conditions and numerical method

The components of the equations of motion of 2nd kind in Eq. (5.2) are given by

$$(t,t): \quad s - F + \kappa\frac{s}{h}\left[\frac{1}{2}\frac{s''}{s} - \frac{1}{4}\left(\frac{s'}{s}\right)^2 - \frac{1}{4}\frac{s'h'}{sh} + \frac{s'}{sr}\right] = 0, \tag{5.39}$$

$$(r,r): \quad h - B + \kappa\left[\frac{1}{2}\frac{s''}{s} - \frac{1}{4}\left(\frac{s'}{s}\right)^2 - \frac{1}{4}\frac{s'h'}{sh} - \frac{h'}{hr}\right] = 0, \tag{5.40}$$

$$(\theta_i,\theta_i): \quad 1 - A + \frac{\kappa}{hr}\left[\frac{1}{2}\frac{s'}{s} - \frac{1}{2}\frac{h'}{h} - \frac{h-1}{r}\right] = 0. \tag{5.41}$$

From conservation of the energy-momentum tensor, $\nabla^g_\mu T^{\mu\nu} = 0$, we have

$$F'(\rho + P) + 2FP' = 0. \tag{5.42}$$

Using Eqs. (5.39)-(5.41), we can eliminate s'' and obtain first-order differential equations for $s(r)$ and $h(r)$. From Eq. (5.42) with the polytropic equation of state Eq. (5.18), we can get a first-order differential equation for $\rho_0(r)$. We impose regularity conditions at the center as follows:

$$s(r) \sim s_0 + s_2 r^2\,, \qquad h(r) \sim 1 + h_2 r^2\,, \qquad \rho_0(r) \sim \rho_0^c + \rho_{02} r^2\,. \tag{5.43}$$

We tune the value of $F(r=0)$ in order to set $s_0 = 1$ by a time reparametrization.

The set of first-order differential equations for $s(r)$, $h(r)$ and $\rho_0(r)$ with the boundary conditions at the origin is solved numerically by using the fourth-order Runge-Kutta method.

5.6. Survey of EiBI Static Star

The solution is completely determined once the density at the center ($\rho_0^c = \rho_0$ at $r = 0$) is given, and some of the solutions obtained for the case of $\kappa = 1$ and $\lambda = 1$ are shown in Figs. 5.1, 5.2, and 5.3. For matter of $\alpha = 1$ and $\beta = 2$, Figs. 5.1 and 5.2 show how the size (R) and the mass (M) of the star vary as the central density ρ_0^c increases. They behave similarly as in the case of Einstein gravity, but are larger than those in the Einstein gravity. For instance, the maximum mass at $\rho_0^c = 0.32$, beyond which the solutions are presumably unstable under small perturbations, is about 6.3 times larger. Note, however, that the size of the star in the EiBI gravity theory decreases more rapidly and that there exists a maximum central density, $\rho_{0\,\max}^c = (\lambda/(\kappa\alpha))^{1/\beta}$, as given by Eqs. (5.12) and (5.18). We also point out that the star in the EiBI gravity theory becomes bulky: *e.g.*, $R_{\rm EiBI} \sim 5.3 R_{\rm GR}$ for the case of $\rho_0^c = 0.1$, which

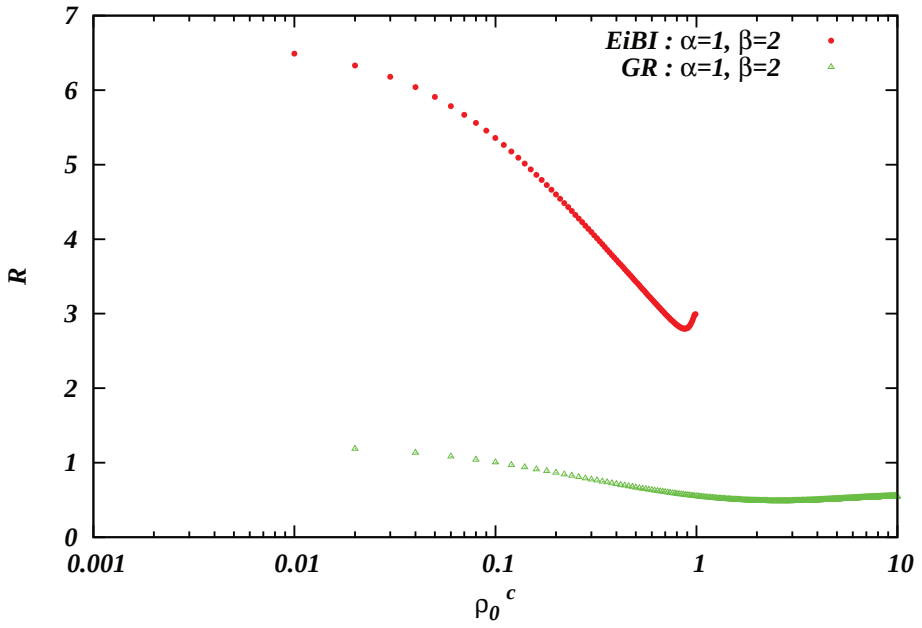

Figure 5.1: Comparison between EiBI and GR TOV solution.

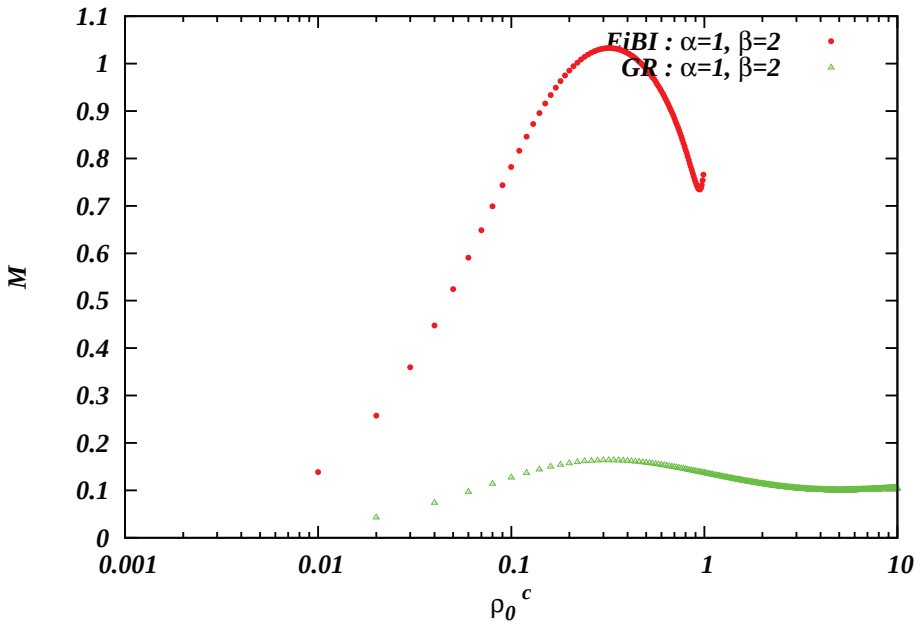

Figure 5.2: Comparison between EiBI and GR TOV solution.

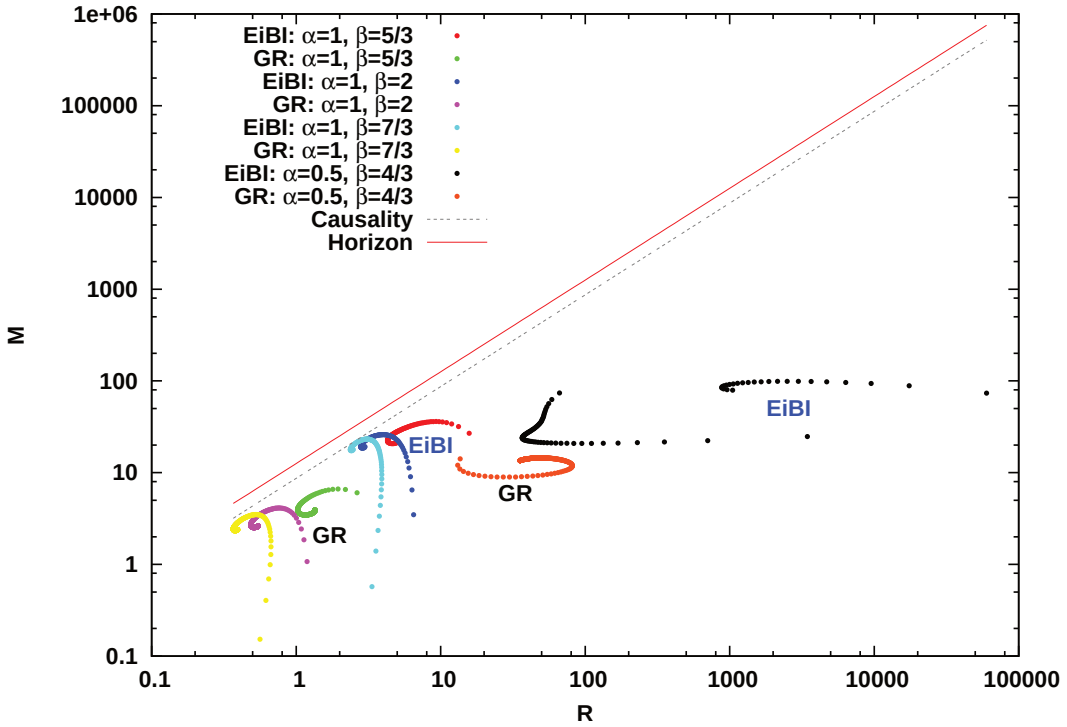

Figure 5.3: Comparison of mass-radius trajectories between the EiBI ($\kappa = 1$) and the GR. Horizon is $R = 2GM/c^2$ and causality constraint is $R > 2.9GM/c^2$.

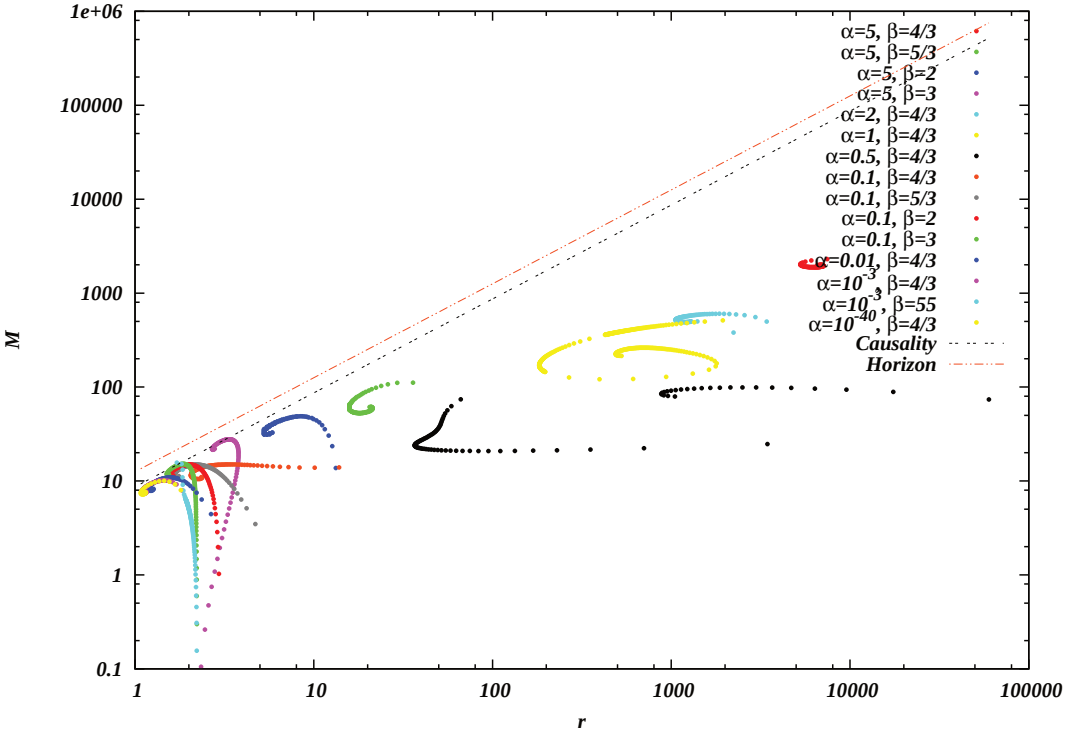

Figure 5.4: Thorough parameter survey of polytropic static star solutions.

is probably due to the repulsive nature in the EiBI theory of gravity. Fig. 5.3 shows how the masses and the sizes of the star solutions distribute as the EOS for matter varies.

We perform thorough parameter survey of EiBI polytropic static stars. Fig. 5.4 shows the results. For different κ, one can obtain solutions not by solving the equations of motion but by using the scaling behavior, Eqs. (5.31), (5.32), and

$$\tilde{\rho_0} = \kappa\rho_0 \ , \qquad \tilde{\alpha} = \kappa^{1-\beta}\alpha \, . \tag{5.44}$$

We summarize our survey as follows:

- As α grows, the curves go right up, but far from the horizon.
- As β grows, the curves approach the horizon, but do not touch.
- It seems there is no static configuration inside the horizon.
- Very large star configuration seems to exist in EiBI theory.

It seems there are diverging configurations of polytropic static stars in EiBI theory. (See Fig. 5.5)

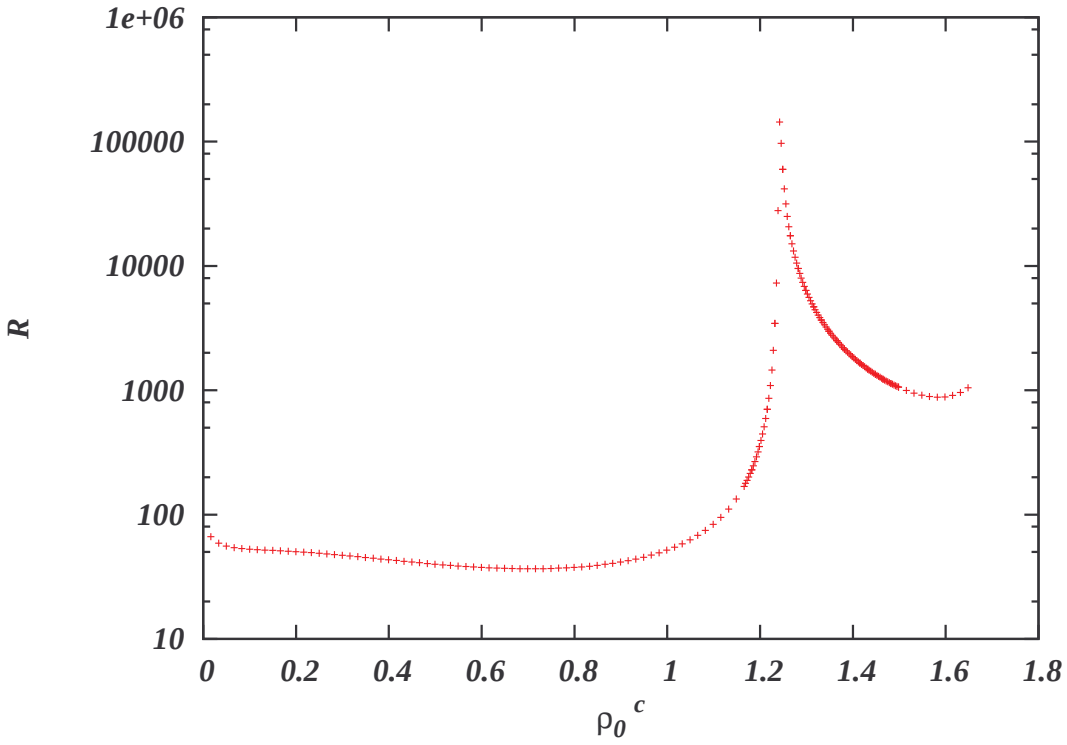

Figure 5.5: $\alpha = 0.5$, $\beta = 4/3$, and $\kappa = 1$

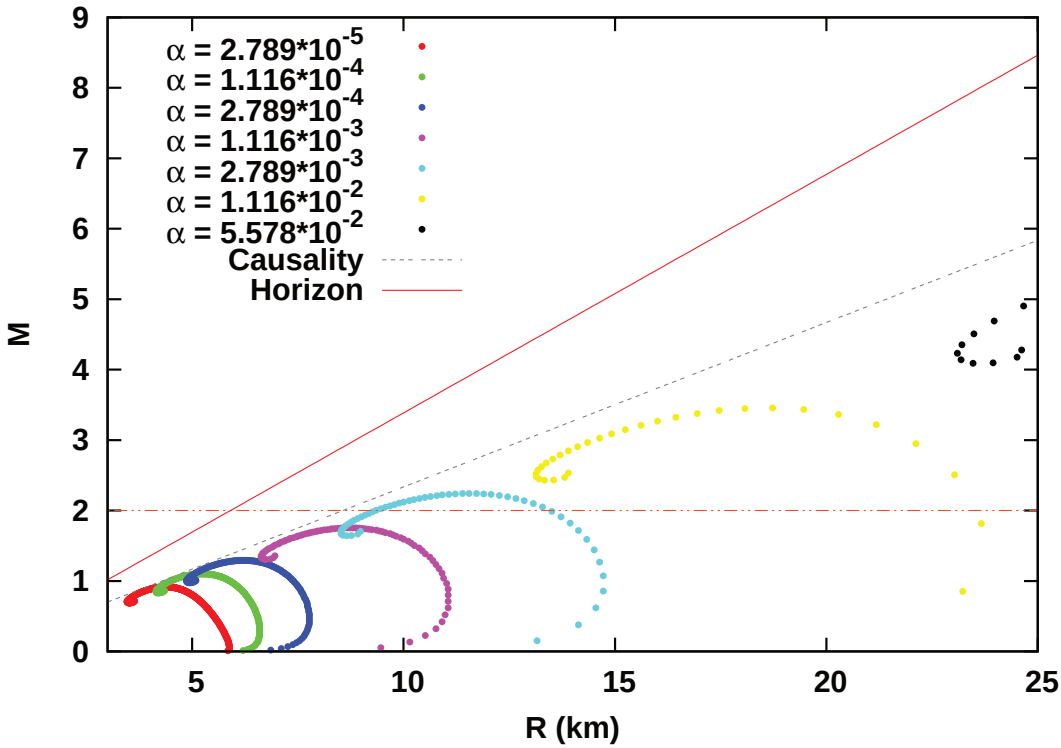

Figure 5.6: ($\kappa\rho_{CNS} = 0.1$ and $\beta = 2.34$) $\rho_{CNS} = 8 \times 10^{17} kg/m^3$, typical central density of neutron stars

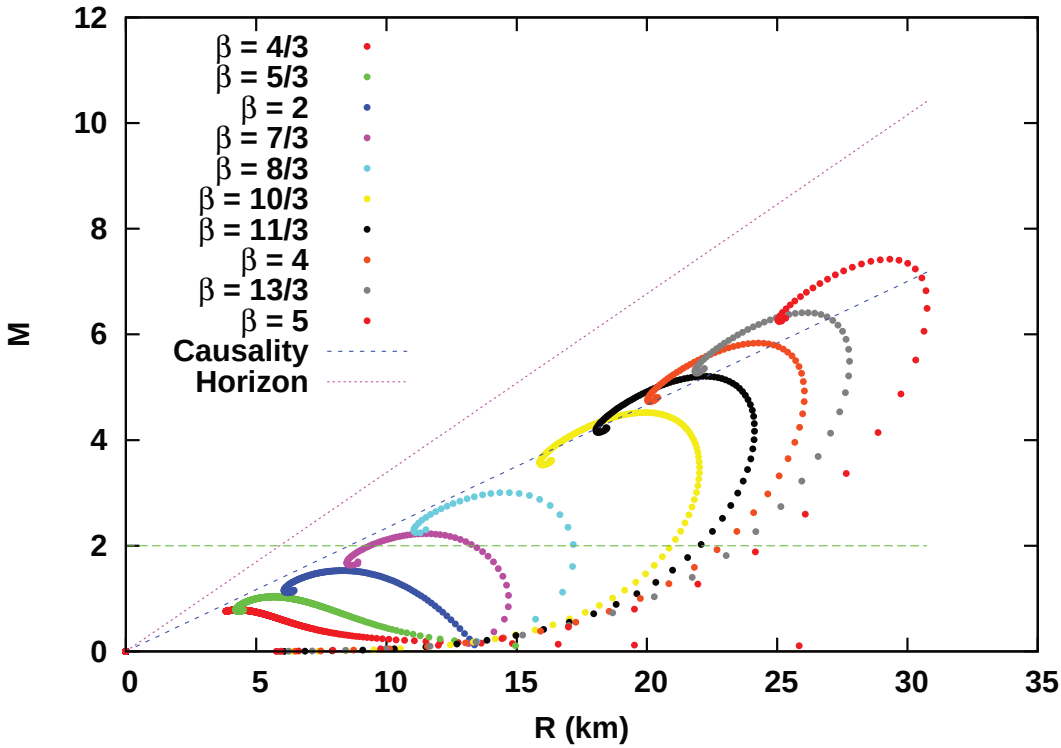

Figure 5.7: ($\kappa\rho_{CNS} = 0.1$ and $\alpha = 2.789 \times 10^{-3}$) $\rho_{CNS} = 8 \times 10^{17} kg/m^3$, typical central density of neutron stars

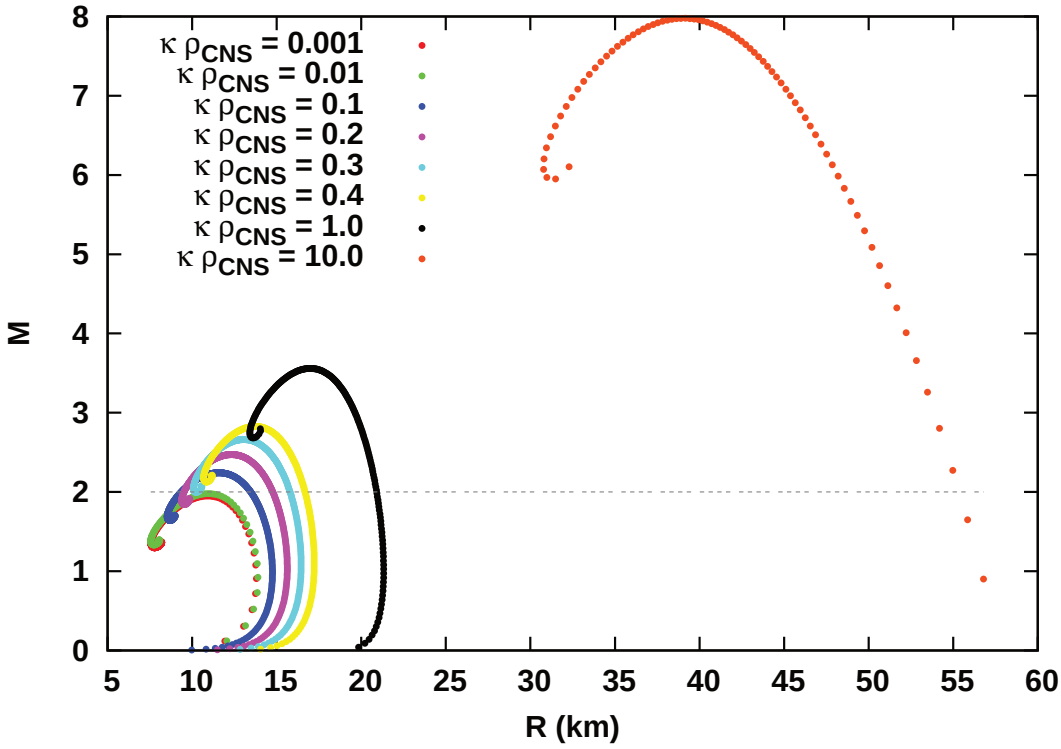

Figure 5.8: ($\alpha = 1.544$ (in cgs unit) and $\beta = 2.34$)

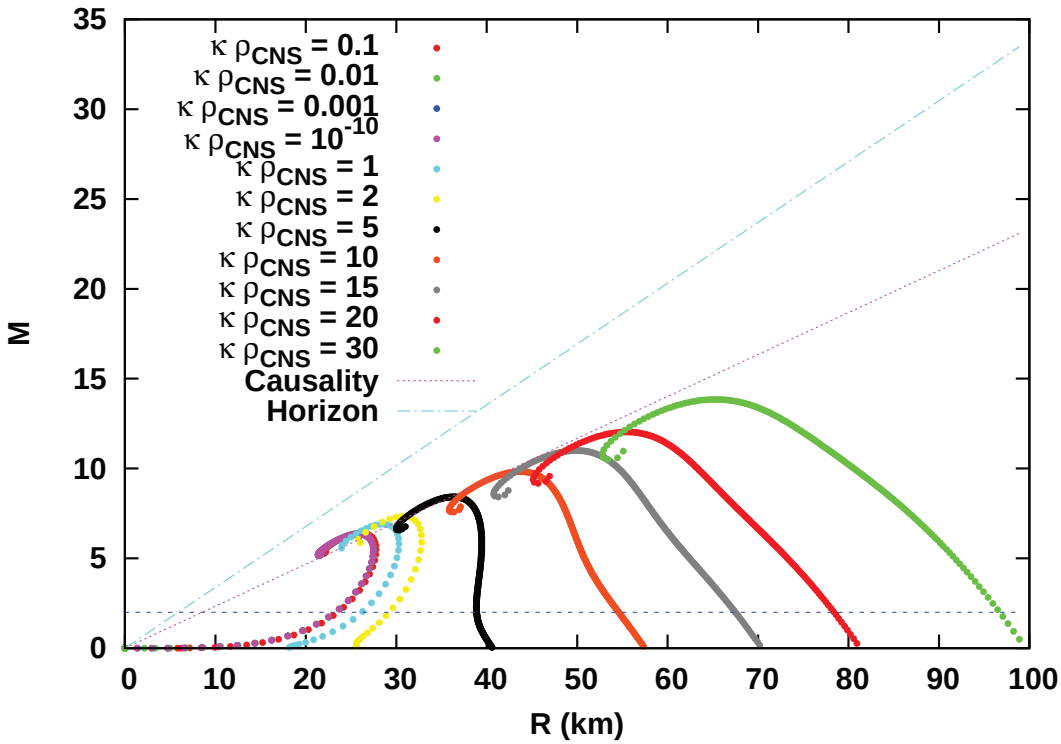

Figure 5.9: Varying κ where mass-radius trajectory crosses the GR causality limit. ($\alpha = 1.544$ (in cgs unit) and $\beta = 13/3$)

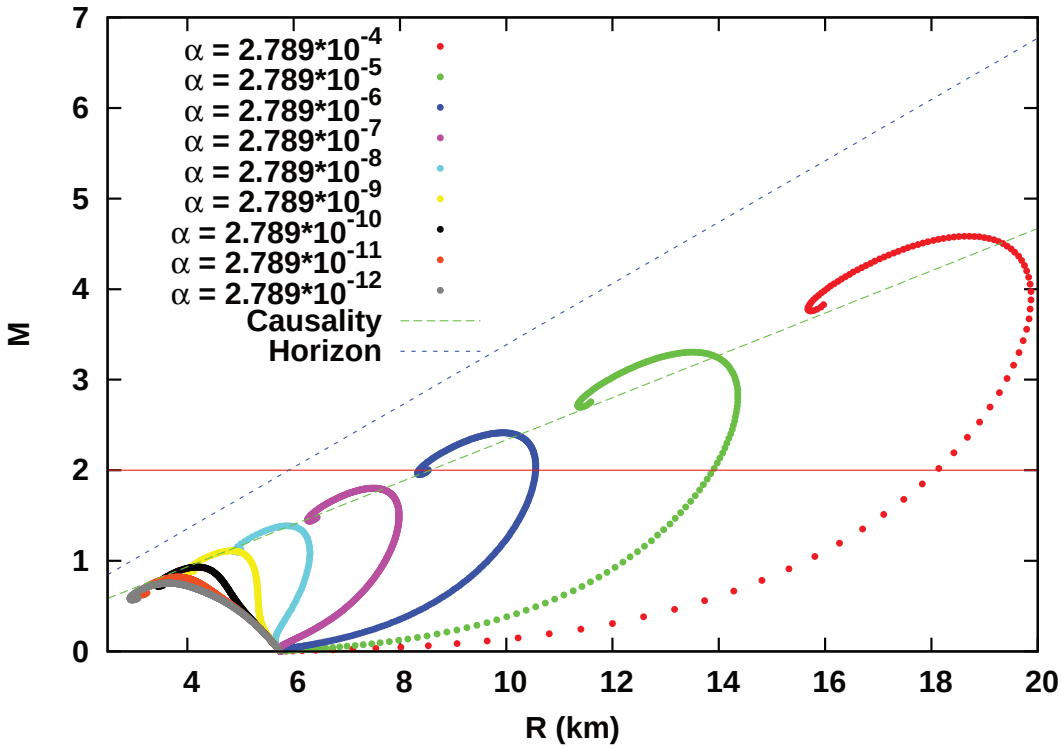

Figure 5.10: Varying α where mass-radius trajectory crosses the GR causality limit. ($\kappa\rho_{CNS} = 0.1$ and $\beta = 13/3$)

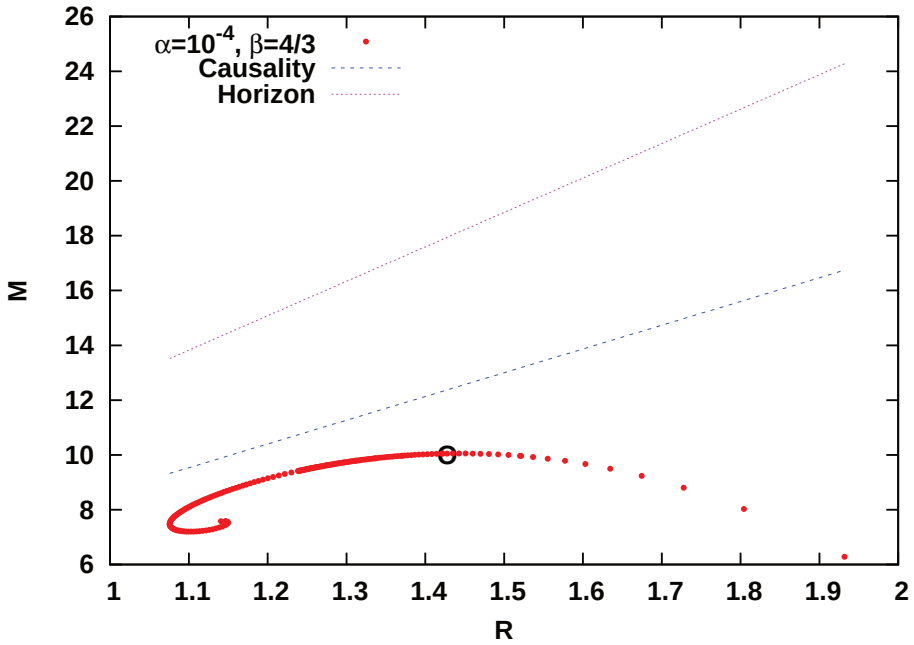

Figure 5.11: Mass-radius trajectories ($\kappa = 1$, $\alpha = 10^{-4}$ and $\beta = 4/3$)

Patterns with varying α (Figs. 5.6 and 5.10), β (Fig. 5.7), and κ (Figs. 5.8 and 5.9).

Figure 5.12 shows the profile of metric functions.

Figure 5.13 shows the "tail" of mass-radius trajectory of EiBI theory. It is similar to GR.

When the trajectory crosses the causal boundary, Figs. 5.14, 5.15, and 5.16 show the sound velocity limit.

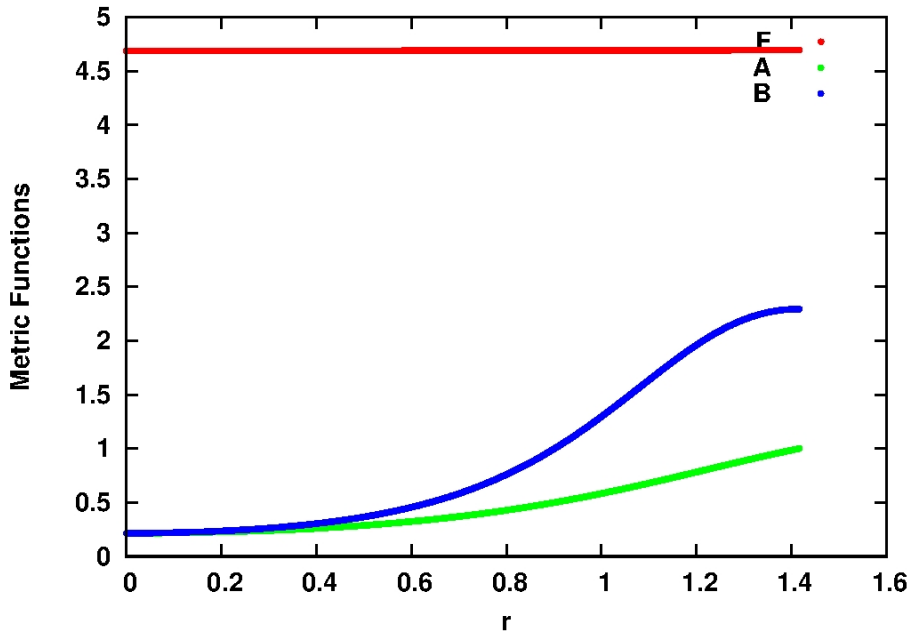

Figure 5.12: Metric functions $F(r)$, $A(r)$ and $B(r)$ at the point "O" in Figure (5.11). ($\kappa = 1$, $\alpha = 10^{-4}$ and $\beta = 4/3$)

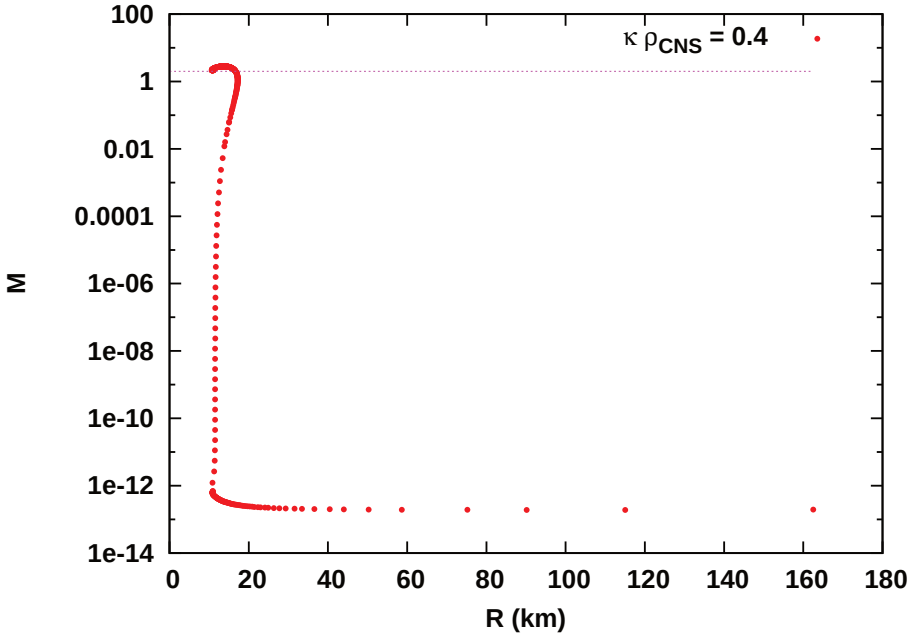

Figure 5.13: Mass-radius trajectory. ($\kappa\rho_{CNS} = 0.4$, $\alpha = 2.789 \times 10^{-3}$ and $\beta = 2.34$)

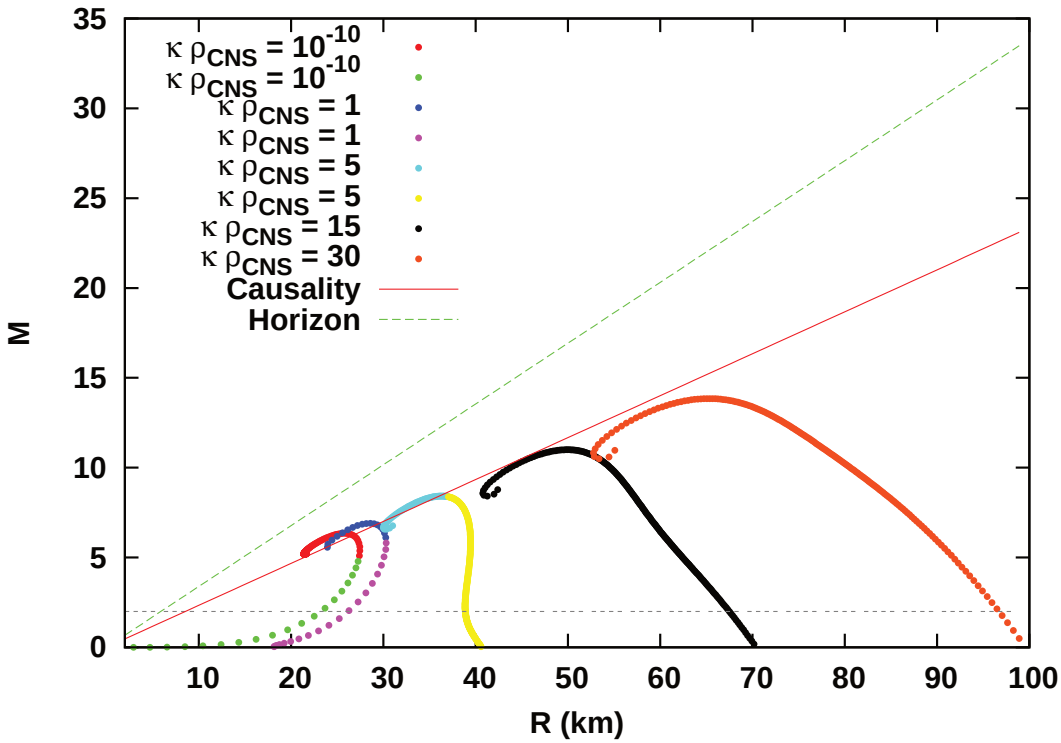

Figure 5.14: Sound velocity limit, $\rho_0^{\beta-1} = \frac{\beta-1}{(\beta-2)\beta\alpha}$ ($\alpha = 1.544$ (in cgs unit) and $\beta = 13/3$)

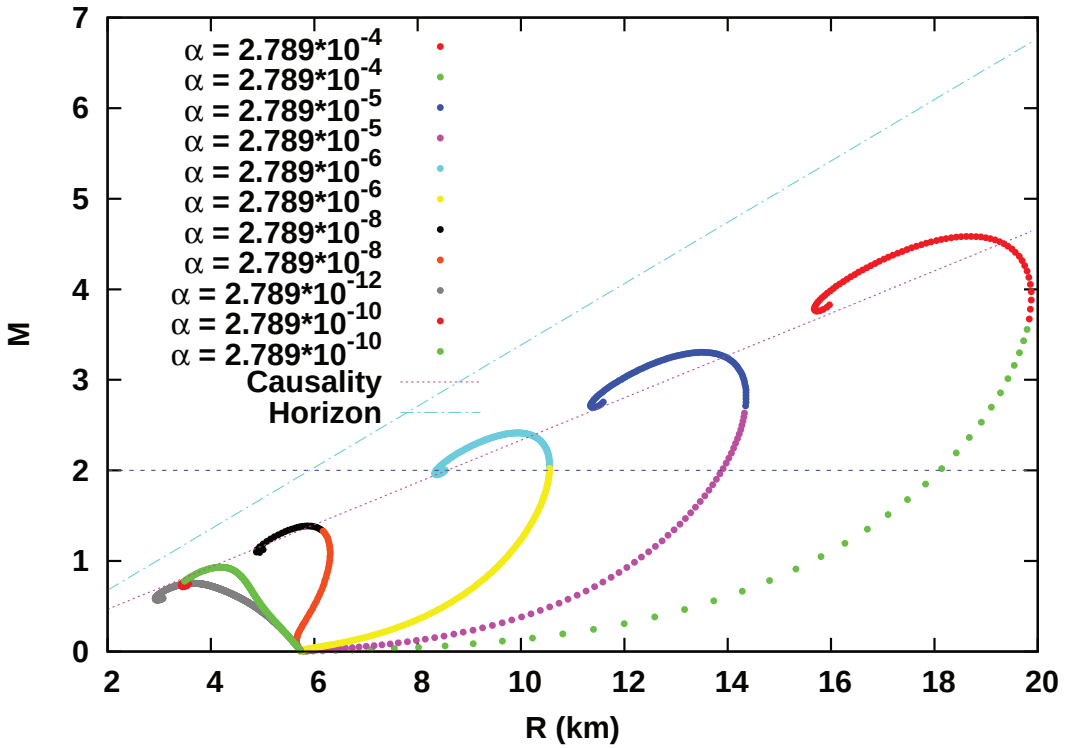

Figure 5.15: Sound velocity limit, $\rho_0^{\beta-1} = \frac{\beta-1}{(\beta-2)\beta\alpha}$ ($\kappa\rho_{CNS} = 0.1$ and $\beta = 13/3$)

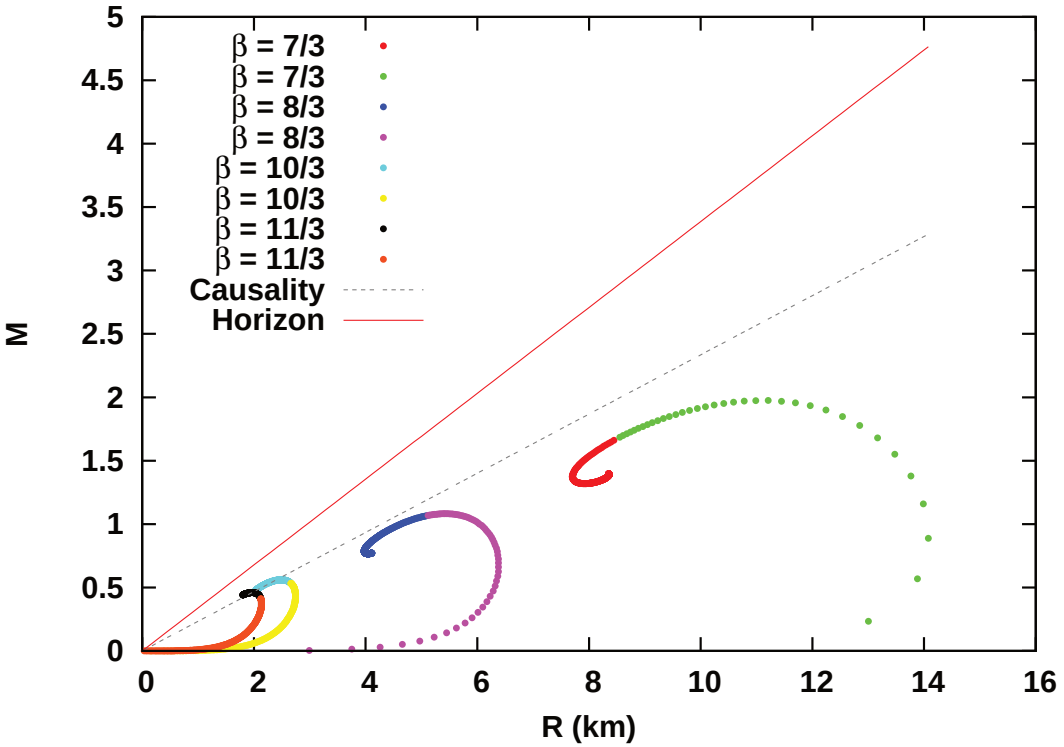

Figure 5.16: GR case. Because there is no central density upper limit, there always exists the density satisfying the sound velocity limit, $\rho_0^{\beta-1} = \frac{\beta-1}{(\beta-2)\beta\alpha}$. ($\alpha = 1187.0$)

6. CONCLUSION

In this thesis, we described the formulations and the numerical methods used to implement a fully general relativistic code that can be used to simulate a system of spherically symmetric perfect fluid matter. The accuracy and the convergence of my numerical code are verified by performing several test problems such as the relativistic blast wave problem, relativistic spherical accretion of matter onto a black hole, a TOV star and an OS dust collapse. Spherical blast wave test shows hydrodynamic part of my code handles discontinuous solution well. From the relativistic spherical accretion simulation, my code evolve to the stationary state well and the results and exact solutions are in good agreement. The code evolve static TOV solution stably for a long time, and the radial pulsation mode frequencies are in excellent agreement. From the Oppenheimer-Snyder dust collapse, my code is fully tested. The evolution results match the exact solution well except around the origin and near the dust boundary. It may be due to the non-zero pressure and boundary effect. We surveyed large parameter space for TOV stars in EiBI gravity theory. So far there is no static star configuration inside the event horizon, i.e., collapsing star to a black hole can not avoid $r = 0$ singularity.

Although my developed code passed all four main tests well, we give several comments for further improvement of the code. For the slicing condition, we considered the maximal slicing only. Polar slicing and other slicing conditions are possible. After some investigations with the choice of coordinate systems, one can clarify the advantages and disadvantages of the gauge choices. For the coordinate system choice, I chose 3+1 conformal coordinates with future tests and comparisons of multidimensional simulation codes in mind. The coordinate-transformation skill implemented numerically here will be useful for testing multidimensional simulation codes. For the flux calculations, I concentrated on a couple of successful implementations, namely, Roe and HLLE methods with an MC limiter. However, I found not much difference in the results between them. I did not consider many other choices of numerical flux calculations and limiters. Implementation using other methods is of interest, and I leave it for the future work.

In the TOV test, I observed the numerical results for the radial pulsation mode frequencies in excellent agreement with the known ones. However, I also observe additional small peaks, as can be seen in Fig. 4.10. These peaks are thought to be caused by the use of a finite-time series in the Fourier transformation. In OS collapse test, there are deviations from the exact solution at the center and on the star boundary. The discrepancy also reported in[31], they

guessed the reason is due to diverging terms near the origin. Finally, I mention that extension of our code to 3D and incorporating various micro-physics for matter are necessary to simulate more realistic astrophysical phenomena.

Appendix A. PARTIAL DERIVATIVES

A.1. Determinant of Partial Derivatives

Let us define the determinant of partial derivatives,[1]

$$\frac{D(A,B)}{D(C,D)} \equiv \begin{vmatrix} \left.\frac{\partial A}{\partial C}\right|_D & \left.\frac{\partial B}{\partial C}\right|_D \\ \left.\frac{\partial A}{\partial D}\right|_C & \left.\frac{\partial B}{\partial D}\right|_C \end{vmatrix}. \tag{A.1}$$

This determinant (A.1) has following properties,

Property 1

$$\begin{aligned} \frac{D(A,B)}{D(C,D)} &= -\frac{D(A,B)}{D(D,C)} = \frac{D(B,A)}{D(D,C)} \\ &= -\frac{D(B,A)}{D(C,D)} \end{aligned} \tag{A.2}$$

Property 2

$$\frac{D(A,B)}{D(C,B)} = \left.\frac{\partial A}{\partial C}\right|_B \tag{A.3}$$

Property 3

$$\frac{D(A,B)}{D(C,D)} = \frac{D(A,B)}{D(P,Q)}\frac{D(P,Q)}{D(C,D)} \tag{A.4}$$

where (C,D) and (P,Q) are complete basis.

Property 3 can be proved using the chain rule of partial derivatives,

$$\left.\frac{\partial A}{\partial C}\right|_D = \left.\frac{\partial A}{\partial P}\right|_Q \left.\frac{\partial P}{\partial C}\right|_D + \left.\frac{\partial A}{\partial Q}\right|_P \left.\frac{\partial Q}{\partial C}\right|_D,$$

$$\left.\frac{\partial B}{\partial D}\right|_C = \left.\frac{\partial B}{\partial P}\right|_Q \left.\frac{\partial P}{\partial D}\right|_C + \left.\frac{\partial B}{\partial Q}\right|_P \left.\frac{\partial Q}{\partial D}\right|_C,$$

$$\left.\frac{\partial B}{\partial C}\right|_D = \left.\frac{\partial B}{\partial P}\right|_Q \left.\frac{\partial P}{\partial C}\right|_D + \left.\frac{\partial B}{\partial Q}\right|_P \left.\frac{\partial Q}{\partial C}\right|_D,$$

[1] I am grateful to Prof. Shoichi Yamada for helping me to manipulate the partial derivatives with different complete basis using this definition.

$$\left.\frac{\partial A}{\partial D}\right|_C = \left.\frac{\partial A}{\partial P}\right|_Q \left.\frac{\partial P}{\partial D}\right|_C + \left.\frac{\partial A}{\partial Q}\right|_P \left.\frac{\partial Q}{\partial D}\right|_C .$$

Then the left-hand side of (A.4) is

$$\frac{D(A,B)}{D(C,D)} = \left.\frac{\partial A}{\partial C}\right|_D \left.\frac{\partial B}{\partial D}\right|_C - \left.\frac{\partial B}{\partial C}\right|_D \left.\frac{\partial A}{\partial D}\right|_C$$

and the right-hand side of (A.4) is

$$\begin{aligned}\frac{D(A,B)}{D(P,Q)}\frac{D(P,Q)}{D(C,D)} &= \left(\left.\frac{\partial A}{\partial P}\right|_Q \left.\frac{\partial B}{\partial Q}\right|_P - \left.\frac{\partial B}{\partial P}\right|_Q \left.\frac{\partial A}{\partial Q}\right|_P\right)\left(\left.\frac{\partial P}{\partial C}\right|_D \left.\frac{\partial Q}{\partial D}\right|_C - \left.\frac{\partial Q}{\partial C}\right|_D \left.\frac{\partial P}{\partial D}\right|_C\right) \\ &= \left.\frac{\partial A}{\partial C}\right|_D \left.\frac{\partial B}{\partial D}\right|_C - \left.\frac{\partial B}{\partial C}\right|_D \left.\frac{\partial A}{\partial D}\right|_C .\end{aligned}$$

■

A.2. Partial Derivative with Different Complete Basis

Consider two coordinate basis (τ, χ) and (t, r). We can write down the relation between the two coordinates as

$$\tau = \tau(t,r), \qquad \chi = \chi(t,r). \tag{A.5}$$

Then, the infinitesimal change $d\tau$ and $d\chi$ can be written

$$d\tau = \left.\frac{\partial \tau}{\partial t}\right|_r dt + \left.\frac{\partial \tau}{\partial r}\right|_t dr, \tag{A.6}$$

$$d\chi = \left.\frac{\partial \chi}{\partial t}\right|_r dt + \left.\frac{\partial \chi}{\partial r}\right|_t dr. \tag{A.7}$$

Now, let us change the coordinate basis to (t, χ). τ and r can be written in terms of (t, χ) as

$$\tau = \tau(t,\chi), \qquad r = r(t,\chi), \tag{A.8}$$

and

$$d\tau = \left.\frac{\partial \tau}{\partial t}\right|_\chi dt + \left.\frac{\partial \tau}{\partial \chi}\right|_t d\chi, \tag{A.9}$$

$$dr = \left.\frac{\partial r}{\partial t}\right|_\chi dt + \left.\frac{\partial r}{\partial \chi}\right|_t d\chi. \tag{A.10}$$

From (A.6), (A.7), (A.9), and (A.10), we can obtain following relations of par-

tial derivatives,

$$\left.\frac{\partial\tau}{\partial t}\right|_r = \left.\frac{\partial\tau}{\partial t}\right|_\chi - \frac{\left.\frac{\partial r}{\partial t}\right|_\chi}{\left.\frac{\partial r}{\partial\chi}\right|_t}\left.\frac{\partial\tau}{\partial\chi}\right|_t, \tag{A.11}$$

$$\left.\frac{\partial\tau}{\partial r}\right|_t = \frac{\left.\frac{\partial\tau}{\partial\chi}\right|_t}{\left.\frac{\partial r}{\partial\chi}\right|_t}, \tag{A.12}$$

$$\left.\frac{\partial\chi}{\partial t}\right|_r = -\frac{\left.\frac{\partial r}{\partial t}\right|_\chi}{\left.\frac{\partial r}{\partial\chi}\right|_t}, \tag{A.13}$$

$$\left.\frac{\partial\chi}{\partial r}\right|_t = \frac{1}{\left.\frac{\partial r}{\partial\chi}\right|_t}. \tag{A.14}$$

One can obtain the relations (A.11), (A.12), (A.13), and (A.14) more systematically using the determinant introduced in Section A.1.

$$\begin{aligned}\left.\frac{\partial\tau}{\partial t}\right|_r &= \frac{D(\tau,r)}{D(t,r)} = \frac{D(\tau,r)}{D(t,\chi)}\frac{D(t,\chi)}{D(t,r)}\\ &= \begin{vmatrix} \left.\frac{\partial\tau}{\partial t}\right|_\chi & \left.\frac{\partial r}{\partial t}\right|_\chi \\ \left.\frac{\partial\tau}{\partial\chi}\right|_t & \left.\frac{\partial r}{\partial\chi}\right|_t \end{vmatrix} \frac{1}{\frac{D(r,t)}{D(\chi,t)}}\\ &= \left.\frac{\partial\tau}{\partial t}\right|_\chi - \frac{\left.\frac{\partial r}{\partial t}\right|_\chi}{\left.\frac{\partial r}{\partial\chi}\right|_t}\left.\frac{\partial\tau}{\partial\chi}\right|_t.\end{aligned}$$

$$\begin{aligned}\left.\frac{\partial\tau}{\partial r}\right|_t &= \frac{D(\tau,t)}{D(r,t)} = \frac{D(\tau,t)}{D(t,\chi)}\frac{D(t,\chi)}{D(r,t)}\\ &= \frac{D(\tau,t)}{D(\chi,t)}\frac{1}{\frac{D(r,t)}{D(\chi,t)}} = \frac{\left.\frac{\partial\tau}{\partial\chi}\right|_t}{\left.\frac{\partial r}{\partial\chi}\right|_t}.\end{aligned}$$

$$\begin{aligned}\left.\frac{\partial\chi}{\partial t}\right|_r &= \frac{D(\chi,r)}{D(t,r)} = \frac{D(\chi,r)}{D(t,\chi)}\frac{D(t,\chi)}{D(t,r)}\\ &= -\frac{D(r,\chi)}{D(t,\chi)}\frac{1}{\frac{D(r,t)}{D(\chi,t)}} = -\frac{\left.\frac{\partial r}{\partial t}\right|_\chi}{\left.\frac{\partial r}{\partial\chi}\right|_t}.\end{aligned}$$

$$\left.\frac{\partial \chi}{\partial r}\right|_t = \frac{D(\chi,t)}{D(r,t)} = \frac{1}{\frac{D(r,t)}{D(\chi,t)}} = \frac{1}{\left.\frac{\partial r}{\partial \chi}\right|_t}\,.$$

Bibliography

[1] M. M. May and R. H. White, "Hydrodynamic calculations of general-relativistic collapse," *Physical Review* **141** (1966) 1232–1241. http://link.aps.org/doi/10.1103/PhysRev.141.1232. 1

[2] J. A. Font, "Numerical hydrodynamics and magnetohydrodynamics in general relativity," *Living Rev. Relativity* **11** (2008) 7. http://www.emis.ams.org/journals/LRG/Articles/lrr-2008-7/download/lrr-2008-7BW.pdf. 1

[3] J. R. Wilson and G. J. Mathews, *Relativistic Numerical Hydrodynamics*. Cambridge University Press, New York, 2003. http://dx.doi.org/10.1017/CBO9780511615917. 1

[4] M. Alcubierre, *Introduction to 3+1 numerical relativity*. International series of monographs on physics. Oxford Univ. Press, Oxford, 2008. 1

[5] T. W. Baumgarte and S. L. Shapiro, *Numerical Relativity: Solving Einsteins Equations on the Computer*. Cambridge University Press, New York, 2010. 1

[6] J. R. Oppenheimer and H. Snyder, "On continued gravitational contraction," *Phys. Rev.* **56** (1939) 455–459. http://link.aps.org/doi/10.1103/PhysRev.56.455. 1, 4.4

[7] M. Banados and P. G. Ferreira, "Eddington's theory of gravity and its progeny," *Phys. Rev. Lett.* **105** (2010) 011101, arXiv:1006.1769 [astro-ph.CO]. 1, 5.1, 5.1

[8] V. C. P. Pani and T. Delsate, "Compact stars in Eddington inspired gravity," *Phys. Rev. Lett.* (2011) 031101, arXiv:1106.3569 [gr-qc]. 1, 5.1

[9] "http://laplace.physics.ubc.ca/Group/Software.html." http://laplace.physics.ubc.ca/Group/Software.html. 1

[10] R. M. Wald, *General Relativity*. University of Chicago Press, Chicago, 1984. 2.1

[11] J. James W. York, *Kinematics and dynamics of general relativity:* Sources of Gravitational Radiation. Cambridge University Press, Cambridge, 1979. 2.1, 2.1.1.2

[12] E. Gourgoulhon, "3+1 formalism and bases of numerical relativity," arXiv:gr-qc/0703035 [GR-QC]. 2.1

[13] U. Sperhake, "Nonlinear numerical schemes in general relativity," arXiv:gr-qc/0201086 [gr-qc]. 2.1

[14] I. I. Olabarrieta, *Relativistic Hydrodynamics and other topics in Numerical Relativity.* PhD thesis, University of British Columbia, 2004. http://bh0.phas.ubc.ca/Members/matt/Doc/Theses/Phd/olabarrieta.pdf. 2.1

[15] A. Lichnerowicz, *Relativistic Hydrodynamics and Magnetohydrodynamics.* Benjamin, New York, 1967. 2.2.1.1

[16] M. Shibata, *Basic equations and methods of GRHD and GRMHD.* lectures at 2007 Summer School on Computational Methods in Gravitation and Astrophysics, APCTP, Pohang, 2007. 2.2.1.4

[17] P. L. Roe, "Approximate Riemann solvers, parameter vectors, and difference schemes," *Journal of Computational Physics* **43** no. 2, (1981) 357 – 372. http://www.sciencedirect.com/science/article/pii/0021999181901285. 3.2

[18] A. Harten, P. Lax, and B. Leer, "On upstream differencing and Godunov-type schemes for hyperbolic conservation laws," *SIAM Review* **25** no. 1, (1983) 35–61. http://epubs.siam.org/doi/abs/10.1137/1025002. 3.2

[19] B. Einfeld, "On Godunov-type methods for gas dynamics," *SIAM J. Numer. Anal.* **25** no. 2, (1988) 294–318. http://dx.doi.org/10.1137/0725021. 3.2

[20] L. Baiotti, *Numerical relativity simulations of non-vaccum spacetimes in three dimensions.* PhD thesis, SISSA, 2004. http://digitallibrary.sissa.it/bitstream/id/288/146_89.pdf/. 3.2.5

[21] F. Guzman, F. Lora-Clavijo, and M. Morales, "Revisiting spherically symmetric relativistic hydrodynamics," *Rev. Mex. Fis.* **E58** (2012) 84–98, arXiv:1212.1421 [gr-qc]. 4.1, 4.1

[22] H. Bondi, "On spherically symmetrical accretion," *Monthly Notices of the Royal Astronomical Society* **112** (1952) 195. 4.2

[23] F. Michel, "Accretion of matter by condensed objects," *Astrophysics and Space Science* **15** (1972) 153–160. http://dx.doi.org/10.1007/BF00649949. 4.2

[24] S. L. Shapiro and S. A. Teukolsky, *Black holes, white dwarfs, and neutron stars: the physics of compact objects*. Wiley, New York, 1983. 4.2

[25] P. Papadopoulos and J. A. Font, "Relativistic hydrodynamics around black holes and horizon adapted coordinate systems," *Phys. Rev. D* **58** (1998) 024005. http://link.aps.org/doi/10.1103/PhysRevD.58.024005. 4.2, 4.2, 4.2

[26] C. W. Misner, K. S. Thorne, and J. A. Wheeler, *Gravitation*. W. H. Freeman, 1973. 4.3.5

[27] J. M. Bardeen, K. S. Thorne, and D. W. Meltzer, "A catalogue of methods for studying the normal modes of radial pulsation of general-relativistic stellar models," *Astrophysical Journal* **145** (1966) 505. 4.3.5

[28] S. Yoshida and Y. Eriguchi, "Quasi-radial modes of rotating stars in general relativity," *Monthly Notices of the Royal Astronomical Society* **322** no. 2, (2001) 389–396. http://dx.doi.org/10.1046/j.1365-8711.2001.04115.x. 4.3.5

[29] J. A. Font, T. Goodale, S. Iyer, M. Miller, L. Rezzolla, E. Seidel, N. Stergioulas, W.-M. Suen, and M. Tobias, "Three-dimensional numerical general relativistic hydrodynamics. II. long-term dynamics of single relativistic stars," *Phys. Rev. D* **65** (2002) 084024. http://link.aps.org/doi/10.1103/PhysRevD.65.084024. 4.3.5

[30] J. V. Romero, J. M. A. Ibanez, J. M. A. Marti, and J. A. Miralles, "A new spherically symmetric general relativistic hydrodynamical code," *Astrophysical Journal* **462** (1996) 839, arXiv:astro-ph/9509121. 4.4.3

[31] E. O'Connor and C. D. Ott, "A New Open-Source Code for Spherically-Symmetric Stellar Collapse to Neutron Stars and Black Holes," *Class. Quant. Grav.* **27** (2010) 114103, arXiv:0912.2393 [astro-ph.HE]. 4.4.3, 4.4.3, 6

[32] L. I. Petrich, S. L. Shapiro, and S. A. Teukolsky, "Oppenheimer-snyder collapse with maximal time slicing and isotropic coordinates," *Physical Review D* **31** (1985) 2459. http://prd.aps.org/abstract/PRD/v31/i10/p2459_1. 4.4.3

[33] H. C. K. I. Cho and T. Moon, "Universe driven by perfect fluid in Eddington-inspired Born-Infeld gravity," *Phys. Rev. D* **86** (2012) 084018, arXiv:1208.2146 [gr-qc]. 5.1

[34] T. D. P. Pani and V. Cardoso, "Eddington-inspired Born-Infeld gravity. phenomenology of non-linear gravity-matter coupling," *Phys. Rev. D* **85** (2012) 084020, arXiv:1201.2814 [gr-qc]. 5.1, 5.2

[35] B. G. A. De Felice and S. Jhingan, "Cosmological constraints for an Eddington-Born-Infeld field," arXiv:1205.1168 [gr-qc]. 5.1

[36] P. P. Avelino, "Eddington-inspired Born-Infeld gravity: astrophysical and cosmological constraints," *Phys. Rev. D* **85** (2012) 104053, arXiv:1201.2544 [astro-ph.CO]. 5.1

[37] I. L. J. Casanellas, P. Pani and V. Cardoso, "Testing alternative theories of gravity using the sun," *Astrophys. J.* **745** (2012) 15, arXiv:1109.0249 [astro-ph.SR]. 5.1

[38] M. B. C. Escamilla-Rivera and P. G. Ferreira, "A tensor instability in the Eddington-inspired Born-Infeld theory of gravity," *Phys. Rev. D* **85** (2012) 087302, arXiv:1204.1691 [gr-qc]. 5.1

[39] P. P. Avelino and R. Z. Ferreira, "Bouncing Eddington-inspired Born-Infeld cosmologies: an alternative to inflation?," arXiv:1205.6676 [astro-ph.CO]. 5.1

[40] H. G. Y. X. Liu, K. Yang and Y. Zhong, "Domain wall brane in Eddington-inspired Born-Infeld gravity," *Phys. Rev. D* **85** (2012) 124053, arXiv:1203.2349 [hep-th]. 5.1

[41] T. Delsate and J. Steinhoff, "New insights on the matter-gravity coupling paradigm," *Phys. Rev. Lett.* **109** (2012) 021101, arXiv:1201.4989 [gr-qc]. 5.1

[42] M. B. J. H. C. Scargill and P. G. Ferreira, "Cosmology with Eddington-inspired gravity," *Phys. Rev. D* **86** (2012) 103533, arXiv:1210.1521 [astro-ph.CO]. 5.1

[43] L. M. L. Y. H. Sham and P. T. Leung, "Radial oscillations and stability of compact stars in Eddington-inspired Born-Infeld gravity," *Phys. Rev. D* **86** (2012) 064015, arXiv:1208.1314 [gr-qc]. 5.1

[44] P. Pani and T. P. Sotiriou, "Surface singularities in Eddington-inspired Born-Infeld gravity," *Phys. Rev. Lett.* **109** (2012) 251102, arXiv:1209.2972 [gr-qc]. 5.1

국문초록

Development of a General Relativistic Hydrodynamic Code in Spherical Symmetry
구대칭 일반상대론적 유체역학 코드의 개발

자체의 중력 효과를 고려하는 구대칭 완전 유체 전산모사 연구를 위해 일반상대론적 유체역학 코드를 이 분야 연구자들을 위한 공개용으로 개발하였다. 이 코드는 3+1 ADM (Arnowitt-Deser-Misner) 공식과 등방 공간 좌표를 사용하였다. 시공간 기하를 구하기 위해 극한값 썰기 (maximal slicing) 조건과 함께 세 개의 제한 방정식을 풀었고, 시공간을 채우는 물질인 유체는 근사 리만 해법을 사용한 HRSC (high resolution shock capturing) 기법으로 오일러 관찰자 시점에서 풀었다. 이 코드의 수렴성과 정확성을 검증하기 위해 상대론적인 구대칭 충격파 비교 분석, 블랙홀로 빨려 들어가는 상대론적 구대칭 강착, TOV (Tolman-Oppenheimer-Volkoff) 별 및 OS (Oppenheimer-Snyder) 붕괴 코드 테스트를 수행하였다. 특히, 이 코드의 동적 진화 테스트인 OS 붕괴의 경우 해석적인 해와 결과를 비교하기 위하여 좌표변환을 수치 계산으로 수행하였다. 아인슈타인의 일반상대성 이론을 넘어서는 변형된 중력이론 중 하나로 최근 제시된 EiBI (Eddington-inspired Born-Infeld) 이론에서 TOV 별의 해가 일반상대성 이론과 어떠한 차이를 보이는지 살펴 보았고, 그 이론에서도 물질이 붕괴하여 블랙홀을 만드는 경우 특이점이 형성되는지 고찰해 보았다.

주요어 : 일반상대론적 유체역학, 구대칭 수치코드, EiBI 중력 이론

학번 : 2003-30091

감사의 글

무엇보다 논문 지도를 해 주신 이형목 교수님 도움이 없었더라면, 이 논문은 나오지 못했을 겁니다. 이 자리를 빌어 교수님께 깊은 감사의 말씀을 올립니다. 제 논문 심사일은 징검다리 연휴일이자 크리스마스 이브였습니다. 그 자리에서 날카롭게 헛점을 짚어주신 김웅태 교수님, 인자하게 코멘트를 주신 구본철 교수님, 먼 곳임에도 선뜻 와 주신 이창환 교수님 그리고 묵묵히 뒤를 봐 주신 강궁원 박사님께 다시 한 번 감사의 말씀 드립니다.

제 박사과정을 돌이켜보면 목적지를 정하지 않고 떠난 항해 같았습니다. 많이 돌아왔고, 그럼에도 어느 지점까지 왔고, 앞으로 계속 항해를 이어가려 합니다. 여기까지 오면서 지금의 제가 있기까지 도움을 주시고 영향을 주신 분들께 고마움의 말씀을 전하고 싶습니다.

우선 어머니, 아버지, 감사합니다. 두 분은 여러모로 저를 있게 한 근본이십니다. 특히, 어머니의 끊임없는 격려와 지원, 관심은 제게 큰 힘이 되었습니다. 논제가 무어냐고 물으실 때 제대로 답해드리지 못한 것이 아쉬움으로 남아 있습니다. 이제 이 논문을 어머니께 바칩니다.

대전에 내려와 있을 때, 아니 그 이전 그 이후에도, 물심양면으로 저를 도와 준 누나에게 그리고 자형, 똑똑한 성빈이, 마음씨 고운 유림이 그리고 귀여운 성호에게 깊은 고마움을 표하고 싶습니다. 그리고, 형 대신 든든한 직장에서 일하는 내 동생 한석이, 대견하다.

부족한 사위이지만 응원해 주시고, 잘 챙겨주시고, 살갑게 대해 주시는 장모님, 장인어른 감사합니다. 앞으로 더 잘 되는 모습으로 보답하도록 노력하겠습니다.

제가 이 논문에서 코드를 개발했다고 했지만, 컴퓨터의 "컴"자도 제대로 아는지 아직 모르겠습니다. 하지만 주위에 동료들이 있었기에 여기까지 올 수 있었습니다. 내 코드를 직접 봐주고 도와줬던 진호에게 진심으로 고맙다는 말 하고 싶다. Jakob, you are my mentor like no other. I'm very grateful for your help! 컴퓨터로 헤멜 때 물으러 가면 척척 도와주는 배태길씨에게도 고마운 마음을 전합니다.

수치상대론 연구모임을 이끌고 KISTI에 자리를 마련해 주신 강궁원 박사님께 다시 한 번 감사의 말씀을 전합니다. 워킹그룹을 이끌어 오시는 김희일 박사님 멤버인 수일이형, Mew-Bing, 찬에게도 고맙습니다.

서울대를 떠나 온 후 같은 연구실에서 연구하며 지내던 동료들은, KISTI로 내려오고 오랜 시간이 지나면서 아련한 추억으로만 남았습니다. 하지만 미국에서 열심히 적응하시고 계신 주호형, 연락 주시고 격려해 주셔서 고마웠습니다.

박사과정 동안 제가 제일 잘 한 일이 있다면, 아마 제 인생의 동반자 영이를 만난 것이라 확신합니다. 나와 함께 하는 마음 고맙고, 사랑한다.

입춘에 관악에서